

Analysis and modeling to forecast in time series: a systematic review

Fatoumata Dama[†] and Christine Sinoquet[†]

[†]LS2N / UMR CNRS 6004, Nantes University, France
`{fatoumata.dama, christine.sinoquet}@univ-nantes.fr`

Abstract

Forecasting in time series is an important area of machine learning, with a plethora of application domains including weather forecast, decision-making in finance and business, quality process control in industry, management of power flows, risk assessment in medicine. This paper surveys state-of-the-art methods and models dedicated to time series analysis and modeling, with the final aim of prediction. This review aims to offer a structured and comprehensive view of the full process flow, and encompasses time series decomposition, stationary tests, modeling and forecasting. Besides, to meet didactic purposes, a unified presentation has been adopted throughout this survey, to present decomposition frameworks on the one hand and linear and nonlinear time series models on the other hand. First, we decrypt the relationships between stationarity and linearity, and further examine the main classes of methods used to test for weak stationarity. Next, the main frameworks for time series decomposition are presented in a unified way: depending on the time series, a more or less complex decomposition scheme seeks to obtain nonstationary effects (the deterministic components) and a remaining stochastic component. An appropriate modeling of the latter is a critical step to guarantee prediction accuracy. We then present three popular linear models, together with two more flexible variants of the latter. A step further in model complexity, and still in a unified way, we present five major nonlinear models used for time series. Amongst nonlinear models, artificial neural networks hold a place apart as deep learning has recently gained considerable attention. A whole section is therefore dedicated to time series forecasting relying on deep learning approaches. A final section provides a list of R and Python implementations for the methods, models and tests presented throughout this review. In this document, our intention is to bring sufficient in-depth knowledge, while covering a broad range of models and forecasting methods: this compilation spans from well-established conventional approaches to more recent adaptations of deep learning to time series forecasting.

Keywords time series decomposition, time series modeling, forecasting, prediction, autocorrelation, stationarity, linearity, nonlinearity

1 Introduction

Time series data are amongst the most ubiquitous data types that capture information and record activity in most aeras. In any domain involving temporal measurements *via* sensors, censuses, transaction records, the capture of a sequence of observations indexed by time stamps first allows to provide insights on the past evolution of some measurable quantity. Beyond this goal, the pervasiveness of time series has generated an increasing demand for performing various tasks on time series data (visualization, discovery of recurrent patterns, correlation discovery, classification, clustering, outlier detection, segmentation, forecasting, data simulation).

Temporal *visualization* is one of the simplest and quickest ways to represent time series data. More importantly, graphical analysis is a crucial step of time series analysis, whatever the downstream data processing line. Notably, it should be the first step before starting with time series modeling.

In online recommendation systems, *correlation mining* aims at identifying Internet users sharing similar shopping patterns, for instance. The final objective is to provide dynamic recommendations based on the correlation between a given customer and other customers' behaviors. In the stock market sector, identifying correlations amongst stock prices can lead stockbrokers to spot investment opportunities.

Spatio-temporal *classification* may open up new possibilities, for example in geographical information systems, to manage land use and its evolution. However, time series classification requires reference data collection: in the absence of label information, this deep retrospective analysis represents a tough task generally hampered by the complexity of thematic classes and their lack of formal description in time series. Unsupervised *clustering* is often used, which offers a solution based upon the data alone.

Outlier detection represents another prominent field of time series analysis. Outlier detection is central to understand the normal behavior of data streams and detect situations that deviate from the norm.

The aim of time series *segmentation* is to identify the boundary points of segments in the data flow, to characterize the dynamical properties associated with each segment.

Forecasting in time series is an important area of machine learning. Time series analysis helps in analyzing the past, to forecast the future. Forecasting is of prime importance in many domains: in finance and business, to plan policies by various organizations; in industrial quality process control and digital transactions, to detect abnormal or fraudulent situations; in electric power distribution, to control loads *via* advanced monitoring and cope with disturbances in power flows; in meteorology, to guide informed decision-making for agriculture, air and maritime navigation; in biology, to gain knowledge on the activity of genes given affected/unaffected status; in medicine, to predict the spread of a disease, estimate mortality rates or assess time-dependent risk.

Recent reviews focussed on time series data were more or less dedicated to specific methods or applications. The surveys in (Susto et al., 2018) and (Fawaz et al., 2019) focus on classification. To our knowledge, the most recent review addressing clustering in stream data dates back to 2015 (Aghabozorgi et al., 2015). In (Ali et al., 2019), the authors review both classification and clustering methods devoted to visual analytics in time series. Two recent state-of-the-art documents on anomaly detection are provided in (Braei and Wagner, 2020) and (Blázquez-García et al., 2020). As regards forecasting in time series, we found few recent substantial surveys, which are moreover all entirely devoted to deep learning (Lim and Zohren, 2020; Sezer et al., 2020). Even less could we identify a survey meeting the objectives sought through the writing of the present document. Drafting this survey was motivated by three goals:

A compilation bringing an informed choice for modeling and forecasting purposes

Multiple media encompassing journal articles, tutorials and blog posts allow to catch valuable though fragmented information on prediction in time series. With a focus on operationality (code source examples are generally provided) and illustration, the two latter media can only tackle specific aspects of time series (for instance, introduction to the fundamentals of time series data and analysis (APTECH, 2020); how to decompose time series data into trend and seasonality (Brownlee, 2020b); Using Python and Auto ARIMA to Forecast Seasonal Time Series (Portilla, 2018); Holt-Winters Forecasting Simplified (Solarwinds, 2019)). On the other hand, several books and e-books dealing with time series were written. In this category, one finds large textbooks that offer a generalist approach for time series analysis and forecasting (*e.g.*, (Montgomery et al., 2016)). Other books and e-books target hands-on approaches (*e.g.*, (Nielsen, 2019)). Finally, several writings are entirely dedicated to a few methods or models (*e.g.*, (Brownlee, 2020a)), to a specific application field (*e.g.*, (Brooks, 2019)) or to one language (*e.g.*, (Avishek and Prakash, 2017)).

However, the exponential increase in the volume of data, including time series data in all sectors

of industry, finance, economy, biology, medicine, together with the growing availability of software programs, announces in particular the appropriation of time series prediction tools by scientists that are nonspecialists of time series. In complement to these media targeting "how to" aspects, and to the aforementioned books and e-books, our aim is to provide readers a quick access to sufficiently detailed information, over a large methodological spectrum. In particular, we wished to offer a compilation allowing nonspecialists to step back and make an informed choice to process their stream data for modeling and forecasting purposes.

A sufficiently broad panorama covered by substantial developments

Time series modeling, stationarity analysis and forecasting ability are intimately related. Numerous publications target cutting-edge theoretical developments on stationarity. Other publications are entirely dedicated to the description of some specific variant of a linear or nonlinear framework, to model time series data. Currently, insights on linear and nonlinear time series modeling are generally presented separately in books (Paoletta, 2018; Tsay and Chen, 2018). In addition, no recent survey could be identified that substantially develops a sufficiently broad panorama on time series modeling upstream forecasting. Moreover, a compilation accessible to scientists without sharp expertise was lacking, that would put in perspective stream data preprocessing, various facets of time series modeling and forecasting.

A dictatorial and unified presentation

Finally, strong didactical concerns have motivated the design of this survey. Besides the guideline from time series preprocessing to forecasting, a unified presentation has been adopted as far as possible for entire parts of this compilation.

A time series is a sequence of data points (observations) ordered in time. Time is supposed discrete here. A time series represents the temporal evolution of a dynamic system that one searches to describe, explain and predict. Correlation analysis allows to model how a time series is related to its delayed values. This analysis is crucial to design a forecasting procedure, a major aim of time series data processing. Forecasting is based on the following principle: knowing the past behaviors of a system, it is possible to make predictions on its nearby or long-term behaviors.

Let $\mathbf{x} = x_1, x_2, \dots, x_T$ be a time series describing a dynamic system of interest; \mathbf{x} is a realization of the stochastic process $\mathbf{X} = \{X_1, X_2, \dots\} = \{X_t\}_{t=1}^\infty$. Prediction requires the modeling of the relationship between past and future values of the system:

$$X_t = f(t, X_{t-1}, X_{t-2}, \dots) + g(t, X_{t-1}, X_{t-2}, \dots)\epsilon_t, \quad (1)$$

where $\{\epsilon_t\}$ is a series of noises such that the ϵ_t 's are independent and identically distributed (i.i.d) with 0 mean and unit variance, and are also independent from past values of X_t , and where f and g are respectively the conditional mean and variance of X_t (given the past values). The conditional mean and variance are possibly time-dependent. The key to prediction in time series is the ability to model the dependencies between current and lagged values (or autocorrelation).

In what follows h designates f or g . To model h , the approaches described in the literature break down into two main categories: parametric and nonparametric models.

Nonparametric models suppose that h belongs to some flexible class of functions. For instance, the review by (Härdle, Lütkepohl, and Chen, 1997) put forward approaches relying on functions that belong to the C_1 class (that is functions that are differentiable over some interval I , and whose derivative function f' is continuous on I). In contrast, parametric models specify h within a class of parametric functions, such as the class of polynomial functions (Tong, 1990; Hamilton, 1994). A nonparametric model can be seen as a parametric framework with a high number of parameters to instantiate, thus requiring a large volume of data to learn the model. Flexibility and interpretability are respective advantages of nonparametric and parametric models. Nonetheless, flexibility may be increased in parametric models. Notably, this survey will show that it is possible to increase flexibility by enabling more complex relationships between the value at time step t and its lagged values. To note, it is possible

to use a parametric model for f and a nonparametric model for g , and *vice-versa*.

This survey aims at presenting a state-of-the-art of parametric models dedicated to time series analysis, with the purpose of prediction. These models are divided into two categories: **linear** and **nonlinear** models. In this survey, we will decrypt in particular the links between linearity and stationarity, and under which conditions they hold for some of the linear models presented. We will also see that stationarity and nonlinearity may be compatible.

This survey is organized as follows. Section 2 deals with the stationarity concept and reviews the main classes of methods to test for weak stationarity. The main frameworks for times series decomposition are presented in Section 3 in a unified way. Section 4 is devoted to the unified presentation of three popular linear models used for time series modeling, each time detailing autocovariance, parameter learning algorithms and forecasting. This section ends with the description of more flexible models, to escape the limits of the previous models. A step further, but still in a unified manner, Section 5 depicts five major nonlinear models used for time series. Amongst nonlinear models, artificial neural networks hold a place apart as deep learning has recently gained considerable attention. Section 6 therefore brings methodological insights in time series forecasting with deep learning. This section describes a selection of five models. Finally, for the report, Section 7 provides a list of R and Python implementations for the methods, models and tests presented throughout this review.

To recapitulate, we highlight the following contributions:

- To the best of our knowledge, this is the first comprehensive survey dedicated to forecasting in time series, with the concern to take a comprehensive view of the full process flow, and encompassing decomposition, stationary tests, modeling and forecasting.
- This survey offers, as far as possible, a unified presentation of decomposition frameworks, on the one hand, and of linear and nonlinear time series models on the other hand.
- The relationships between stationarity and linearity are decrypted, with the aim of bringing them within the reach of scientists that are nonspecialists of time series.
- In this document, our intention is to bring sufficient in-depth knowledge, while covering a broad range of models and forecasting methods: this compilation spans from well-established conventional approaches to more recent adaptations of deep learning to time series forecasting.

2 Stationarity

This subsection will first recall the definitions of strong and weak stationarity. Then it will briefly describe the main categories of methods employed to test for stationarity. Finally, a recapitulation of methods within these categories will be provided.

2.1 Stationary Stochastic Process

A stochastic process \mathbf{X} is *stationary* if its statistical properties are time-independent. A distinction is made between *strong* stationarity and *weak* stationarity.

2.1.1 Strong Stationarity

\mathbf{X} is a strongly stationary process if its distribution satisfies the following property:

$$\mathbb{P}(X_1, X_2, \dots, X_T) = \mathbb{P}(X_{1+\tau}, X_{2+\tau}, \dots, X_{T+\tau}), \quad \forall T, \tau \in \mathbb{N}^*. \quad (2)$$

Stationarity means that the distribution of \mathbf{X} is the same over time or, in other words, that it is invariant to any time shift. In particular, any *i.i.d* stochastic process is strongly stationary. In practice, it is difficult to test property (2). Thus, a weak version, named *weak stationarity*, was introduced.

2.1.2 Weak Stationarity

\mathbf{X} is a weakly stationary (or mean-covariance stationary) process if its mean and covariance verify the following properties:

$$\begin{aligned} \mathbb{E}[X_t] &= \mu \quad (\text{mean stationarity}), \\ \text{Cov}(X_t, X_{t+h}) &= \gamma(h) \implies \text{Var}(X_t) = \gamma(0) < \infty \quad (\text{covariance stationarity}), \end{aligned} \tag{3}$$

where Cov and Var respectively denote covariance and variance, and γ is symmetric ($\gamma(-h) = \gamma(h)$) and bounded ($|\gamma(h)| \leq \gamma(0) < \infty$). Formula (3) expresses that the mean and autocovariance of \mathbf{X} are time-independent and that its variance is finite.

Weak stationarity relaxes the strong stationarity property by only constraining the first moment and autocovariance function of \mathbf{X} instead of its whole distribution. Thus, *strong stationarity* implies *weak stationarity*. Figure 1 shows an example for *weak stationarity*, *mean stationarity*, *variance stationarity* and *mean and variance nonstationarity*. Weak stationarity is also called *second-order stationarity*. *First-order stationarity* refers to the case where only the mean is constant.

From now on, the term "weak" will be omitted for the sake of simplicity, that is **weak stationarity will be referred to as stationarity**.

2.2 How to Test for Stationarity?

Testing the stationarity for a time series is of great importance for its modeling. To assess the stationarity of a stochastic process \mathbf{X} based on a realization $\{x_t\}_{t=1}^T$, we can use either *graphical methods* or *statistical tests*.

2.2.1 Graphical Methods

Analysis of time series plot Stationarity can be visually assessed from time series plots on which prominent seasonality, trend and changes in variances are investigated. For instance, the time series of atmospheric concentration of CO_2 in Hawaii (Figure 4c) has an increasing trend and a yearly seasonal pattern.

Plotting rolling statistics *Rolling statistics* graphs plot means and variances computed within sliding time windows. Such graphs can provide insights on stationarity. Indeed, if these graphs exhibit time-invariance, then the studied time series will probably be stationary.

Figure 2 displays an application of the rolling mean method to two stationary and nonstationary time series. Note that the rolling graph is time-invariant for the (stationary) white noise process (Figure 2a) while it shows an increase for the nonstationary time series (Figure 2b).

Correlogram vs covariogram In time series analysis, a *correlogram* and a *covariogram* are respectively the graphs of the autocorrelation function (ACF) and of the scaled autocovariance function. These functions are defined as follows:

$$\rho(h) = \frac{\text{Cov}(X_t, X_{t+h})}{\sqrt{\text{Var}(X_t)\text{Var}(X_{t+h})}} \quad (\text{autocorrelation function}) \tag{4}$$

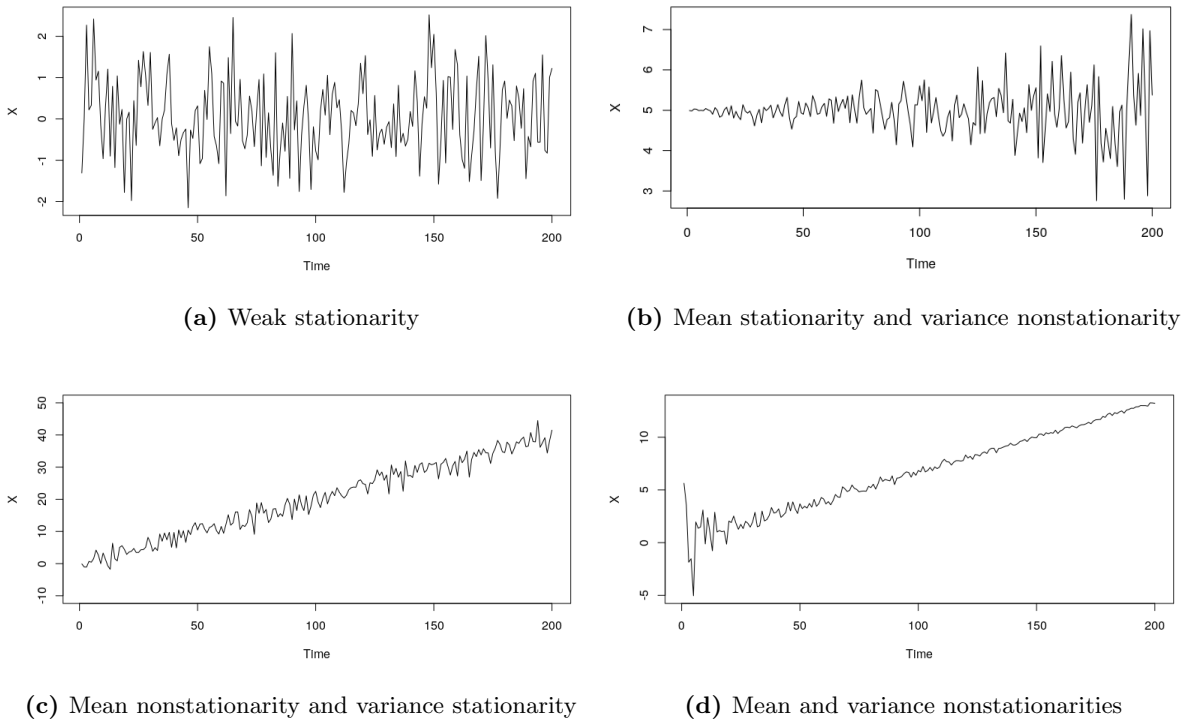


Figure 1 Illustration of stationarity and nonstationarity on simulated time series. $\mathcal{N}(\mu, \sigma)$ represents the *normal* law with mean μ and variance σ^2 . **(a)** Weak stationarity: uncorrelated white noise simulated through $X_t \sim \mathcal{N}(0, 1)$; $\mathbb{E}[X_t] = 0$; $\text{Var}[X_t] = 1$. **(b)** Mean stationarity: $X_t \sim \mathcal{N}(5, \sigma_t)$ with $\sigma_t = \frac{t+1}{200}$, $\mathbb{E}[X_t] = 5$ and $\text{Var}[X_t] = \sigma_t^2$ increases with time. **(c)** Variance stationarity: $X_t = t/5 + \mathcal{N}(0, 2)$, $\mathbb{E}[X_t] = t/5$ increases with time and $\text{Var}(X_t) = 4$. **(d)** Mean and variance nonstationarities: $X_t = t/15 + \mathcal{N}(0, \sigma_t)$ with $\sigma_t = \frac{20}{t}$, $\mathbb{E}[X_t] = t/15$ and $\text{Var}[X_t] = \sigma_t^2$. Mean increases with time whereas variance decreases.

$$\rho_s(h) = \frac{\text{Cov}(X_t, X_{t+h})}{\text{Var}(X_t)} \quad (\text{scaled autocovariance}). \quad (5)$$

Correlograms and covariograms allow to graphically describe temporal dependencies existing within the observations. A correlogram (respectively a covariogram) plots the value of the ACF (respectively the scaled autocovariance) for increasing lags. It has to be highlighted that correlograms and covariograms are identical for stationary time series (since $\text{Var}(X_t) = \text{Var}(X_{t+h})$). Besides, it was proven that correlograms tend to better discriminate between stationarity and nonstationarity than covariograms (Nielsen, 2006). In particular, correlograms show a quick decrease down to zero for stationary processes, unlike nonstationary ones for which the decay is slower. Figure 3 illustrates this fact.

However, visual investigations of stationarity do not always allow to conclude. In this case, more rigorous *statistical tests* have to be used.

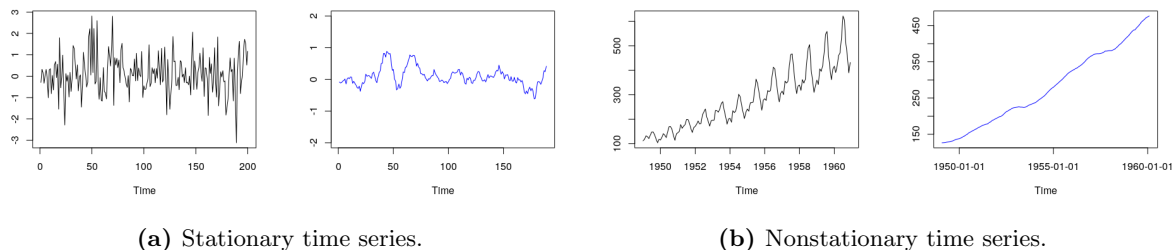
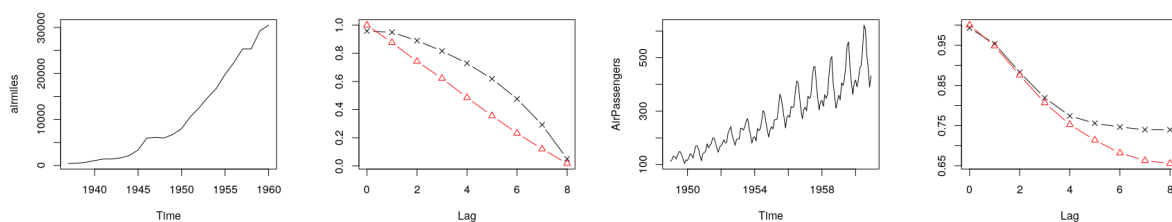


Figure 2 Rolling mean method applied to examples of stationary and nonstationary time series. Window size equals 12. **(a)** White noise process $\mathcal{N}(0, 1)$ where \mathcal{N} stands for gaussian law (left), rolling mean graph (right). **(b)** USA monthly airline numbers of passengers (left), rolling mean graph (right).



(a) Revenue passenger miles flown by commercial airlines in the United States. **(b)** Monthly airline numbers of passengers in the United States.

Figure 3 Correlogram (cross) vs covariogram (triangle) applied to two nonstationary time series.

2.2.2 Statistical Tests

A short reminder about statistical tests

A statistical test is used to decide between two hypotheses, the null hypothesis H_0 and the alternative hypothesis H_1 , where H_0 is the hypothesis considered true if no evidence is brought against it. The risk to wrongly accept H_1 , $\mathbb{P}_{H_0}(H_1) = \alpha$, is referred to as *type I error*. Symmetrically, the risk $\mathbb{P}_{H_1}(H_0) = \beta$ is called *type II error*. $1 - \alpha$ and $1 - \beta$ are respectively called **test confidence** and **test power**. α and β were proven to vary inversely.

Formally, a statistical test relies on a *test statistic*, S . The *observed statistic* S_{obs} is a numerical summary of the information contained in the observed dataset, whereas S is the random variable summarizing the information for any dataset in the whole distribution of possible datasets. Provided we can compute or approximate the law of S under H_0 , $\mathbb{P}_{H_0}(S)$, we can evaluate the probability to obtain a *test statistic* more atypical than S_{obs} in the direction of the alternative. This probability is called the *p-value*. For example, in a right (respectively left) uni-lateral test, H_0 is rejected when S_{obs} is too high (respectively too low), that is if $p\text{-value} = \mathbb{P}_{H_0}(S > S_{obs}) \leq \theta$ (respectively $p\text{-value} = \mathbb{P}_{H_0}(S < S_{obs}) \leq \theta$), with some user-defined threshold θ . H_0 rejection entails H_1 acceptance. Finally, the higher the $|p\text{-value} - \theta|$ difference, the safer the decision. Moreover, the lower the threshold θ , the higher the test confidence.

Stationarity tests

When relying on statistical tests to analyze time series, we must pay attention to the choice of the hypotheses. If we test H_0 (nonstationarity) against H_1 (stationarity), the lower the α type I error (high

confidence), the safer it is to conclude to stationarity. In contrast, if we test H_0 (stationarity) against H_1 (nonstationarity), the lower the β type II error (high power), the safer it is to decide stationarity. The statistical tests proposed to test whether a stochastic time series is stationary or not can roughly be grouped into two categories: tests that mostly work in the frequency domain and those that work in the time domain.

Frequency domain methods A natural way to analyze a signal (for instance a time series) consists in plotting its behavior against time. However, this temporal representation does not offer insight on the frequencies contained in the signal. For a brief reminder, just consider the simple cosine signal $x_t = A \cos(2\pi ft + \phi)$, where amplitude A determines the maximum absolute height of the signal, frequency f controls how rapidly the signal oscillates and ϕ is the phase at origine. This simple signal contains only one frequency, but more complex functions such as times series can be viewed as a sum of cosine waves with varying amplitudes, frequencies and phases at origine, for example $X_t = 3 \cos(\frac{\pi}{4}t) - 2 \cos(\frac{\pi}{3}t + \frac{\pi}{2}) + \cos(\frac{\pi}{2}t + \frac{\pi}{6})$. The spectrum of a signal plots the amplitudes of the various components existing in the signal against the frequencies. Moreover, it is recalled that the Fourier series expansion of a signal writes as a sum of trigonometric function of all frequencies, for instance $A_i \sin(\omega it + \phi_i)$, $i = 1, 2, \dots$, where $\omega = 2\pi f$. Short-time Fourier transform uses a sliding window, which provides information of both time and frequency. To increase the resolution in frequency, Wavelet transform is another standard function based on small wavelets with limited duration.

Several methods testing for (non)stationarity rely on some spectral decomposition of the time series under analysis. Therein, we find approaches testing the constancy of spectral characteristics (Priestley and Rao, 1969; Paparoditis, 2010), methods comparing a time-varying spectral density estimate with its stationary approximation (Dette et al., 2011; Preuß et al., 2013; Puchstein and Preuß, 2016) and approaches based on Fourier transform (Basu et al., 2009; Dwivedi and Subba Rao, 2011) or on wavelets (Nason, 2013; Cardinali and Nason, 2013). Recently, a class of dynamic processes exhibiting a functional time-varying spectral representation was established (van Delft and Eichler, 2018). In particular, this class includes time-varying *functional ARMA* processes which have been shown to be functional locally stationary. ARMA processes will be described in Subsection 4.3. Functional-coefficient Autoregressive processes will be presented in Subsection 5.2.

Frequency analysis is dedicated to discover underlying periodicities in time series. This periodic behavior can be very complex. Frequency domain analysis is useful if the time series under study is known to remain invariant within a certain time interval. Issues arise if the frequency changes over time.

Time domain methods Unit root tests represent standard methods to identify nonstationarity. To convey the intuition behind this concept, we introduce unit roots in the case of a linear autoregressive process AR(p): $X_t = \phi_0 + \sum_{i=1}^p \phi_i X_{t-i} + \epsilon_t$, where the ϵ_i 's are usually uncorrelated white noise processes. The reformulation as $(1 - \phi_1 L - \phi_2 L^2 - \dots - \phi_p L^p)X_t = \phi_0 + \epsilon_t$, where L represents the lag operator ($LX_t = X_{t-1}$, $t > 1$) allows to identify the so-called characteristic equation of X_t : $1 - \phi_1 y - \phi_2 y^2 - \dots - \phi_p y^p = 0$. An AR(p) process has a unit root if one of the roots of the characteristic equation is equal to 1. Unit roots are one cause for nonstationarity. An AR(p) process with a unit root can be transformed into a stationary process through a given number of differentiation transformations (see equation 11, Subsection 3.2.1). An AR(p) process with unit root and multiplicity m for this root exactly requires m successive differentiations to become stationary. Such a process is said to be integrated to order m .

Standard unit root tests, such as *Phillip-Perron test* (Phillips and Perron, 1988) and *Dickey-Fuller test* (Dickey and Fuller, 1979), check stationarity under one-order serial correlation assumption and constant trend assumption for the former, linear trend for the latter. In the *KPSS test*, the time series under study is written as the sum of a linear trend, a random walk process RW (defined as $RW_t = RW_{t-1} + u_t$ where the u_t 's are i.i.d($0, \sigma^2$)) and a standard error (Kwiatkowski et al., 1992). *Augmented Dickey-Fuller*

(*ADF*) test checks the stationarity around a linear trend under a p -order serial correlation (Cheung and Lai, 1995; Dolado et al., 2002; Elliott et al., 1996). The works reported in (Phillips, 1987) extend unit root-based tests to the random walk and more general ARIMA models (to be presented in Subsection 4.4.1).

Several methods were proposed to deal with time series in which break points are known or suspected (Perron, 1989). The *Zivot and Andrews test* tests the null hypothesis of unit root existence against the stationary alternative with a unique structural break point (Zivot and Andrews, 2002).

Other methods are able to cope with more than one break point. The CUSUM test is widely used to test for parameter changes in time series. The method described in (Lee et al., 2003) implements a CUSUM test, to handle the break point problem for parameters other than the mean and variance. Thus, parameter stability can be tested for random coefficient autoregressive models, as well as autocovariance stationary for infinite-order moving average processes (to be presented in Subsection 4.2).

In the same category, the piece-wise locally stationary (PLS) time series model described in (Zhou, 2013) allows both abrupt and smooth changes in the temporal dynamics of the process. In this framework, a bootstrap procedure is used to approximate the null distribution for a CUSUM test statistic (H_0 : the time series is PLS). The proposed method goes beyond testing changes in mean. It can be extended to testing structural stability for multidimensional parameters, in second and higher-order nonstationary time series. Further in this line, another CUSUM approach (Dette et al., 2015) relying on bootstrapping was designed to relax assumptions: for instance, when testing for the stability of autocovariance, it is not required that mean and variance be constant under H_0 ; moreover, this approach allows break points at different times, for variance and autocovariance.

Table 1 sums up the (non)stationarity tests that perform in time domain analysis and were presented in this section.

Method	Trend T_t	Test	Hypotheses	H_0	Reference		
Unit root	Constant	Phillips-Perron	$X_t = T_t + AR(1)$	NS	Phillips and Perron (1988)		
		Dickey-Fuller			Dickey and Fuller (1979)		
	Linear	KPSS	$X_t = T_t + RW_t + \epsilon_t$	S	Kwiatkowski et al. (1992)		
		ADF			$X_t = T_t + AR(p)$	NS	Cheung and Lai (1995)
							Dolado et al. (2002)
				Elliott et al. (1996)			
Unit root and break point	Constant	Phillips	$X_t = T_t + RW_t + \epsilon_t$ or $X_t = T_t + ARIMA$	NS	Phillips (1987)		
	Linear	Perron Zivot and Andrews	unique known breakpoint in trend unique unknown breakpoint in trend	NS	Perron (1989) Zivot and Andrews (2002)		
Break point analysis	Constant	Lee	random coefficient autoregressive model infinite-order moving average process	S	Lee et al. (2003)		
		Zhou			Zhou (2013)		
		Dette <i>et al</i>			Dette et al. (2015)		

Table 1 Stationary tests that perform in time domain. ADF: augmented Dickey-Fuller test. S: stationary. NS: nonstationary. RW: random walk process. ARIMA: autoregressive integrated moving average. The ARIMA model is a generalization of the autoregressive (AR) model. These models are presented in Subsections 4.4.1 and 4.1, respectively. LS: locally stationary. In an LS time series model, the process is assumed to be smoothly changing over time. PLS: piecewise locally stationary. In the PLS time series framework, the time series is divided into several time intervals, and the process is assumed to be stationary in each interval.

3 Time Series Decomposition

Subsection 3.1 will describe the motivation behind the decomposition of nonstationary time series into nonstationary effects and a remaining component. Then, various decomposition schemes will be described

through Subsections 3.2 to 3.4. Subsection 3.5 will offer a recapitulation of the most popular models and methods designed for time series decomposition. Further, Subsection 3.6 will address prediction in the decomposition scheme.

3.1 Objectives of Time Series Decomposition

Nonstationary time series can be decomposed into nonstationary effects (the deterministic components) and a remaining component (the stochastic constituent), to allow further tasks. Such tasks encompass the characterization of the cause for nonstationarity, together with prediction. The commonly studied nonstationary effects are trend and seasonality, which are taken into account in many time series analysis models such as ARIMA (Usman et al., 2019; Nyoni, 2019), SARIMA (Samal et al., 2019; Valipour, 2015; Martinez et al., 2011), exponential smoothing-based methods (Pegels, 1969; Taylor, 2003a; Aryee et al., 2019).

In such a decomposition scheme, the deterministic components are predictable and contribute to the prediction task through their estimations or through extrapolation. For example, the evolution of a trend can be modeled and extrapolation will thus contribute to build the predicted values. Similarly, seasonality (that is, periodic fluctuation) can be modeled, to yield the corresponding deterministic contribution to the predicted values. As a complement, attempts to improve the prediction accuracy require an analysis of the remaining stochastic component. Therefore, depending on the time series, a more or less complex decomposition scheme seeks to obtain the remaining stochastic component. It is important to highlight here that in general, the stochastic component is structured, because of *auto-correlation*. In contrast, noise (or chaos) is the effect of unknown factors or factors that cannot be measured.

Autocorrelation is the key concept that allows future prediction in time series. Informally, autocorrelation is a measure that reflects the degree of dependence between the values of a time series over successive time intervals. Otherwise stated, a high autocorrelation means that values are highly dependent on their lagged values. Thus, many models attempting to capture autocorrelation have been proposed in the literature. Stationary models are preferred when possible.

Stationarity is a central and desirable property in time series analysis. Intuitively, stationarity can be explained as follows: if a dynamic system represented by a stochastic process $\mathbf{X} = \{X_t\}_{t=1}^{\infty}$ is characterized by a given behavior at time t , this behavior will likely reproduce at time $t + 1$. In other words, the system behavior is time-invariant. This implies stability for the relation between X_t and its lagged values. A key property inherent to stationarity is therefore exploited to model the stochastic process: the autocorrelation is invariant with time. Such models will offer a simplified framework, to predict future values, based on autocorrelation.

The link between stationarity and linearity was established in Wold’s theorem (1938) (Wold, 1954). In a nutshell, Wold’s theorem states that any stationary stochastic process can be expressed as an infinite weighted sum of uncorrelated white noise errors. In other words, the process may be represented through an MA(∞) model, where MA(∞) represents a (linear) moving average model with an infinite number of parameters (see Subsection 4.2).

Conversely, a linear model is not necessarily stationary. In Section 4, we will see that the moving average (MA) model is stationary by definition. In the same section, we will discuss conditions to guarantee stationarity for two other linear models (linear autoregressive: AR; autoregressive moving average: ARMA).

It should also be emphasized here that numerous stochastic processes exist that show stationarity but are nonlinear. The reason lies in Wold’s representation not being adapted or realistic: namely, this representation does not allow to fit a limited amount of data with a reasonable number of parameters and to provide reliable predictions. In such stationary processes, the link between X_t and its lagged values is nonlinear; in other cases, X_t is subject to regime changes.

The phenomenon that governs a stationary time series may be linear or nonlinear. However, if a series is nonstationary, the underlying phenomenon is generally nonlinear. For instance, a nonlinear model may be envisaged in the case when a stochastic process switches from regime to regime. Regime switching is an acknowledged cause for nonstationarity. A compromise is nonetheless proposed by some models that describe jumps between locally stationary processes (Zhou, 2013). Other situations may require still more complex modeling, such as in financial markets, where periods of low variations are interspersed with periods of high variations. Essentially, wherever there is time-varying variance (or so-called "volatility"), the time series do not conform to a linear model (see for instance the GARCH model, Subsection 5.5). But the border is not so clear-cut in the case of time-varying variance: nonlinearity does not necessarily imply nonstationarity. Several works have established conditions to guarantee the stationarity for specific variants of the GARCH model (see for example Bollerslev (1986a); Bougerol and Picard (1992); Panorska, Mitnik, and Rachev (1995); Mohammadi (2017)).

Decomposition aims at preprocessing a raw time series to yield a remaining stochastic component. The latter is further modeled as a linear or nonlinear process, if possible. Moreover, stationarity is a desirable situation as it simplifies modeling and prediction tasks.

Whereas the trend and seasonal components are deterministic and time-dependent, the remaining stochastic component (stationary or not, linear or not) is expected to display no apparent trend and seasonal variations and to contain the information about the autocorrelation of observations. In this favourable situation, the aims pursued by time series decomposition are then to describe the autocorrelation structure and to perform accurate prediction based on the autocorrelation inherent to this remaining part. To achieve the second aim, the remaining component is obtained by filtering out the deterministic components from the raw series. In particular, \mathbf{X} is stationary if the remaining stochastic component is stationary while the other components are null; otherwise, it is nonstationary.

Subsection 2.1.2 described three classes of nonstationarity: mean, variance, mean and variance nonstationarity. The next three Subsections 3.2 to 3.4 will exhibit the connection between these former descriptions and various decomposition schemes combining trend, seasonality and the remaining stochastic component. From weakest to strongest level of weak nonstationarity, we can enumerate *mean nonstationarity*, *variance nonstationarity* and *mean and variance nonstationarity*.

3.2 Additive Decomposition - Nonstationary Mean

\mathbf{X} is a nonstationary mean process if its mean varies over time, that is $\mathbb{E}[X_t] = \mu(t)$, while its variance stays constant. This situation is described by an additive decomposition model defined as follows:

$$X_t = \mu(t) + Z_t, \tag{6}$$

where Z_t is the remaining stochastic component of \mathbf{X} . Z_t is hypothesized to be stationary, with mean and variance respectively equal to 0 and σ^2 .

It has to be noted that if an estimator of $\mu(t)$ is known, that of the stationary component can be found as follows: $\hat{Z}_t = X_t - \hat{\mu}(t)$. Generally, $\mu(t)$ is either a trend T_t or a seasonal component S_t or any combination of both. In what follows, we will present the classical models widely studied in the literature: **additive trend** ($\mu(t) = T_t$), **additive seasonality** ($\mu(t) = S_t$) and **additive trend and seasonality** ($\mu(t) = T_t + S_t$). Figure 4 shows examples of real-life time series that can be modeled through additive decomposition.

3.2.1 Additive Trend Scheme: $\mu(t) = T_t$

The trend T_t represents the long-term evolution of \mathbf{X} . The trend can be increasing, decreasing, polynomial, *etc.* It can be either estimated then removed from X_t , or (much less easily) modeled then removed from

X_t . Otherwise, T_t can be directly removed from X_t by transformation.

• **Estimation of T_t in the additive trend scheme**

In this line, we will mention three categories of methods.

- ***Moving average (rolling mean)***

Generally speaking, smoothing methods take an important place in time series analysis, particularly, in time series trend estimation. In this context, the *moving average* method, also referred to as *rolling mean* method, can adjust to a large range of trends. *Moving average* is a very simple *scatterplot smoother* for which the initial data points X_t are replaced with the means computed from successive intervals $I_t = \{X_{t'}, t' \in [a_t, b_t]\}$, with $a_t = \max(1, t - w)$, $b_t = t - 1$ and w the *span size*. The trend estimate is then defined as follows:

$$\hat{T}_t = \frac{1}{|I_t|} \sum_{i \in I_t} X_i, \quad (7)$$

where $|I_t|$ stands for the cardinal of I_t . The smoothness of the estimated trend depends on the span size w : the larger w , the smoother the trend. It has to be noted that this method is particularly sensitive to outliers.

In this scheme, if the series is observed till time step t , at horizon $h > 0$, prediction is made as follows: the trend \hat{T}_{t+h} is extrapolated according to equation (7), relying on observed values and previously extrapolated values $\hat{T}_{t+h'}, 0 < h' < h$.

- ***Damped Holt additive trend method (generalized Holt method)***

We first explain *Simple exponential smoothing*, equivalently, *exponentially weighted moving average*, a well-known smoothing method that also relies on a sliding window (Perry, 2010). This method is suited to noisy time series without trend. It is defined by the following recursion scheme:

$$\tilde{X}_t = \alpha X_t + (1 - \alpha) \tilde{X}_{t-1}, \quad (8)$$

with \tilde{X}_t the smoothed value (or *level*) at time t , and α the *smoothing parameter* comprised between 0 and 1.

It has to be noted that the lower the α parameter, the stronger the smoothing. No general method exists that allows to choose the best value for α . The α parameter is generally adjusted thanks to expert knowledge that indicates how much weight should be given to the current *versus* past observations. Other data-driven selection methods were proposed (Gelper et al., 2010).

The difference with the previously seen *moving average* method is that each data point is smoothed based on weights that are exponentially decreasing as the observations are older. Thanks to the exponential decay of weights, *exponential smoothing* is less sensitive to outliers than *moving average*.

The *damped Holt additive trend method*, also referred to as *generalized Holt method*, is suited to time series that exhibit an increasing or decreasing trend (Gardner Jr and Mc Kenzie, 1985; Taylor, 2003a). This method intertwines two exponential smoothings:

$$\begin{aligned} \tilde{X}_t &= \alpha X_t + (1 - \alpha)(\tilde{X}_{t-1} + \phi \hat{T}_{t-1}), \\ \hat{T}_t &= \beta(\tilde{X}_t - \tilde{X}_{t-1}) + (1 - \beta) \phi \hat{T}_{t-1}, \end{aligned} \quad (9)$$

where \tilde{X}_t is the smoothed series, \hat{T}_t is the estimated trend, α and β are the smoothing parameters comprised between 0 and 1, and ϕ is the dampening parameter that gives more control over trend exploration. The first *exponential smoothing* removes random variations (noise), to produce the level of the series at time step t , and the second one smoothes the trend.

If $\phi = 1$, we obtain the standard **Holt additive trend** method (Holt, 2004). If $\phi = 0$, we obtain the *simple exponential smoothing* method (no trend). If $0 < \phi < 1$, the trend extrapolation is damped and approaches an horizontal asymptote given by $\hat{T}_t \phi / (1 - \phi)$. If $\phi > 1$, \hat{T}_{t+h} has an exponential growth; this setting seems to be suited to series with exponential trends.

At horizon $h > 0$, the trend is extrapolated as follows:

$$\hat{T}_{t+h} = \sum_{i=1}^h \phi^i \hat{T}_t. \quad (10)$$

- Local polynomial smoothing, locally estimated scatterplot smoothing

More flexible smoothing methods based on *moving regression* have been introduced in the literature. These methods decompose the time series into trend and remaining component Z_t , following a scheme alternative to exponential smoothing. In this category, the **local polynomial** (LP) smoothing method fits a polynomial (usually a straight line or parabola) on datapoints within time-windows centered at each time step t (Fan and Gijbels, 1996). A simple or weighted *least squares* method is used for this purpose. Then, the smoothed value at time t equals the value of the corresponding polynomial at that time. The smoothing becomes stronger as the sliding window size increases. By removing the smoothed value from X_t , one obtains the stochastic component $Z_t = X_t - T_t$.

In the same category, the *locally estimated scatterplot smoothing* (LOESS) method introduces robustness to outliers into LP smoothing (Cleveland et al., 2017). This method operates iteratively. At each iteration, a weighted LP smoothing is performed on the raw series (local polynomials are fitted using weighted least-squares), and the weights are corrected as described hereafter.

At iteration n , the weight assignment to datapoints is governed by two aspects: (i) their distances to the datapoint under consideration (the one recorded at time step t); (ii) the residuals of the smoothing achieved at iteration $n - 1$ (that is the difference between each datapoint and its smoothed version calculated at previous iteration). Following (i), close neighbors are assigned large weights. According to (ii), large residuals yield low weights. In this way, outliers characterized by very large residuals are assigned very low weights and will have a negligible effect in the next iteration.

• Parametric modeling of T_t in the additive trend scheme

The previously mentioned methods were designed to estimate the trend, to be further removed from the raw process \mathbf{X} . Alternatively, T_t can be modeled by a parametric function of the time, that is $T_t = F(t; \theta)$, whose parameters θ are usually estimated by the *least squares* method. However, in the overwhelming majority of time series, the trend model is unknown, which impedes the wide application of such parametric methods.

• Transformation of X_t in the additive trend scheme

In the above presented methods, the trend is either estimated or modeled, to be further removed from the raw process \mathbf{X} . An alternative is to transform \mathbf{X} through **differentiation**. Differentiation is an iterative process that ends up removing T_t from the raw series. However, this method is suitable when the trend is regular and has a slow variation (as for polynomial functions). The differentiation operator is described as follows:

$$\begin{aligned} \Delta^1 X_t &= \Delta X_t = (1 - L)X_t, \\ \Delta^k X_t &= \Delta^{k-1}(\Delta X_t) = (1 - L)^k X_t, \end{aligned} \quad (11)$$

where ΔX_t is the first-order difference of X_t , $\Delta^k X_t$ the k^{th} order difference and L the backward shift operator with $LX_t = X_{t-1}$ and $L^j X_t = X_{t-j}$.

In practice, successive differentiations are performed until a series without trend is obtained. \mathbf{X} is said to be integrated to order k if it becomes stationary after the k^{th} application of first-order differentiation operator. Moreover, the removed trend T_t is a k -degree polynomial function. X_t can be recovered from $\Delta^k X_t$ and $\{X_{t-j}\}_{j=1}^k$ by inverse differencing using binomial expansion of $(1 - L)^k$:

$$\begin{aligned}\Delta^k X_t &= (1 - L)^k X_t = \left[\sum_{j=0}^k \binom{k}{j} (-1)^j L^j \right] X_t \\ \implies X_t &= \Delta^k X_t - \sum_{j=1}^k \binom{k}{j} (-1)^j X_{t-j}.\end{aligned}\tag{12}$$

The most popular additive trend-based model that uses differentiation is the ARIMA (Autoregressive Integrated Moving Average) model (Usman et al., 2019; Nyoni, 2019). This model will be presented in Subsection 4.4.1.

3.2.2 Additive Seasonality Scheme: $\mu(t) = S_t$

In time series analysis, a seasonal phenomenon is characterized by variations that repeat after a fixed duration m called period. As with additive trend, S_t can be estimated, or directly removed from \mathbf{X} .

• Estimation of S_t in the additive seasonal scheme

Pegels (1969) proposed an exponential smoothing method that copes with additive seasonal effect. The estimates are calculated as follows:

$$\begin{aligned}\tilde{X}_t &= \alpha(X_t + \hat{S}_{t-m}) + (1 - \alpha)\tilde{X}_{t-1}, \\ \hat{S}_t &= \gamma(\tilde{X}_t - X_t) + (1 - \gamma)\hat{S}_{t-m},\end{aligned}\tag{13}$$

with \tilde{X}_t the smoothed series, \hat{S}_t the m -periodic seasonal component estimate, α and γ the smoothing parameters comprised between 0 and 1.

At period $t + h, h > 0$, the seasonal effect is computed by periodicity, that is $\hat{S}_{t+h} = \hat{S}_{t+h-m}$.

• Parametric modeling of S_t in the additive seasonal scheme

In a parametric setting, S_t can be modeled by an m -periodic parametric function (trigonometric polynomial function), $S_t = G(t; \theta)$, whose parameters are estimated by *least squares*.

• Transformation of S_t in the additive seasonal scheme

If S_t is an m -seasonal component, it can be removed from X_t by successive m -order differentiations. This operation is called seasonal differentiation and is defined as follows:

$$\Delta_m X_t = \Delta_m^1 X_t = X_t - X_{t-m}, \quad \Delta_m^k X_t = \Delta_m(\Delta_m^{k-1} X_t).\tag{14}$$

3.2.3 Additive Trend and Seasonality Scheme: $\mu(t) = T_t + S_t$

In this decomposition scheme, one has to correct for both additive trend and seasonality. Hereafter we present four categories of methods.

- *Sequential correction*

S_t and T_t can be removed from the original time series one after another: a first correction is made with respect to the seasonal component S_t ; then T_t is removed. This procedure is implemented by the specific case SARIMA($p, d, q, P = 0, D, Q = 0$) of the Seasonal Autoregressive Integrated Moving Average model (Samal et al., 2019; Valipour, 2015; Martinez et al., 2011). In this specific case, d denotes the number of classical differentiations (equation 11, Subsection 3.2.1) and D is the number of seasonal differentiations (equation 14, Subsection 3.2.2). The SARIMA model will be depicted in Section 4.4.2.

- Simultaneous correction in additive Holt-Winters method

In contrast to the previous case, the *additive Holt-Winters method* performs the two corrections simultaneously, using triple exponential smoothing (Aryee et al., 2019). This extension of the standard *Holt additive trend* method was specifically designed to cope with additive seasonal components. Herein, three *exponential smoothing* processes are interwoven, that respectively smooth the series level (\tilde{X}_t), the trend and the seasonal components. To note, this method only supports increasing or decreasing trends. This method involves the three equations below:

$$\begin{aligned}\tilde{X}_t &= \alpha(X_t - \hat{S}_{t-m}) + (1 - \alpha)(\tilde{X}_{t-1} + \hat{T}_{t-1}), \\ \hat{T}_t &= \beta(\tilde{X}_t - \tilde{X}_{t-1}) + (1 - \beta)\hat{T}_{t-1}, \\ \hat{S}_t &= \gamma(\tilde{X}_t - X_t) + (1 - \gamma)\hat{S}_{t-m},\end{aligned}\tag{15}$$

with \tilde{X}_t the smoothed series, \hat{T}_t the trend estimate, \hat{S}_t the m -periodic seasonal component estimate, α, β and γ the smoothing parameters comprised between 0 and 1.

At horizon $h > 0$, the trend is extrapolated and the seasonal effect is computed by periodicity:

$$\hat{T}_{t+h} = h \hat{T}_t, \quad \hat{S}_{t+h} = \hat{S}_{t+h-m}.\tag{16}$$

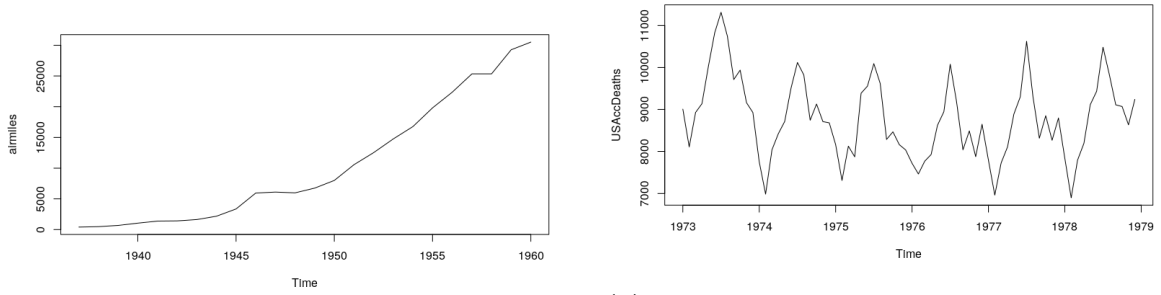
- Decomposition dedicated to quarterly and monthly data

X11 and **SEATs** (**Seasonal Extraction in ARIMA Time Series**) are two popular methods that are limited to decomposing quarterly and monthly data. The reader interested in these specific methods is referred to (Dagum and Bianconcini, 2016). To note, X11 can handle both additive and multiplicative decompositions (see Subsection 3.3).

- Flexible Seasonal Trend decomposition using Loess

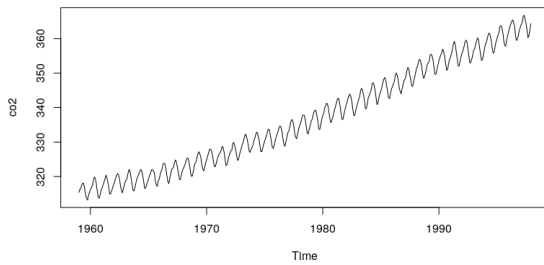
In contrast to the above mentioned X11 and SEATs methods, Seasonal Trend decomposition using Loess (STL) is one of the most widely used decomposition methods that can accommodate whatever trend and whatever periodicity (Cleveland et al., 1990; Bergmeir et al., 2016). Thus daily, weekly, monthly, yearly, etc time series may be processed.

The STL iterative procedure essentially relies on LOESS smoothing (previously introduced). STL decomposition runs two embedded loops: (i) the inner loop iterates a user-specified number of iterations in which seasonal smoothing followed by trend smoothing respectively update the seasonal and trend components; (ii) in each outer loop iteration, a complete run of the inner loop is followed by the computation of robustness weights: for any datapoint, the neighborhood weight used throughout whole $(k + 1)^{th}$ run of inner loop is that of k^{th} run multiplied by the robustness weight. These robustness weights are used to control for aberrant behavior. We now briefly describe an inner loop iteration. At iteration k , the detrended series $X_t - T_t^{(k)}$ is first obtained. Cycle-subseries are distinguished (for example, in a monthly series with a yearly periodicity, cycle-subseries are the series related to January observations, February observations, etc.). Each subseries of the detrended series is then smoothed using LOESS. The collection of all smoothed cycle-subseries values, $\{C_t^{(k+1)}\}$, is obtained. A succession of moving average steps followed by LOESS is applied to $\{C_t^{(k+1)}\}$, to obtain $\{L_t^{(k+1)}\}$. The seasonal

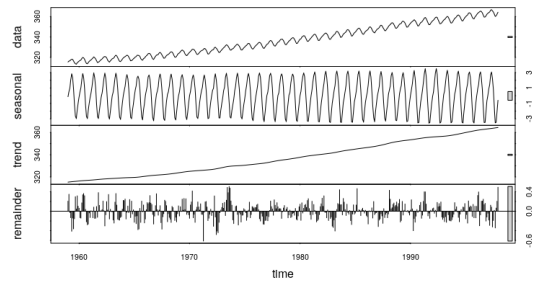


(a) Nonstationary mean with exponentially increasing trend. Revenue passenger miles flown by commercial airlines in the United States.

(b) Nonstationary mean with additive seasonality. Monthly totals of accidental deaths in the United States.



(c) Nonstationary mean with additive trend and seasonality. Mauna Loa (Hawaii) atmospheric concentration of CO_2 , expressed in parts per million (ppm); monthly observation from 1959 to 1997.



(d) Seasonal Trend Decomposition (STL) of time series shown in (c).

Figure 4 Illustration of nonstationary-mean real-life time series and of additive decomposition.

component obtained at $(k + 1)^{th}$ iteration is then computed as follows: $\{S_t^{(k+1)}\} = \{C_t^{(k+1)}\} - L_t^{(k+1)}$. Finally, trend smoothing is applied on the deseasonalized series $X_t - \{S_t^{(k+1)}\}$, using LOESS. These smoothed values constitute the trend component at $(k + 1)^{th}$ iteration.

Figures 4c and 4d show the STL decomposition of "Mauna Loa" volcano CO_2 concentration time series.

3.3 Multiplicative Decomposition - Nonstationary Variance

\mathbf{X} is a nonstationary variance process if its variance is time-dependent, that is $\text{Var}(X_t) = \sigma^2(t)$. This situation is modeled as follows:

$$X_t = \sigma(t) \times Z_t, \quad (17)$$

where Z_t is the remaining stochastic component which is assumed to be stationary, and has a zero mean and a unit variance.

As for the $\mu(t)$ component in additive decomposition, three schemes may be described. $\sigma(t)$ is generally either a trend T_t (**multiplicative trend**) or a seasonal phenomenon S_t (**multiplicative seasonality**), or any combination of both (**multiplicative trend and seasonality**). Multiplicative seasonality is

illustrated with the following example: if in the summer months, 1,000 more property transactions are performed than in the winter months, the seasonality is additive. In contrast, multiplicative seasonality corresponds to the situation where 10% more transactions are performed in summer months than in winter months. In the multiplicative trend and seasonality case, a classical model consists in considering the product $T_t \times S_t$. In other words, under the additive (respectively multiplicative) seasonality assumption, the amplitude of the seasonal pattern does not depend (respectively depends) on the level of the series. Again, as for additive decomposition, the $\sigma(t)$ component in multiplicative decomposition can be estimated, then removed (in this case, $\hat{Z}_t = \frac{X_t}{\hat{\sigma}_t}$), or $\sigma(t)$ can be directly extracted from \mathbf{X} by transformation.

• **Estimation of σ_t in the multiplicative scheme**

Multiplicative trend, multiplicative seasonality and multiplicative trend and seasonality schemes are described in the comprehensive presentation of all nine combinations of trend and seasonal effects in additive form, multiplicative form or absence of effect, reported in (Pegels, 1969). Exponential smoothing methods were customized to deal with these three schemes:

$$\tilde{X}_t = \alpha X_t + (1 - \alpha)\tilde{X}_{t-1} \hat{T}_{t-1} \quad (\text{multiplicative trend}), \quad (18)$$

$$\tilde{X}_t = \alpha \frac{X_t}{\hat{S}_{t-m}} + (1 - \alpha)\tilde{X}_{t-1} \quad (\text{multiplicative seasonality}), \quad (19)$$

$$\tilde{X}_t = \alpha \frac{X_t}{\hat{S}_{t-m}} + (1 - \alpha)\tilde{X}_{t-1} \hat{T}_{t-1} \quad (\text{multiplicative trend and seasonality}), \quad (20)$$

where \tilde{X}_t is the smoothed series, \hat{T}_t the trend estimate, \hat{S}_t the m -periodic seasonal component estimate, α is a smoothing parameter taking its value within $[0, 1]$, and the multiplicative trend and seasonal components are derived from the formulas below:

$$\hat{T}_t = \beta \frac{\tilde{X}_t}{\tilde{X}_{t-1}} + (1 - \beta)\hat{T}_{t-1}, \quad (21)$$

$$\hat{S}_t = \gamma \frac{X_t}{\tilde{X}_t} + (1 - \gamma)\hat{S}_{t-m}, \quad (22)$$

with β and γ smoothing parameters taking their values in $[0, 1]$, and specified initial values $\tilde{X}_1, \hat{T}_1, \hat{S}_1, \dots, \hat{S}_m$.

At horizon $h > 0$, depending on the decomposition scheme, the trend is extrapolated and the seasonal effect is computed by periodicity:

$$\hat{T}_{t+h} = (\hat{T}_t)^h \quad (23)$$

$$\hat{S}_{t+h} = \hat{S}_{t+h-m}. \quad (24)$$

The multiplicative trend assumption involves equations (18) and (21), the multiplicative seasonality assumption relies on equations (19) and (22), whereas the multiplicative trend and seasonal hypothesis builds on equations (20), (21) and (22).

Pegels suggests that a multiplicative trend "appears more probable in real-life applications" than an additive trend. However, additive trend is most used in practice. The reason lies in that the additive trend scheme yields a more conservative trend extrapolation (that is a linear extrapolation, in contrast

to an exponential extrapolation for the multiplicative trend). Therefore, the additive trend assumption may be more robust when applied to a large variety of time series data. Following this observation, [Taylor \(2003a\)](#) proposed a damped version of Pegels multiplicative trend model, in which the trend projection is damped by an extra parameter, in an analogous fashion to the damped Holt additive trend model (equation 9). This model is defined below:

$$\begin{aligned}\tilde{X}_t &= \alpha X_t + (1 - \alpha)\tilde{X}_{t-1}\hat{T}_{t-1}^\phi, \\ \hat{T}_t &= \beta \frac{\tilde{X}_t}{\tilde{X}_{t-1}} + (1 - \beta)\hat{T}_{t-1}^\phi,\end{aligned}\tag{25}$$

where \tilde{X}_t , \hat{T}_t , α and β have the same meaning as previously.

At horizon $h > 0$, we obtain:

$$\hat{T}_{t+h} = \hat{T}_t^{\sum_{i=1}^h \phi^i}.\tag{26}$$

If $\phi = 1$, we obtain the Pegels multiplicative trend model (equations 18 and 21). If $\phi = 0$, the method is identical to simple exponential smoothing (equation 8). If $0 < \phi < 1$, the multiplicative trend is damped and extrapolations approach an horizontal asymptote given by $\hat{T}_t^{\phi(1-\phi)}$. If $\phi > 1$, the trend extrapolation exponentially increases over time.

Empirical studies on 1,428 time series from various domains pointed out that damped Pegels multiplicative trend outperforms standard Pegels multiplicative trend ([Taylor, 2003a](#)). To note, the same observation is done for damped Holt additive trend and standard Holt additive trend.

• Transformation of X_t in the multiplicative scheme

Log transformations and power transformations may stabilize the variance, prior to the use of an additive model. In the power transformation framework, parameter adjustment motivated multiple works.

- *Logarithmic transformation*

In purely multiplicative decomposition, $\sigma(t) = T_t \times S_t$, the logarithmic transformation results in an additive decomposition (see time series in Figure 5), that is $Y_t = \ln(X_t) = \ln(T_t) + \ln(S_t) + \ln(Z_t)$, which has a constant variance. However, the logarithmic transformation is limited to time series with strictly positive values.

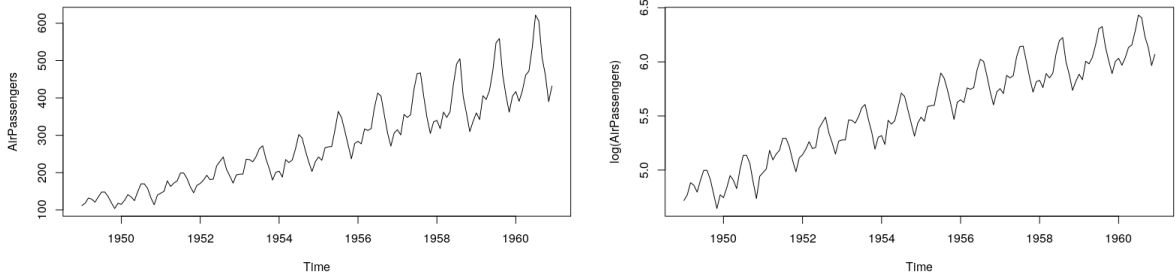
- *Box-Cox parametric power transformations*

Box and Cox proposed parametric power transformations, to stabilize the variance, obtain more linear resulting series, as well as render the data more normal distribution-like ([Box and Cox, 1964](#); [Bergmeir et al., 2016](#)).

We illustrate below this category of transformations with the two following widely-used variants:

$$Y_t = \begin{cases} \frac{X_t^{\lambda_1} - 1}{\lambda_1} & \text{if } \lambda_1 \neq 0 \\ \ln(X_t) & \text{if } \lambda_1 = 0 \end{cases} \quad ; \quad Y_t = \begin{cases} \frac{(X_t + \lambda_2)^{\lambda_1} - 1}{\lambda_1} & \text{if } \lambda_1 \neq 0 \\ \ln(X_t + \lambda_2) & \text{if } \lambda_1 = 0 \end{cases}\tag{27}$$

The left transformation is defined for strictly positive processes only, while the right one allows negativity through the appropriate choice of λ_2 's (real) value ($X_t > -\lambda_2$). Parameter λ_1 is real-valued and has to be calibrated. Many extensions of the original Box-Cox transformation have been introduced in the literature, in order to accommodate for such properties as bimodality and asymmetry ([Sakia, 1992](#); [Hossain, 2011](#)).



(a) Initial time series.

(b) Logarithmic decomposition of the time series in (a).

Figure 5 Illustration of logarithmic transformation applied in the purely multiplicative decomposition framework. Monthly airline numbers of passengers from 1949 to 1960 in the United States, in thousands. \mathbf{X} : initial time series. \mathbf{Y} : time series obtained by transformation of \mathbf{X} . (a) Initial real time series \mathbf{X} . In this example, the trend is increasing and a period of 12 seems to exist. (b) Multiplicative decomposition: $X_t = \sigma(t) \times Z_t$. In the purely multiplicative decomposition, $\sigma(t) = T_t \times S_t$. Thus, $Y_t = \ln(X_t) = \ln(T_t) + \ln(S_t) + \ln(Z_t)$, which results in an additive decomposition.

- Parameter adjustment in parametric power transformations

In their seminal paper (1964), Box and Cox proposed maximum likelihood and Bayesian estimates for λ_1 .

Alternatively, the procedure introduced by Guerrero (1993) allows to estimate the λ_1 parameter in equation (27). We now shortly describe the principle underlying this procedure. If \mathcal{T} denotes the power transformation function ($\mathcal{T}(X_t) = Y_t$), and \mathcal{T}' denotes the derivative of \mathcal{T} , the Taylor expansion of $\mathcal{T}(X_t)$ about $\mathbb{E}[X_t]$ yields a linear approximation: $\text{Var}(\mathcal{T}(X_t)) = \mathcal{T}'(\mathbb{E}(X_t))^2 \text{Var}(X_t)$. A variance-stabilizing power transformation for X must then satisfy: $[\text{Var}(X_t)]^{(1/2)}/[\mathbb{E}(X_t)]^{1-\lambda_1} = a$ for some constant $a > 0$. In practice, when only one observation is available at each time step t , it is impossible to estimate the variance. To solve this problem, the time series under consideration can be divided into H subseries; thus, a local estimate of variance and mean can now be computed within each subseries. The objective is then to stabilize the variance between subseries.

Osborne (2010) introduced a graphical protocol, to select λ_1 by hand. This procedure chains four steps: (i) to start with, the time series under consideration is divided into at least 10 subseries; (ii) within each subseries, the mean and standard deviation are estimated; (iii) then, the curve *log(standard deviation) versus log(mean)* is plotted; (iv) λ_1 is estimated as $1 - b$, where b is the slope of the previous curve.

Finally, visual inspection selection procedure is widely used by experienced analysts. It consists in applying power transformation using different values of λ_1 and comparing the plots obtained. The drawbacks of this procedure are its inaccuracy and the subjectivity involved in the visual inspection. Moreover, it can be time-consuming, especially if the tested λ_1 values are arbitrarily chosen.

3.4 Mixed Decomposition - Nonstationary Mean and Variance

To cope with \mathbf{X} 's both nonstationary mean and variance, we can use a model combining additive and multiplicative decompositions:

$$X_t = \mu(t) + \sigma(t) \times Z_t, \quad (28)$$

where Z_t is the remaining stochastic component which is supposed to be stationary and has a zero mean and a unit variance, and where $\mu(t)$ and $\sigma^2(t)$, respectively the mean and variance of X_t , have the same meaning as in previous Subsections 3.2 and 3.3.

To note, the stationary component Z_t can be extracted by successively applying the procedures previously presented for nonstationary mean (Subsection 3.2) and nonstationary variance (Subsection 3.3). On the other hand, further refined models resorting to the mixed decomposition framework were proposed, that exhibit trend and seasonality. In the remainder of this subsection, we mention two of these models.

3.4.1 Additive Trend and Multiplicative Seasonal Component, Multiplicative Holt-Winters:

$$X_t = (T_t + Z_t)S_t$$

In *multiplicative Holt-Winters*, $X_t = (T_t + Z_t)S_t$, that is $\mu(t) = T_t \times S_t$ and $\sigma(t) = S_t$, which means that additive trend and multiplicative seasonal components are considered (Holt, 1957, 2004; Winters, 1960; Aryee et al., 2019). As in *additive Holt-Winters* method (dedicated to additive trend and seasonality, $X_t = (T_t + S_t) + Z_t$), this method performs a triple exponential smoothing defined by the following equations:

$$\begin{aligned}\tilde{X}_t &= \alpha \frac{X_t}{\hat{S}_{t-m}} + (1 - \alpha)(\tilde{X}_{t-1} + \hat{T}_{t-1}), \\ \hat{T}_t &= \beta(\tilde{X}_t - \tilde{X}_{t-1}) + (1 - \beta)\hat{T}_{t-1}, \\ \hat{S}_t &= \gamma \frac{X_t}{\tilde{X}_t} + (1 - \gamma)\hat{S}_{t-m},\end{aligned}\tag{29}$$

with \tilde{X}_t the smoothed series, \hat{T}_t the additive linear trend estimate, \hat{S}_t the multiplicative m -periodic seasonal component estimate, α, β and γ the smoothing parameters chosen from $[0, 1]$.

At period $t + h, h > 0$, the trend is extrapolated and the seasonal component is determined thanks to periodicity:

$$\hat{T}_{t+h} = h \hat{T}_t, \quad \hat{S}_{t+h} = \hat{S}_{t+h-m}.\tag{30}$$

3.4.2 Multiplicative Trend and Additive Seasonal Component, Pegels Mixed Model: $X_t = S_t + T_t Z_t$

Not only did Pegels propose multiplicative model schemes. To tackle mixed decomposition, in contrast to multiplicative Holt-Winters, the model introduced in (Pegels, 1969) considers a multiplicative trend and additive seasonal effect. This model also relies on triple exponential smoothing:

$$\begin{aligned}\tilde{X}_t &= \alpha(X_t + \hat{S}_{t-L}) + (1 - \alpha)\tilde{X}_{t-1} \hat{T}_{t-1}, \\ \hat{T}_t &= \beta \frac{\tilde{X}_t}{\tilde{X}_{t-1}} + (1 - \beta)\hat{T}_{t-1}, \\ \hat{S}_t &= \gamma(\tilde{X}_t - X_t) + (1 - \gamma)\hat{S}_{t-m},\end{aligned}\tag{31}$$

with \tilde{X}_t the smoothed series, \hat{T}_t the multiplicative trend estimate, \hat{S}_t the additive m -periodic seasonal component estimate, α, β and γ the smoothing parameters which take values within $[0, 1]$.

At horizon $h > 0$, the trend is extrapolated and the seasonal effect is computed by periodicity:

$$\hat{T}_{t+h} = (\hat{T}_t)^h, \quad \hat{S}_{t+h} = \hat{S}_{t+h-m}.\tag{32}$$

Decomposition	Characteristics	Trend and seasonal components	Models	References			
Additive decomposition $X_t = \mu(t) + Z_t$	nonstationary mean	Additive trend: $\mu(t) = T_t$	differentiation (ARIMA)(p, d, q) ⁽¹⁾	Usman et al. (2019) Nyoni (2019)			
			Damped Holt additive trend method (generalized Holt method)	Taylor (2003a)			
			Holt additive trend method	Holt (2004)			
			Local polynomial smoothing	Fan and Gijbels (1996)			
		Locally estimated scatterplot smoothing (LOESS)	Cleveland et al. (2017)				
		Additive seasonality: $\mu(t) = S_t$	Pegels additive seasonality (double exponential smoothing)	Pegels (1969)			
			m -order differentiation (m : seasonality period)				
		Additive trend and seasonality: $\mu(t) = T_t + S_t$	SARIMA(p, d, q)($P = 0, D, Q = 0$) $_m$ ⁽²⁾ (m : seasonality period)	Samal et al. (2019) Valipour (2015) Martinez et al. (2011)			
			Additive Holt-Winters method	Holt (2004) Aryee et al. (2019)			
			Quarterly and monthly data X11, Seasonal Extraction in ARIMA Time Series (SEATs)	Dagum and Bianconcini (2016)			
Flexible Seasonal Trend decomposition using Loess (STL)	Cleveland et al. (1990) Bergmeir et al. (2016)						
Multiplicative decomposition $X_t = \sigma(t) \times Z_t$	nonstationary variance	Multiplicative trend: $\sigma(t) = T_t$	Damped multiplicative trend model	Taylor (2003a)			
			Multiplicative seasonality: $\sigma(t) = S_t$	Pegels multiplicative models (exponential smoothing)	Pegels (1969)		
		Multiplicative trend and seasonality: $\sigma(t) = T_t \times S_t$ ⁽³⁾ $\sigma(t) = T_t \times S_t$ ⁽⁴⁾ $\sigma(t) = \text{function}(T_t, S_t)$ ⁽⁵⁾				Logarithmic transformation	
						Box-Cox transformations (power transformations)	Box and Cox (1964)
		Mixed decomposition $X_t = \mu(t) + \sigma(t) \times Z_t$	nonstationary mean and variance	Additive trend and multiplicative seasonality: $\mu(t) = T_t \times S_t, \sigma(t) = S_t$ $X_t = (T_t + Z_t) S_t$	Multiplicative Holt-Winters method	Holt (1957, 2004) Winters (1960) Aryee et al. (2019)	
Multiplicative trend and additive seasonality: $\mu(t) = S_t, \sigma(t) = T_t$ $X_t = S_t + T_t Z_t$	Pegels mixed model (triple exponential smoothing)			Pegels (1969)			

Table 2 Time series decomposition and examples of corresponding models. X_t : initial time series. Z_t : the remaining component assumed to be stationary, with a zero mean and a unit variance. On the one hand, X_t can be characterized through its moments: $\mu(t)$ (mean), $\sigma(t)$ (variance). On the other hand, in the decomposition scheme, X_t can be characterized as the combination of a trend T_t , a seasonality S_t and Z_t . ⁽¹⁾ ARIMA(p, d, q) is described in Subsection 4.4.1. ⁽²⁾ SARIMA(p, d, q)($P = 0, D, Q = 0$) $_m$ is a specific instantiation of the SARIMA model (Subsection 4.4.2 ; Table 5) for which the seasonal component reduces to D m -order differentiations, with m the seasonality period. ⁽³⁾ Pegels multiplicative models. ⁽⁴⁾ Logarithmic transformation. ⁽⁵⁾ Box-Cox transformations.

3.5 Recapitulation for Time Series Decomposition models

Table 2 provides a quick overview of the main categories of approaches dedicated to time series decomposition.

3.6 Time Series Decomposition and Prediction

Except for exponential smoothing-based decomposition methods, the aim of time series decomposition is to filter out the deterministic features from a raw time series, and capture the remaining stochastic component. The latter is expected to show no apparent trend and seasonal variations. One step further

this preprocessing task, modeling this remaining stochastic component is the basis to design a forecasting procedure. To achieve this aim, one attempts to fit some model on \mathbf{Z} : linear and nonlinear models will be presented in Sections 4 and 5. Taking into account \mathbf{Z} 's autocorrelation structure, when it exists, allows to increase prediction accuracy for the initial time series \mathbf{X} . Autocorrelation, the key to forecasting, is captured in such linear and nonlinear models through the modeling of the conditional mean and conditional variance. These latter notions will be detailed in Sections 4 and 5. To note, the autocorrelation function is known for simple linear models, whereas it is very complicated to derive it for nonlinear models. The **Ljung-Box statistical test** allows to assess the absence of *residual* autocorrelation at lag $r \geq 1$, relying on the squared sample autocorrelation function (Ljung and Box, 1978). When this test is applied to residuals obtained from some fitted model, it allows to determine whether the model has captured the dependencies within the data. One expects that the more dependencies the model has captured, the more accurate the prediction relying on this model will be.

In contrast, the autocorrelation in the initial time series is implicitly modeled in exponential smoothing-based decomposition methods. Indeed, the very aim of these specific decomposition methods is prediction. Therefore, the two next subsections will describe prediction in general when \mathbf{Z} has been isolated by decomposition, and prediction in the specific case of exponential smoothing-based decomposition.

3.6.1 Prediction Focused on Isolated Stochastic Component

If autocorrelation can be assessed and modeled for the process \mathbf{Z} , the forecast for \mathbf{X} at period $h > 0$, denoted by \hat{X}_{t+h} , depends on the decomposition method used. If a transformation was used for multiplicative decomposition, \hat{X}_{t+h} is computed from \hat{Z}_{t+h} through inverse transformation: in a nutshell, the prediction is made for the transformed series (\mathbf{Z}); then the inverse transformation yields the prediction for the initial series; in this case, $\mu(t)$ and $\sigma(t)$ are directly filtered out from the original series. Apart from this specific transformation case, the deterministic components $\mu(t)$ and $\sigma(t)$ are estimated and \hat{X}_{t+h} is obtained as a function of $\hat{\mu}(t+h)$ estimate, $\hat{\sigma}(t+h)$ estimate and \hat{Z}_{t+h} forecast, following the decomposition scheme.

When the process \mathbf{Z} is stationary, the relationship existing between X_t and its lagged values is time-invariant, which simplifies the prediction. Nonetheless, nonstationary autocorrelation can exist indeed. For example, conditions guaranteeing stationarity have been established for the linear autoregressive model and the nonlinear GARCH model presented in Subsections 4.1 and 5.5 respectively.

In the context of power-transformed time series (Box-Cox transformation, equation 27, Subsection 3.3), it has been shown that the forecasts obtained for the transformed series become biased after the inverse transformation has been applied. The reason lies in the difference in scales between transformed and initial time series. Methods devoted to correct the resulting bias have been proposed in the literature (Guerrero, 1993).

3.6.2 Prediction in the Case of Exponential Smoothing-based Decomposition

In the decomposition framework, exponential smoothing-based methods hold a place apart. Indeed, no attention is paid therein to capture a remaining stochastic component. The reason lies in that these methods were designed for a prediction purpose, from the outset. Therefore, autocorrelation is implicitly acknowledged in \mathbf{X} 's modeling: applying exponential smoothing amounts to use an autoregressive model (see Subsection 4.1) in which the coefficients decrease exponentially with time.

To note, exponential smoothing parameters can be chosen by minimizing the mean squared ahead-forecast errors (Gelper et al., 2010). The same procedure can be used in order to select the *damping parameter* in generalized Holt method and damped multiplicative trend model (Taylor, 2003a). On the other hand, initial values for the smoothed level, trend and seasonal components must also be chosen. To

this end, methods respectively based on linear regression, averaging and maximum likelihood have been described in the literature (Gardner Jr and Everette, 2006). It is important to note that the smaller the smoothing parameters, the more sensitive forecasts will be to the initial values (since a strong weight is attributed to past values).

Table 3 summarizes forecasting functions for the exponential smoothing-based methods introduced in Subsections 3.2 to 3.4.

If a significant autocorrelation is found in the residuals of an exponential smoothing method, defined by $\epsilon_t = X_t - \hat{X}_t$ (\hat{X}_t is computed using Table 3: $\hat{X}_t = \hat{X}_{(t-1)+h}$ with $h = 1$), this indicates that the corresponding forecasts are suboptimal. In this case, prediction accuracy can be improved by adjusting a zero-mean first-order autoregressive AR(1) model (see Subsection 4.1) to the terms ϵ_t 's (Gardner Jr, 1985; Taylor, 2003b). Thus, at period h , the forecasts provided in Table 3 are modified by adding the term $(\phi_1)^h \epsilon_t$ where ϕ_1 is the autoregressive coefficient of the AR(1) model.

Model	Decomposition	Trend \hat{T}_{t+h}	Seasonality \hat{S}_{t+h}	Forecast \hat{X}_{t+h}
Damped Holt additive trend	$X_t = T_t + Z_t$	$\sum_{i=1}^h \phi^i \hat{T}_t$	-	$\hat{X}_t + \hat{T}_{t+h}$
Pegels additive seasonality	$X_t = S_t + Z_t$	-	\hat{S}_{t+h-m}	$\hat{X}_t + \hat{S}_{t+h}$
Additive Holt-Winters	$X_t = T_t + S_t + Z_t$	$h \hat{T}_t$	\hat{S}_{t+h-m}	$\hat{X}_t + \hat{T}_{t+h} + \hat{S}_{t+h}$
Taylor damped multiplicative trend	$X_t = T_t Z_t$	$\hat{T}_t \sum_{i=1}^h \phi^i$	-	$\hat{X}_t \hat{T}_{t+h}$
Pegels multiplicative seasonality	$X_t = S_t Z_t$	-	\hat{S}_{t+h-m}	$\hat{X}_t \hat{S}_{t+h}$
Pegels multiplicative trend and seasonality	$X_t = T_t S_t Z_t$	$(\hat{T}_t)^h$	\hat{S}_{t+h-m}	$\hat{X}_t \hat{T}_{t+h} \hat{S}_{t+h}$
Multiplicative Holt-Winters	$X_t = (T_t + Z_t) S_t$	$h \hat{T}_t$	\hat{S}_{t+h-m}	$(\hat{X}_t + \hat{T}_{t+h}) \hat{S}_{t+h}$
Pegels mixed model	$X_t = S_t + T_t Z_t$	$(\hat{T}_t)^h$	\hat{S}_{t+h-m}	$\hat{X}_t \hat{T}_{t+h} + \hat{S}_{t+h}$

Table 3 Forecasting function for methods based on exponential smoothing.

4 Linear Time Series Models

As seen in section 3, time series are generally decomposed into trend and seasonal effects, and a remaining stochastic component, following a decomposition model: additive, multiplicative, or mixed (equations 6, 17, 28, respectively). In this section, we will focus on how the remaining stochastic component denoted by $\mathbf{Z} = \{Z_t\}_{t=1}^{\infty}$ can be modeled in order to make accurate predictions on Z_t . This prediction task requires the modeling of the relationship between past and future values of \mathbf{Z} :

$$Z_t = f(Z_{t-1}, Z_{t-2}, \dots) + g(Z_{t-1}, Z_{t-2}, \dots) \epsilon_t, \quad (33)$$

where ϵ_t 's are i.i.d.(0, 1) white noise processes, f and g^2 are respectively the conditional mean and conditional variance of Z_t , that is $Z_t | Z_{t-1}, Z_{t-2}, \dots \sim \mathcal{D}(f, g^2)$ with \mathcal{D} the law of residuals. Given information from the past, f is the optimal forecast of Z_t and g^2 is the forecast variance. This yields a forecast interval $[f - g, f + g]$.

f and g can be modeled in a nonparametric way. This approach is outside the scope of the present survey. Further details can be found in the interesting review of nonparametric time series models presented in Härdle et al. (1997). The present survey will focus on the parametric modeling of f and g .

When f and g are linear, that is when the relationship between Z_t and its past values is linear, the model is said to be **linear**. Otherwise, the model is said to be **nonlinear** (see Section 5). Linear time series models have been widely studied and applied in the literature (Ge and Kerrigan, 2016; Gomes and Castro, 2012) because of their simplicity and strong theoretical foundation. These models rely on

the stationarity hypothesis. As already highlighted in Subsection 3.1, a relationship exists between stationarity and linearity: Wold's theorem (1938) shows that every stationary process can be represented as an infinite weighted sum of error terms.

The most popular linear models dedicated to time series analysis are presented in the remainder of this section: linear autoregressive (AR), moving average (MA) and autoregressive moving average (ARMA). These models differ from each other in the design of the conditional mean f . In contrast, they all assume a constant conditional variance g^2 . These models are mainly analyzed under three aspects: autocorrelation function structure, model fitting methods and forecasting procedure. In the last subsection, ARMA-based models such as ARIMA and SARIMA (autoregressive integrated moving average and seasonal ARIMA, respectively) are briefly introduced. For presentation convenience, the SARIMA variant is mentioned in the same Section as ARMA, but it should be highlighted that SARIMA is not a linear model.

4.1 Linear Autoregressive Model - AR(p)

The linear autoregressive model has been introduced in the seminal paper of Yule in 1927. It is a regression model in which regressors are the p lagged values of the response variable Z_t , where p is called AR process order. The AR process is described as:

$$Z_t = \phi_0 + \sum_{i=1}^p \phi_i Z_{t-i} + \sigma \epsilon_t, \quad (34)$$

where the terms ϵ_t are i.i.d.(0,1) white noise processes (usually, gaussian white noise is used), p is a hyper-parameter to be fixed and $\{\phi_0, \phi_1, \dots, \phi_p, \sigma^2\}$ are the model parameters.

The AR framework models the conditional mean f of Z_t given its past values as a linear regression of its p past values, whereas its conditional variance g^2 is constant and equal to σ^2 .

It has to be noted that Z_t is independent of future error terms $\{\epsilon_{t'}, t' > t\}$ and is correlated to past ones $\{\epsilon_{t'}, t' < t\}$ through its past values. For instance, in the AR(1) model, Z_t depends on Z_{t-1} , which itself depends on ϵ_{t-1} and Z_{t-2} , which depends on ϵ_{t-2} and Z_{t-3} and so on. In the end, Z_t depends of all past error terms. This is the substantial difference between AR and **moving average** processes introduced in Subsection 4.2.

4.1.1 Autocovariance Function

AR process first and second order moments write:

$$\mathbb{E}[Z_t] = \phi_0 + \sum_{i=1}^p \phi_i \mathbb{E}[Z_{t-i}] \implies \mathbb{E}[Z_t] = \frac{\phi_0}{1 - \sum_{i=1}^p \phi_i}, \quad (35)$$

$$\gamma(h) = \text{Cov}(Z_t, Z_{t+h}) = \text{Cov}(Z_t, \sum_{i=1}^p \phi_i Z_{t+h-i} + \sigma \epsilon_{t+h}) = \sum_{i=1}^p \phi_i \gamma(h-i), \quad h = 0, 1, 2, \dots \quad (36)$$

Note that if ϕ_0 is null, then \mathbf{Z} is a zero-mean process. Moreover, an AR process has a finite mean if and only if $\sum_{i=1}^p \phi_i \neq 1$.

When an AR process is stationary, its autocovariance function $\gamma(h)$ has an infinite scope with an exponential decay, that is Z_t is more correlated to nearby values in time than high-order lagged values. Let us show this result for the AR(1) process. It is straightforward to show that $\gamma(h) = \gamma(0) (\phi_1)^h$. Following the stationarity property (equation 3, Subsection 2.1.2), $\gamma(h)$ should go to zero when h

goes to infinity, which means $|\phi_1| < 1$. This result can be generalized to the AR(p) model, that is $|\phi_i| < 1$, $i = 1, \dots, p$.

4.1.2 Partial Autocorrelation Function

The definition of the autocorrelation function was provided in equation 4 (Subsection 2.2.1). The partial autocorrelation (PAC) function at lag h is the autocorrelation between Z_t and Z_{t+h} in which the dependencies of Z_t on Z_{t+1} through Z_{t+h-1} have been removed. Mathematically, PAC does not supply any new information on the studied process. In practice, a PAC plot is commonly used to identify the order of the AR process since the partial autocorrelation of an AR(p) process is null from lag $p + 1$. Estimation based on sample PAC is sensitive to outliers (see for instance Maronna, Martin, and Yohai (2006), pp. 247–257). Several robust algorithms are reviewed in Dürre et al. (2015).

4.1.3 Parameter Learning Algorithms

An AR(p) model has $p + 2$ parameters, $\phi = \{\phi_0, \phi_1, \dots, \phi_p\}$ and σ^2 , which have to be estimated from observations $\{z_t\}_{t=1}^T$. To this end, the following methods can be used:

Maximum likelihood The conditional likelihood function \mathcal{L}_c of a p -order autoregressive model is the probability of observing sample $\{z_t\}_{t=p}^T$ knowing the first p values and parameters (ϕ, σ^2) . It writes as follows:

$$\mathcal{L}_c(\phi, \sigma^2) = P(Z_p^T = z_p^T | Z_1^p = z_1^p; \phi, \sigma^2) = \prod_{t=p}^T P(Z_t = z_t | Z_{t-1}^{t-p} = z_{t-1}^{t-p}; \phi, \sigma^2), \quad (37)$$

where $Z_t^{t'} = (Z_t, \dots, Z_{t'})$, with $t \leq t'$, and the conditional probability $P(Z_t = z_t | Z_{t-1}^{t-p} = z_{t-1}^{t-p}; \phi, \sigma^2)$ is given by the law of residuals ϵ_t via equation (34). For instance, when a gaussian white noise is considered, the conditional probability is gaussian too, with mean $\phi_0 + \sum_{i=1}^p \phi_i z_{t-i}$ and variance σ^2 .

A maximum likelihood estimator is obtained by maximizing the logarithm of \mathcal{L}_c with respect to parameters (ϕ, σ^2) . This maximization is generally driven numerically, but, in the case of a gaussian white noise, analytical expressions can be derived.

Ordinary least squares (OLS) AR(p) parameters can be estimated by the least squares method:

$$\hat{\phi}_{LS} = (D^t D)^{-1} Z D, \quad (38)$$

where $D = \{D_{i,j} = z_{i-j}\}_{i=p+1, \dots, T, j=1, \dots, p}$ is the $(T-p) \times p$ design matrix. Computing the OLS estimator requires a $p \times p$ matrix inversion at the cost of $\mathcal{O}(p^3)$. However, if $D^t D$ is singular, pseudo-inverse methods can be considered at the price of poor precision.

Method of moments This method chains three steps: (i) establish a relationship between the moments of Z_t and the model parameters, (ii) estimate these moments empirically, and (iii) solve the equation obtained via (i) with the estimates obtained through (ii). Equation (36) establishes a relationship between the autocovariance function of Z_t and parameters ϕ . After dividing by $\text{Var}(Z_t)$ in (36), we obtain the same relationship in which autocovariance function γ has been replaced with autocorrelation function ρ :

$$\rho(h) = \sum_{i=1}^p \phi_i \rho(h-i), \quad h = 0, 1, 2, \dots \quad (39)$$

The matricial reformulation of equation (39) yields:

$$\rho = R \phi \quad \text{with} \quad \rho = (\rho(1), \dots, \rho(p))^t, \quad R = \{R_{i,j} = \rho(i-j)\}_{i,j=1,\dots,p}, \quad (40)$$

where ρ is a column vector and R is a $p \times p$ symmetric, semi-definite positive matrix. Equation (40) is referred to as the **Yule-Walker** equation.

Once ρ and R have been estimated from sample autocorrelations, Yule-Walker equation can be solved either by matrix inversion ($\hat{\phi}_{YW} = \hat{R}^{-1}\hat{\rho}$) at the cost of $\mathcal{O}(p^3)$ operations, or using **Levinson-Durbin algorithm** (Durbin, 1960) that requires a number of operations proportional to p^2 only. The latter method is an iterative procedure that solves a series of AR(p') truncated problems, with $0 \leq p' \leq p$. At each step, the size of the problem p' is incremented.

4.1.4 Forecasting

Once the AR model parameters have been estimated using observations $\{Z_t = z_t\}_{t=1}^T$, one-step ahead prevision is done as follows:

$$\hat{Z}_{T+1} = \hat{\phi}_0 + \sum_{i=1}^p \hat{\phi}_i Z_{T+1-i}, \quad (41)$$

where $\{\hat{\phi}_0, \hat{\phi}_1, \dots, \hat{\phi}_p\}$ are autoregressive coefficient estimates.

When performing h -step ahead previsions ($h > 1$), previous forecasts are used as predictors. For instance, in an AR(2) process, 3-step ahead prevision writes:

$$\begin{aligned} \hat{Z}_{T+1} &= \hat{\phi}_0 + \hat{\phi}_1 Z_T + \hat{\phi}_2 Z_{T-1}, \\ \hat{Z}_{T+2} &= \hat{\phi}_0 + \hat{\phi}_1 \hat{Z}_{T+1} + \hat{\phi}_2 Z_T, \\ \hat{Z}_{T+3} &= \hat{\phi}_0 + \hat{\phi}_1 \hat{Z}_{T+2} + \hat{\phi}_2 \hat{Z}_{T+1}, \end{aligned}$$

where the unobserved terms Z_{T+1} and Z_{T+2} have been substituted with their predictions \hat{Z}_{T+1} and \hat{Z}_{T+2} . It can be shown that these substitutions increase the variance of forecast errors. Following the previous example, the forecast errors write:

$$\begin{aligned} Z_{T+1} - \hat{Z}_{T+1} &= \epsilon_{T+1}, \\ Z_{T+2} - \hat{Z}_{T+2} &= \epsilon_{T+2} + \hat{\phi}_1(Z_{T+1} - \hat{Z}_{T+1}) = \epsilon_{T+2} + \hat{\phi}_1 \epsilon_{T+1}, \\ Z_{T+3} - \hat{Z}_{T+3} &= \epsilon_{T+3} + \hat{\phi}_1(Z_{T+2} - \hat{Z}_{T+2}) + \hat{\phi}_2(Z_{T+1} - \hat{Z}_{T+1}) = \epsilon_{T+3} + \hat{\phi}_1 \epsilon_{T+2} + (\hat{\phi}_1^2 + \hat{\phi}_2) \epsilon_{T+1}. \end{aligned}$$

As ϵ_t 's are i.i.d.(0, $\hat{\sigma}^2$), the means of forecast errors are equal to zero and their variances write:

$$\begin{aligned} \text{Var}(Z_{T+1} - \hat{Z}_{T+1}) &= \hat{\sigma}^2, \\ \text{Var}(Z_{T+2} - \hat{Z}_{T+2}) &= \hat{\sigma}^2(1 + \hat{\phi}_1^2), \\ \text{Var}(Z_{T+3} - \hat{Z}_{T+3}) &= \hat{\sigma}^2(1 + \hat{\phi}_1^2 + (\hat{\phi}_1^2 + \hat{\phi}_2)^2). \end{aligned}$$

4.2 Moving Average Model - MA(q)

Moving average is a linear regression model in which the regressors are the q prediction error terms. This model is depicted as follows:

$$Z_t = \alpha_0 + \sum_{i=1}^q \alpha_i \epsilon_{t-i} + \epsilon_t, \quad (42)$$

where ϵ_t 's are error terms that are i.i.d. $(0, \sigma^2)$ (usually, the normal law is used), q is the MA process order and $\{\alpha_0, \alpha_1, \alpha_2, \dots, \alpha_q, \sigma^2\}$ are the model parameters.

In the MA model, the conditional mean f of Z_t given its past values is a linear function of the past q prediction errors, whereas its conditional variance g^2 is constant and equal to σ^2 .

4.2.1 Autocovariance Function

An MA process oscillates around a long term equilibrium defined by its mean, where oscillation amplitude depends on error variance σ^2 . Thus, by construction, this process is stationary. Its first and second order moments write:

$$\mathbb{E}[Z_t] = \alpha_0, \quad \text{Var}(Z_t) = \sigma^2 \left(1 + \sum_{i=1}^q \alpha_i^2\right). \quad (43)$$

$$\begin{aligned} \gamma(h) = \text{Cov}(Z_t, Z_{t+h}) &= \mathbb{E} \left[\left(\alpha_0 + \sum_{i=1}^q \alpha_i \epsilon_{t-i} + \epsilon_t \right) \left(\alpha_0 + \sum_{j=1}^q \alpha_j \epsilon_{t+h-j} + \epsilon_{t+h} \right) \right] - \alpha_0^2 \\ &= \begin{cases} \sigma^2 (\alpha_h + \sum_{i=1}^{q-h} \alpha_i \alpha_{i+h}), & 0 \leq h \leq q \\ 0 & h > q. \end{cases} \end{aligned} \quad (44)$$

Note that the autocovariance function $\gamma(h)$ is null from lag $q+1$, that is Z_t and $Z_{t+\tau}$ are uncorrelated for all lags $\tau > q$. This property characterizes the MA process and is used to select hyper-parameter q . Indeed, q is fixed at h value such that $\hat{\gamma}(h+1)$ is null, where $\hat{\gamma}(h)$'s are sample autocovariances.

4.2.2 Infinite Autoregressive Representation

It is well known that the MA(q) process has an infinite autoregressive representation in which the autoregressive coefficients are defined by a recursion scheme (Galbraith and Zinde-Walsh, 1994). This representation is obtained through successive substitutions of the error terms in equation (42):

$$Z_t = \epsilon_t + \sum_{i=1}^{\infty} \phi_i Z_{t-i}, \quad (45)$$

where the coefficients ϕ_i verify the following relation:

$$\begin{aligned} \phi_0 &= \alpha_0 = 0 \\ \phi_1 &= \alpha_1 \\ \phi_2 &= -\alpha_1 \phi_1 + \alpha_2 \\ &\vdots \\ \phi_q &= -\alpha_1 \phi_{q-1} - \alpha_2 \phi_{q-2} - \dots - \alpha_{q-1} \phi_1 + \alpha_q \\ \phi_j &= \sum_{i=1}^q -\alpha_i \phi_{j-i} \quad (j = q+1, \dots), \end{aligned} \quad (46)$$

with $\{\alpha_i\}$ the regression coefficients of the MA process.

In the case when the MA process has a nonzero mean ($\alpha_0 \neq 0$), it can be centered prior using representation (equation 45).

It is important to emphasize that an MA(q) process can be well approximated by a finite autoregressive process of order p , with $p > q$ chosen sufficiently large, if and only if $|\alpha_i| < 1$, $i = 1, \dots, q$ (Durbin, 1959). Indeed, this condition guarantees that the variance of the remaining terms from $p + 1$ goes to zero when p goes to infinity. Therefore, the remaining terms are neglectible for large values of p .

4.2.3 Parameter Learning Algorithms

In the MA(q) process, $q + 2$ parameters $\{\alpha_0, \alpha_1, \alpha_2, \dots, \alpha_q, \sigma^2\}$ have to be estimated from the training dataset $\{z_t\}_{t=1}^T$. In practice, this is a difficult task because of the randomness of the regressors, which are the error terms ϵ_t .

On the one hand, moment estimators have been proven statistically inefficient (Whittle, 1953). On the other hand, even though the likelihood function can be written in terms of the sample covariances (Whittle, 1953), its maximization requires solving a high-order nonlinear equation. Murthy and Kronauer (1973) proposed an approximation method that reduces data storage and computational effort, without substantial loss in the efficiency of the maximum likelihood.

An asymptotically efficient estimation procedure was proposed by Durbin (1959). Durbin's method is one of the most widely used MA fitting techniques. This method relies on the ordinary least squares method (OLS) and implements two steps:

Step 1. Following the infinite autoregressive representation of the moving average model (equation 45), MA(q) is approximated by a p -order autoregressive model, with $p > q$. So, an AR(p) model is fitted to the observations $\{z_t\}$ via an OLS method (equation 38, Subsection 4.1.3). Let $\{\hat{\phi}_i\}_{i=1}^p$ be the OLS estimation of the autoregressive coefficients $\{\phi_i\}_{i=1}^p$.

Step 2. Using the relations (46), a second autoregressive model is formed, in which $\{\hat{\phi}_i\}_{i=1}^p$ are observed data and MA(q) parameters $(\alpha_1, \dots, \alpha_q)$ are coefficients. Then, OLS estimation provides a set of estimates $\{\hat{\alpha}_i\}_{i=1}^q$. Generally, p is set at $2q$ or is selected via Akaike's information criterion (AIC) or Bayesian information criterion (BIC).

In Sandgren et al. (2012), a procedure has been proposed that simplifies Durbin's method by removing its second step. Thus, after the first autoregression fitting (first step of Durbin's method), an estimation of the q moving average parameters is directly computed from the first q relations in (46). This simple estimator appears to outperform Durbin's estimator in small samples and seems more robust to model misspecification (Sandgren et al., 2012).

Finally, it is well known that Durbin's estimator accuracy is degraded when coefficients α_i 's are close to the unit circle (that is when $|\alpha_i| < 1$) for a fixed value of p . In this case, alternative methods with higher performances have been proposed (Sandgren et al., 2012). However, the performance of Durbin's estimator can be improved by increasing the value of p at the cost of a greater computational complexity (Sandgren et al., 2012).

4.2.4 Forecasting

Once MA model parameters have been estimated using observations $\{Z_t = z_t\}_{t=1}^T$, one-step ahead prediction is done as follows:

$$\hat{Z}_{T+1} | \epsilon_{T+1-q}^T = \hat{\alpha}_0 + \sum_{i=1}^q \hat{\alpha}_i \epsilon_{T+1-i}, \quad (47)$$

where $\{\hat{\alpha}_0, \hat{\alpha}_1, \hat{\alpha}_2, \dots, \hat{\alpha}_q, \hat{\sigma}^2\}$ are the parameter estimates and $\epsilon_t = Z_t - \hat{Z}_t$ are the forecast errors.

New predictions are adjusted with respect to the q last forecast errors. Beyond one-step ahead prediction, unknown forecast errors appear in equation (47). For instance, in an MA(2) process, three-step ahead prediction writes:

$$\begin{aligned}\hat{Z}_{T+1} &= \hat{\alpha}_0 + \hat{\alpha}_1 \epsilon_T + \hat{\alpha}_2 \epsilon_{T-1}, \\ \hat{Z}_{T+2} &= \hat{\alpha}_0 + \hat{\alpha}_1 \epsilon_{T+1} + \hat{\alpha}_2 \epsilon_T, \\ \hat{Z}_{T+3} &= \hat{\alpha}_0 + \hat{\alpha}_1 \epsilon_{T+2} + \hat{\alpha}_2 \epsilon_{T+1}.\end{aligned}$$

Since the series has only been observed till time step T , ϵ_{T+1} and ϵ_{T+2} are unknown forecast errors. In multi-step ahead forecasts, the unknown forecast errors are commonly omitted at the price of a variance increase for forecast errors. Thus, the above example yields:

$$\begin{aligned}\hat{Z}_{T+1} &= \hat{\alpha}_0 + \hat{\alpha}_1 \epsilon_T + \hat{\alpha}_2 \epsilon_{T-1} & \text{and} & & Z_{T+1} - \hat{Z}_{T+1} &= \epsilon_{T+1}, \\ \hat{Z}_{T+2} &= \hat{\alpha}_0 + \hat{\alpha}_2 \epsilon_T & & & Z_{T+2} - \hat{Z}_{T+2} &= \epsilon_{T+2} + \hat{\alpha}_1 \epsilon_{T+1}, \\ \hat{Z}_{T+3} &= \hat{\alpha}_0 & & & Z_{T+3} - \hat{Z}_{T+3} &= \epsilon_{T+3} + \hat{\alpha}_1 \epsilon_{T+2} + \hat{\alpha}_2 \epsilon_{T+1}.\end{aligned}$$

As ϵ_t 's are i.i.d.(0, $\hat{\sigma}^2$), the forecast errors have a zero mean and their variances write:

$$\begin{aligned}\text{Var}(Z_{T+1} - \hat{Z}_{T+1}) &= \hat{\sigma}^2. \\ \text{Var}(Z_{T+2} - \hat{Z}_{T+2}) &= \hat{\sigma}^2(1 + \hat{\alpha}_1^2). \\ \text{Var}(Z_{T+3} - \hat{Z}_{T+3}) &= \hat{\sigma}^2(1 + \hat{\alpha}_1^2 + \hat{\alpha}_2^2).\end{aligned}$$

It has to be noticed that the variance of forecast error grows as $\hat{\sigma}^2(1 + \hat{\alpha}_1^2 + \hat{\alpha}_2^2 + \dots)$.

Alternatively, the unknown forecast errors can be simulated as i.i.d.(0, $\hat{\sigma}^2$) processes from the law chosen for error terms.

4.3 Autoregressive Moving Average Model - ARMA(p, q)

Introduced by Box and Jenkins in 1970, the ARMA(p, q) model (also called Box-Jenkins model) is the combination of the autoregressive AR(p) and moving average MA(q) models. The ARMA model is described as below:

$$Z_t = \phi_0 + \sum_{i=1}^p \phi_i Z_{t-i} + \sum_{j=1}^q \alpha_j \epsilon_{t-j} + \epsilon_t, \quad (48)$$

where the ϵ_t 's are error terms that are i.i.d.(0, σ^2) (usually, a normal law is used), (p, q) are hyper-parameters to be fixed and $\{\phi_0, \phi_1, \dots, \phi_p, \alpha_1, \alpha_2, \dots, \alpha_q, \sigma^2\}$ are the model parameters.

When $q = 0$, equation (48) gives an AR(p) process and when $p = 0$, it defines an MA(q) model. We emphasize that the ARMA(p, q) process is stationary if and only if the roots of its AR component are within the unit circle, that is $|\phi_i| < 1$, $i = 1, \dots, p$. If $\phi_0 = 0$, the mean of the ARMA process will be zero.

4.3.1 Autocovariance Function

As seen in Subsection 4.2 (respectively 4.1), the MA(q) model (resp. the AR(p) model) is suited to stationary processes for which the autocovariance function $\gamma(h)$ has a scope q (resp. has an exponential decrease). As a sum of AR(p) and MA(q) processes, ARMA(p, q) model can handle a wider range of autocovariance functions using few parameters. Fitting an AR or MA model to data dynamics

may require a high-order model with many parameters. Mixing AR and MA models allows a more parsimonious description.

It is well known that any stationary ARMA process has an infinite-order moving average MA(∞) representation:

$$Z_t = \phi_0 + \sum_{j=0}^{\infty} \beta_j \epsilon_{t-j} \quad \text{with} \quad \sum_{j=0}^{\infty} |\beta_j| < \infty. \quad (49)$$

Then, the autocovariance function of the ARMA process writes

$$\gamma(h) = \sigma^2 \sum_{j=1}^{\infty} \beta_j \beta_{j+h}. \quad (50)$$

It can be shown that $\gamma(h)$ shows an exponential decrease when h goes to infinity, as for the autocovariance function in AR processes. For instance, in zero-mean ARMA(1, 1) process

$$Z_t = \phi_1 Z_{t-1} + \alpha_1 \epsilon_{t-1} + \epsilon_t,$$

after incorporating $Z_{t-1} = \phi_1 Z_{t-2} + \alpha_1 \epsilon_{t-2} + \epsilon_{t-1}$ into the previous equation, we obtain:

$$Z_t = \phi_1^2 Z_{t-2} + \phi_1 \alpha_1 \epsilon_{t-2} + (\phi_1 + \alpha_1) \epsilon_{t-1} + \epsilon_t.$$

Finally, after substituting all past values Z_{t-2}, Z_{t-3}, \dots , we obtain representation (49), where $\beta_j = \phi_1^{j-1}(\phi_1 + \alpha_1)$ and $\beta_0 = 1$. So, since $|\phi_1| < 1$, $\beta_j \beta_{j+h} = \phi_1^{h+2j-2}(\phi_1 + \alpha_1)^2 \rightarrow 0$ as $h \rightarrow \infty$, whatever the fixed value of j . Therefore, $\gamma(h) \rightarrow 0$ as $h \rightarrow \infty$.

The orders (p, q) of an ARMA process can be chosen relying on the partial auto-correlation function and the autocorrelation function, as is done for AR and MA processes (Box et al., 2015).

4.3.2 Parameter Learning Algorithms

ARMA(p, q) process fitting consists in estimating its parameters $\{\phi_0, \phi_1, \dots, \phi_p, \alpha_1, \alpha_2, \dots, \alpha_q, \sigma^2\}$ from observations $\{z_t\}_{t=1}^T$. In this subsection, some methods proposed in the literature are presented.

In (Jones, 1980), a maximum likelihood estimation of the ARMA model has been proposed in the case of gaussian white noise. This estimation procedure relies on the Markovian representation, an information interface between the future and the past of a discrete-time stochastic process, whose existence was established for ARMA processes (Akaike, 1998). The Markovian representation provides a minimal state-space representation for the recursive calculation of the likelihood function, under the gaussian white noise assumption.

On the other hand, a three-step method was designed for ARMA model fitting, including the estimation of the autoregressive and moving average orders (p, q) (Hannan and Rissanen, 1982; Hannan and Kavalieris, 1984). The three steps are as follows:

Step 1. The error terms $\hat{\epsilon}_t$ are obtained by fitting an AR(n) model to the data, for a large n :

$$\hat{\epsilon}_t = z_t + \sum_{i=1}^n \hat{\phi}_i z_{t-i},$$

with $\{\hat{\phi}_i\}_{i=1}^n$ the autoregressive coefficients estimated via the Yule-Walker equation (39) (see Subsection 4.1).

Step 2. Using $\{z_t\}$ and $\{\hat{\epsilon}_t\}$ as regressors, ARMA(p, q) parameters are estimated by the least squares method. Then, the orders (p, q) are estimated by minimizing the following criterion:

$$\log(\hat{\sigma}^2) + \frac{(p+q)}{T} \log(T),$$

where $\hat{\sigma}^2$ is the least squares estimate of σ^2 and T is the number of observations (that is, the number of time steps). This procedure can be costly when a wide grid of (p, q) values is tested. In the scenario where $p = q$, an efficient algorithm that recursively computes the sequence of ARMA(p, q) regressions has been proposed (Hannan and Rissanen, 1982).

Step 3. Once (p, q) are determined, ARMA(p, q) parameters are estimated through an iterative optimization procedure of the likelihood function. This function is initialized with the ARMA parameters corresponding to (p, q) identified by step 2.

In (Franke, 1985), the **Levinson-Durbin algorithm** used for AR parameter learning has been generalized to ARMA model fitting.

The **Innovation algorithm** is a recursive method used to compute ARMA(p, q) model parameters (Brockwell et al., 1991). Innovation is defined as the difference between the observed value z_t at time step t and the optimal forecast of that value, based on past information. In a parameter estimation framework, the motivation behind the Innovation algorithm lies in that in the innovation time series, the successive terms are uncorrelated with each other, thus yielding a white noise time series. Evaluating the likelihood directly for \mathbf{Z} involves inverting a nondiagonal covariance matrix which may also be a cumbersome function of the model parameters. Instead, the (white noise) innovation series has a diagonal covariance matrix, which is much easier to invert. The work presented in (Sreenivasan and Sumathi, 1998) extends the Innovation algorithm in order to include the selection of the ARMA process orders (p, q).

4.3.3 Forecasting

Once ARMA(p, q) model parameters have been estimated from sample $\{Z_t = z_t\}_{t=1}^T$, forecast at horizon h , \hat{Z}_{T+h} , is the sum of the forecasts for AR (equation 41) and MA (equation 47) components at the same horizon h :

$$\hat{Z}_{T+h} | \epsilon_{T+h-q}, \dots, \epsilon_{T+h-1} = \hat{\phi}_0 + \sum_{i=1}^p \hat{\phi}_i Z_{T+h-i} + \sum_{i=1}^q \hat{\alpha}_i \epsilon_{T+h-i}, \quad (51)$$

where $Z_{T+h-i} = \hat{Z}_{T+h-i}$ when $h - i > 0$.

As for the MA model (see Subsection 4.2.4), the error terms which are unknown are omitted.

4.4 Autoregressive Moving Average-based models

As seen in Subsection 4.3, the *autoregressive moving average* (ARMA) model is the most general linear stationary model that allows to specify the conditional mean. Since trend and seasonal components are observed in most real-world time series, the ARMA model has been extended to include these two deterministic components. The ARIMA and SARIMA models are described in this subsection.

4.4.1 Autoregressive Integrated Moving Average Model - ARIMA(p, d, q)

The *autoregressive integrated moving average* (ARIMA) model falls within the additive trend decomposition scheme (Subsection 3.2.1). The ARIMA(p, d, q) process has a nonstationary mean and is suited

to trended time series whose trends can be removed after d successive differentiations (equation 11, Subsection 3.2.1). Then, the resulting stationary component is an *autoregressive moving average* process of order (p, q) . A time series $\{X_t\}$ follows an ARIMA(p, d, q) process if:

$$\Phi_p(L) (1 - L)^d X_t = \Theta_q(L) \epsilon_t, \quad (52)$$

where $\{\epsilon_t\}$ is a white noise series; p, d, q are integers; L is the backward shift operator ($LX_t = X_{t-1}$, $L^k X_t = X_{t-k}$), Φ_p and Θ_q are polynomials in L , of orders p and q , respectively:

$$\begin{aligned} \Phi_p(L) &= 1 - \phi_1 L - \phi_2 L^2 - \dots - \phi_p L^p, \\ \Theta_q(L) &= 1 - \alpha_1 L - \alpha_2 L^2 - \dots - \alpha_q L^q. \end{aligned}$$

The most known specific instantiations of the ARIMA model are summed up in Table 4.

Instantiation	ARIMA(p, d, q)
White noise	ARIMA(0, 0, 0)
Random walk process	ARIMA(0, 1, 0)
Autoregression	ARIMA($p, 0, 0$)
Moving average	ARIMA(0, 0, q)
ARMA	ARIMA($p, 0, q$)

Table 4 Most popular instantiations of the ARIMA model. p denotes the order of the AR process (see Subsection 4.1), d is the number of differentiations required to detrend the raw series, q is the order of the MA process (see Subsection 4.2).

It has to be underlined that there exists no automatic method to identify the number d of differentiations required to detrend the time series. In practice, different values are tested (1, 2, 3, ...). Then two strategies can be applied: (i) d is set as the first value for which the d^{th} differentiation $(1 - L)^d X_t$ is stationary (see Subsection 2.2); (ii) d is chosen to minimize Akaike's information criterion (AIC) or Bayesian information criterion (BIC).

Let $\{X_t\}$ an ARIMA(p, d, q) process and $\{X_t = x_t\}_{t=1}^T$ the observed data. The stationary component $Z_t = (1 - L)^d X_t = \Delta^d X_t$, with Δ the differentiation operator (equation 11, Subsection 3.2.1), is an ARMA(p, q) process. At horizon h , Z_{T+h} is predicted through formula (51). Then, the forecast \hat{X}_{T+h} for the observed series is obtained by inverse transformation (equation 12, Subsection 3.2.1):

$$\hat{X}_{T+h} = \hat{Z}_{T+h} - \sum_{j=1}^d \binom{d}{j} (-1)^j X_{T+h-j}, \quad (53)$$

where $X_{T+h-j} = \hat{X}_{T+h-j}$ when $h - j > 0$.

4.4.2 Seasonal Autoregressive Integrated Moving Average Model - SARIMA(p, d, q)(P, D, Q) $_m$

As seen in Subsection 4.4.1, the ARIMA model handles additive trend but does not account for seasonal episodes. Seasonal ARIMA overcomes this limitation. It is the most popular model in the field of seasonal time series forecasting. For presentation fluency, the SARIMA extension is mentioned in the same Section as ARIMA, but it must be kept in mind that SARIMA is not a linear model. A time series $\{X_t\}$ is generated by a SARIMA(p, d, q)(P, D, Q) $_m$ process if:

$$\Phi_p(L) \Phi_P(L^m) (1 - L)^d (1 - L^m)^D X_t = \Theta_q(L) \Theta_Q(L^m) \epsilon_t, \quad (54)$$

where $\{\epsilon_t\}$ is a white noise series, p, d, q, P, D, Q and m are integers, L is the backward shift operator ($L^k X_t = X_{t-k}$), and

$$\begin{aligned}\Phi_p(L) &= 1 - \phi_1 L - \phi_2 L^2 - \dots - \phi_p L^p, \\ \Phi_P(L^m) &= 1 - \phi_m L^m - \phi_{2m} L^{2m} - \dots - \phi_{Pm} L^{Pm}, \\ \Theta_q(L) &= 1 - \alpha_1 L - \alpha_2 L^2 - \dots - \alpha_q L^q, \\ \Theta_Q(L^m) &= 1 - \alpha_m L^m - \alpha_{2m} L^{2m} - \dots - \alpha_{Qm} L^{Qm},\end{aligned}$$

are polynomials of degrees p, P, q and Q , respectively, m is the seasonality period, d is the number of classical differentiations (equation 11, Subsection 3.2.1) and D is the number of seasonal differentiations (equation 14, Subsection 3.2.2).

Note that the SARIMA process has one seasonal component (Φ_P, Θ_Q) and one nonseasonal component (Φ_p, Θ_q) . Each component is composed of an autoregressive part and of a moving average part. The autoregressive parts Φ_P and Φ_p are multiplied together; similarly, the moving average parts Θ_Q and Θ_q are multiplied together. For this reason, SARIMA is often referred to as **multiplicative seasonal ARIMA**. In table 5, some specific instantiations of the SARIMA model are presented.

Instantiation	SARIMA(p, d, q)(P, D, Q) $_m$
Seasonal ARMA	SARIMA(0, 0, 0)($P, 0, Q$) $_m$
ARIMA	SARIMA(p, d, q)(0, 0, 0)
Additive trend-seasonality model	SARIMA(p, d, q)(0, $D, 0$) $_m$

Table 5 Specific instantiations of the SARIMA model. p, q and d characterize the nonseasonal component (NSC) of the SARIMA model; they respectively denote the AR process order for the NSC (see Subsection 4.1), the MA process order for the NSC (see Subsection 4.2) and the number of differentiations required to detrend the NSC. P, Q, D and m characterize the seasonal component (SC) of the SARIMA model; P, Q, D represent for the seasonal component what p, q and d represent for the nonseasonal component, except that m -order differentiation is considered for the seasonal component, where m stands for the seasonality period.

5 Nonlinear Time Series Models

Many real-life processes display nonlinear features, such as irregular behavior switching. For such data, linear models (introduced in Section 4) unlikely provide an adequate fit to data when a small number of parameters is used, and/or unlikely yield accurate forecasts. Thus, it seems realistic to consider nonlinear models. However, it must be highlighted that underlying nonlinear structures are not necessarily detectable by visual inspection of the raw series. In this case, preprocessing the raw data series is essential to help decipher its structure (see Section 3). Following the time series model specification already seen in Section 4 (equation 33) and recalled hereafter, adopting a nonlinear framework for the remaining stochastic component Z consists in modeling the conditional mean f or/and the conditional standard deviation g as nonlinear functions. We remind the reader that f is the best forecast for Z_t and that g^2 is the forecast variance:

$$Z_t = f(Z_{t-1}, Z_{t-2}, \dots) + g(Z_{t-1}, Z_{t-2}, \dots) \epsilon_t,$$

with ϵ_t 's i.i.d.(0, 1) white noise processes, f and g^2 respectively the conditional mean and conditional variance of X_t , meaning that $Z_t | Z_{t-1}, Z_{t-2}, \dots \sim \mathcal{D}(f, g^2)$ with \mathcal{D} the law of residuals ϵ_t 's.

In contrast to linear models, autocorrelation is difficult to characterize in nonlinear models. Besides, adopting a nonlinear framework increases the complexity of the model learning process.

The present section will present five categories on parametric nonlinear models proposed in the literature. These models are the following:

- Polynomial Autoregressive Model (PAR)
- Functional-coefficient Autoregressive Model (FAR)
- Markov Switching Autoregressive Model (MSAR)
- Smooth Transition Autoregressive Model (STAR)
- Autoregressive Conditional Heteroscedasticity (ARCH).

5.1 Polynomial Autoregressive Model - PAR(q, p)

In the standard linear autoregressive model (equation 34, Subsection 4.1), the conditional mean f is linear with respect to both the model parameters and the past values. This latter assumption is released by polynomial autoregressive models in which nonlinear dependencies are specified through polynomials (Karakuş et al., 2017). Thus, in the PAR(q, p) model, f is a q -degree polynomial function of the p past values, and the conditional variance g^2 is constant and equal to σ^2 . A stochastic process $\{X_t\}$ follows a PAR(p, q) model if and only if:

$$Z_t = \mu + \sum_{i_1=1}^p \phi_{i_1}^{(1)} Z_{t-i_1} + \sum_{i_1=1, i_2=1}^p \phi_{i_1, i_2}^{(2)} Z_{t-i_1} Z_{t-i_2} + \dots + \sum_{i_1=1, \dots, i_q=1}^p \phi_{i_1, \dots, i_q}^{(q)} Z_{t-i_1} \dots Z_{t-i_q} + \sigma \epsilon_t, \quad (55)$$

where the error terms ϵ_t 's are i.i.d.(0, 1) such that ϵ_t is independent of X_{t-i} for $i > 0$, q is the degree of nonlinearity, p is the autoregressive order and ϕ 's are autoregressive coefficients.

The PAR($q = 1, p$) model is identical to the AR(p) model, and for $p = q = \mu = 0$, we obtain a simple white noise process.

As suggested by equation (55), a PAR process relies on a **Volterra series expansion**, the equivalent of Taylor series functional expansion in the nonlinear framework: the Volterra series differs from the Taylor series in its ability to capture memory effects. PAR models have been successfully used in real-life phenomenon modeling such as in industry (Gruber et al., 2010), short-term wind speed prediction (Lee, 2011), biological systems (Lahaye et al., 2003), seismology (Bekleric, 2008) and communications (Fernandes et al., 2010).

5.1.1 Model Identification and Parameter Learning

So far, we have seen that the autocorrelation function is used for the identification of linear models. For instance, in the Moving Average Model (MA(q), Section 4.2), the autocorrelation function is null as from lagged value $q + 1$. The identification of nonlinear models requires other strategies, which are more complex, since the autocorrelation function is not characterizable in such models.

Regarding PAR model dimension estimation, several values of (q, p) can be considered. Then model selection criteria can be used to identify the final values. This procedure can be costly when a large grid of (q, p) values is tested. An alternative method has been described in (Karakuş et al., 2015). In this method, (q, p) as well as PAR parameters (ϕ 's and σ) are random variables for which prior distributions are defined. The posterior densities of these variables are derived through the well-known Bayes theorem. Then a Reversible Jump Markov Chain Monte Carlo (RJMCMC) sampler is used to obtain an estimation of (q, p) and of the model parameters that maximizes the posterior joint density of the variables.

An interesting and useful feature of PAR models is their linearity with respect to their parameters. Thus, for fixed (q, p) hyper-parameters, model parameters can be estimated by the *non-linear least squares* (NLS) method (Kuruoglu, 2002). NLS provides the optimal estimates in the maximum likelihood sense if gaussian error terms are used ($\epsilon_t \sim \mathcal{N}(0, 1)$). When ϵ_t 's have heavier tails than in a gaussian distribution, such as in α -stable or generalized gaussian distributions, the estimate of variance is not reliable. In this case, alternative techniques such as *non-linear least L_p -norm* estimation can be used (Kuruoglu, 2002).

5.1.2 Forecasting

Once PAR(q, p) model parameters have been estimated from observations $\{z_t\}_{t=1}^T$, one-step ahead prediction is performed as follows:

$$\begin{aligned} \hat{Z}_{T+1} = f(z_T, \dots, z_{T+1-p}) = & \hat{\mu} + \sum_{i_1=1}^p \hat{\phi}_{i_1}^{(1)} z_{T+1-i_1} + \sum_{i_1=1, i_2=1}^p \hat{\phi}_{i_1, i_2}^{(2)} z_{T+1-i_1} z_{T+1-i_2} + \dots \\ & + \sum_{i_1=1, \dots, i_q=1}^p \hat{\phi}_{i_1, \dots, i_q}^{(q)} z_{T+1-i_1} \dots z_{T+1-i_q}, \end{aligned} \quad (56)$$

where f is the conditional mean.

In multi-step ahead predictions, past predicted values are used as new observations.

5.2 Functional-coefficient Autoregressive Model - FAR(p, k)

The functional-coefficient autoregressive model is a direct generalization of the standard linear autoregressive model (equation 34, Subsection 4.1) in which the autoregressive coefficients are functions instead of constants. This class of models is devoted to exploring the nonlinear features of time series data by exploiting their local characteristics. The FAR model proposed in (Chen and Tsay, 1993) is defined as follows:

$$Z_t = \sum_{i=1}^p \phi_i(\mathbf{Z}_{t-i}^*) Z_{t-i} + \sigma_t \epsilon_t, \quad (57)$$

where $\{\epsilon_t\}$ is a sequence of i.i.d.(0,1) error terms such that ϵ_t is independent of Z_{t-i} for $i > 0$, p is the autoregressive order, and the $\phi_i(\mathbf{Z}_{t-i}^*)$ terms are measurable functions from \mathbb{R}^k to \mathbb{R} and

$$\mathbf{Z}_{t-i}^* = (Z_{t-i_1}, Z_{t-i_2}, \dots, Z_{t-i_k}) \quad \text{with } i_j > 0 \quad \text{for } j = 1, \dots, k. \quad (58)$$

\mathbf{Z}_{t-i}^* is referred to as the threshold vector, with i_1, \dots, i_k the threshold lags and Z_{t-i_j} the threshold variables.

When the ϕ_i terms are constant, the FAR model is reduced to an AR model. The FAR model is very flexible and can accommodate most nonlinear features. As a matter of fact, many nonlinear models proposed in the literature are specific cases of the FAR model. For instance, for $\phi_i(\mathbf{Z}_{t-i}^*) = a_i + b_i \exp(-c_i z_{t-d}^2)$, equation (57) is reduced to an **exponential autoregressive** (EXPAR) model (Xu et al., 2019). With $\phi_i(\mathbf{Z}_{t-i}^*) = a_i^{(1)} \mathbb{1}(Z_{t-d} \leq c) + a_i^{(2)} \mathbb{1}(Z_{t-d} > c)$ where $\mathbb{1}$ is the indicator function, equation (57) is reduced to a **threshold autoregressive** (TAR) model (Chan et al., 2015; Hansen, 2011).

The definition of FAR models (equation 57) is flexible. However, only parsimonious models are considered in real-life applications: a small number of threshold variables, for instance $k = 1, 2$, and a low AR order are expected.

5.2.1 Model Identification and Parameter Learning

A FAR model is identified by the AR order p , the threshold lags i_1, \dots, i_k and the functional forms of the ϕ_i terms. To set the value of p , we may test several values and use model selection criteria, such as the Akaike's information criterion (AIC). Threshold lags may be identified from the exploration of the nonlinear feature of the data. To this end, various threshold nonlinearity tests can be used (Tsay, 1989; So et al., 2005; Gospodinov, 2005) can be used. Several functional forms can be tested for each of the ϕ_i terms; then the best one is selected using model selection criteria, in a manner similar to AR-order p identification (see Subsection 4.1.3). For $k = 1$, an alternative data-driven procedure based on *arranged local regressions* has been proposed to select the functionals forms of ϕ_i 's (Chen and Tsay, 1993). To note, in the EXPAR and TAR models, a unique functional form is shared by all coefficients.

We remind the reader that the ϕ_i terms are parametric functions of shape-parameters (for instance, $a_i, b_i,$ and c_i in the case of EXPAR). Once the FAR model has been identified, the ϕ_i 's can be estimated by the conditional least squares method (Klimko and Nelson, 1978).

5.2.2 Forecasting

Once FAR(p, k) model parameters have been estimated from observations $\{z_t\}_{t=1}^T$, one-step ahead prediction yields:

$$\hat{Z}_{T+1} = f(z_T, \dots, z_{T+1-p}) = \sum_{i=1}^p \hat{\phi}_i(\mathbf{z}_{T+1-i}^*) z_{T+1-i}, \quad (59)$$

where f is the conditional mean and $\mathbf{z}_{T+1-i}^* = (z_{T+1-i_1}, z_{T+1-i_2}, \dots, z_{T+1-i_k})$ with $i_j > 0$ for $j = 1, \dots, k$. In multi-step ahead predictions, past predicted values are used as new observations.

5.3 Markov Switching Autoregressive Model - MSAR(q, p)

Many real-life phenomena such as in economic systems (Hamilton, 1989, 1990) and meteorology (Ailliot et al., 2015) are subject to switches in regimes. Intuitively, a stochastic process \mathbf{Z} is subject to switches in regimes if the behavior of the associated dynamic system changes at each break which coincides with the beginning of a regime. The break points are not directly observed and probabilistic inference is required to determine whether and when break points occurred, based on the observed time series.

Let $\mathbf{S} = \{S_t\}_{t=1}^\infty$ a homogeneous Markov process with S_t the regime under which \mathbf{Z} is running at time step t . \mathbf{S} is referred to as the *state process* of \mathbf{Z} . For example, in the economic growth model described in (Hamilton, 1989) S_t can take two values: 1 and 0, respectively, for fast and slow growths. However, in practice, it is not always possible to provide a physical interpretation for the hidden states. From now on, we will indifferently use *regime* or *state*, as well as *regime switching* or *transition*.

Regime switching is a nonlinear feature that must be handled by dedicated time series models. In this context, the Markov switching autoregressive model has been proposed by Hamilton (1990), to offer a flexible alternative to the popular ARMA and ARIMA frameworks. In the MSAR model, the regime shifts are explicitly introduced through a hidden variable. The changes in regime are governed by a homogeneous Markov process (HMP): the transitions are time-independent (*homogeneous* process).

$$Z_t | S_t = s = \phi_0^{(s)} + \sum_{i=1}^p \phi_i^{(s)} Z_{t-i} + \sigma^{(s)} \epsilon_t, \quad (60)$$

$$S_t | S_{t-1}, \dots, S_{t-q} \sim \text{HMP}(q, K), \quad (61)$$

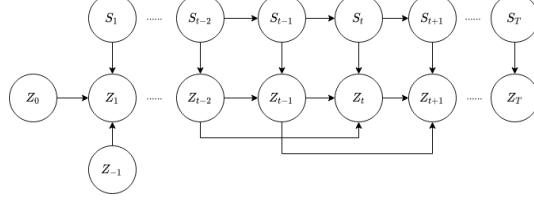


Figure 6 The conditional independence graph of the Markov switching autoregressive model for $q = 1, p = 2$.

where the ϵ_t 's are i.i.d. gaussian white noise processes, \mathbf{S} is a homogeneous Markov process of order q with K states ($K \geq 1$), $\{\phi_0^{(s)}, \dots, \phi_p^{(s)}\}$ and $\sigma^{(s)}$ are respectively the autoregressive parameters and standard deviation for each state s , $s = 1, \dots, K$. The transition between any two successive regimes only depends on the q previous regimes (*Markov* process). Moreover, given the current regime/state S_t , \mathbf{Z} follows an AR(p) model whose parameters are specific to S_t .

Obviously, the conditional mean f and conditional variance g^2 of a MSAR process also switch over time. Thus, given $S_t = s$ with $s = 1 \in \{1, 2, \dots, K\}$, $f_{(s)}(Z_{t-1}, \dots, Z_{t-p}) = \phi_0^{(s)} + \sum_{i=1}^p \phi_i^{(s)} Z_{t-i}$ and $g_{(s)}^2(Z_{t-1}, \dots, Z_{t-p}) = \sigma_{(s)}^2$.

When $K = 1$, the MSAR(q, p) model is reduced to the AR(p) model. When $q = 1$, \mathbf{S} is a Markov chain. The conditional independence graph of the MSAR($q = 1, p = 2$) model is shown in Figure 6: therein, the state at time step t only depends on the state at immediate past time step $t - 1$; moreover, the value of Z_t depends on Z_{t-2} and Z_{t-1} (the autoregressive part of MSAR), as well as on the state at time step t (the switching part of MSAR).

5.3.1 Model Identification and Parameter Learning

In practice, q is usually set to 1 and p is expected to be small. The number of states K and the process order p can be fixed using expert knowledge or it can be chosen using a model selection criterion such as Bayesian information criterion (BIC) or Akaike's information criterion (AIC).

A homogeneous Markov process is parametrized by: (i) the initial state law $\{\pi_k\}_{k=1, \dots, K}$ with π_k the probability for \mathbf{S} to be in state k at initial time step; and (ii) the transition probabilities $P(S_t = s | S_{t-1} = s_1, \dots, S_{t-q} = s_q)$ which is reduced to a transition matrix $\{a_{i,j}\}_{i,j=1, \dots, K}$ when $q = 1$. As the state process \mathbf{S} is unobserved, MSAR parameter learning is performed through the **maximum expectation** algorithm (Hamilton, 1990).

5.3.2 Forecasting

After the parameters related to both autoregressive and switching parts of the the MSAR(q, p) model have been estimated from observations $\{z_t\}_{t=1}^T$, one-step ahead prediction is achieved as follows:

$$\hat{Z}_{T+1} | \hat{S}_{T+1}=s = f_{(s)}(z_T, \dots, z_{T+1-p}) = \hat{\phi}_0^{(s)} + \sum_{i=1}^p \hat{\phi}_i^{(s)} z_{T+1-i}, \quad (62)$$

where \hat{S}_{T+1} is generally inferred by **MAP** (maximum a posteriori). In multi-step ahead predictions, past predicted values are used as new observations.

5.3.3 Variants of the MSAR Model

Some variants of the MSAR model have been proposed in the literature. The variant depicted in (Bessac et al., 2016) considers that the state process \mathbf{S} is directly observed. This specific model is referred to as **observed Markov switching AR**. An MSAR model in which gamma white noise is used instead of the usual gaussian white noise was described in (Ailliot et al., 2003). This adaptation was motivated by a better fit to data (in this case, wind speed for a given month, across several years). In 2015, Ailliot with other co-authors described an MSAR in which \mathbf{S} is a nonhomogeneous Markov process, that is transition from state to state is time-dependent (Ailliot et al., 2015).

5.4 Smooth Transition Autoregressive Model - STAR(p)

The smooth transition autoregressive model is an extension of the linear AR model that allows transitions from an AR model to another (Lin and Teräsvirta, 1994; Eitrheim and Teräsvirta, 1996). It is a nonlinear state-dependent dynamic model like the Markov switching autoregressive model MSAR (Subsection 5.3). In other words, for both MSAR and STAR models, alternative AR dynamics are allowed. The substantial difference between STAR and MSAR models lies in how the autoregressive parameters change over time. The switching part of an MSAR process switches between a finite and relatively small number of AR processes; in this case transitions are said to be abrupt. In contrast, in a STAR model, the autoregressive parameters depend on a transition function which is generally continuous. Thus, the probability to observe exactly the same dynamics at two distinct time steps is null. Therefore, the process switches between an infinite number of AR processes (one per time step). These transitions are said to be smooth.

The STAR model is defined as follows:

$$Z_t = \phi_0^{(1)} + \sum_{i=1}^p \phi_i^{(1)} Z_{t-i} + G(S_t) \left(\phi_0^{(2)} + \sum_{i=1}^p \phi_i^{(2)} Z_{t-i} \right) + \epsilon_t, \quad (63)$$

where $\{\epsilon_t\}$ is a sequence of i.i.d. $(0, \sigma^2)$ error terms, p is the AR order, $\{\phi_0^{(j)}, \dots, \phi_p^{(j)}, \sigma^2\}$ with $j = 1, 2$ is a vector of parameters to be estimated, S_t is the *transition variable* and G is the *transition function* which is bounded between zero and one.

From equation (63), it is easily seen that \mathbf{Z} switches from one AR process to another one with autoregressive coefficients varying according to transition function G . Thus, STAR model dynamics are altered by the transition function, conditional on the transition variable, in a potentially smooth manner. The degree of smoothness depends on how G is modeled. Given the transition variable S_t , the conditional mean $f_{(S_t)}(Z_{t-1}, \dots, Z_{t-p}) = (\phi_0^{(1)} + G(S_t)\phi_0^{(2)}) + \sum_{i=1}^p Z_{t-i}(\phi_i^{(1)} + G(S_t)\phi_i^{(2)})$ is state-dependent, whereas the conditional variance g^2 is constant and equal to σ^2 .

It is important to emphasize that structural changes in regimes are not incompatible with stationarity. If dynamic changes are local phenomena in the process behavior, then long-run statistics (mean and variance) of the process may remain stable. This case has been observed with large-scale medium-frequency events known as the so-called El Niño Southern Oscillations (ENSO) (Ubilava and Helmers, 2013).

5.4.1 Choice of Transition Function and Transition Variable - Parameter Learning

Transition functions define how the autoregressive parameters vary over time. The most frequently used transition functions are the following:

$$G(S_t) = \{1 + \exp[-\xi(S_t - c)]\}^{-1} \quad \text{logistic transition function,} \quad (64)$$

$$G(S_t) = \{1 - \exp[-\xi(S_t - c)^2]\} \quad \text{exponential transition function,} \quad (65)$$

$$G(S_t) = \{1 + \exp[-\xi(S_t^3 + c_1 S_t^2 + c_2 S_t + c_3)]\}^{-1} \quad \text{cubic transition function,} \quad (66)$$

where $\xi \geq 0$ is the smoothness parameter determining the smoothness of transitions, and c, c_1, c_2, c_3 are other shape parameters called location parameters. The transition function in (64) allows a smooth monotonic parameter change with a single structural break for the limiting case $\xi \rightarrow \infty$. Function (65) mimics a nonmonotonic change which is symmetric around c . Equation (66) describes the most flexible transition function which allows both monotonic and nonmonotonic changes. When $\xi \rightarrow 0$, all transition functions (64) to (66) tend to a constant and the STAR model converges to an AR model.

Generally, the transition variable S_t is set as a lagged value of Z_t , such as $S_t = Z_{t-d}$, with $d > 1$ (see for example [Ubilava and Helmers \(2013\)](#)). In this case, the STAR model is a specific instantiation of the functional autoregressive model (equation 57, Subsection 5.2). Alternatively, the literature dedicated to parameter stability or structural change indicates that S_t is a function of time, usually $S_t = t$. The reader interested in further details is referred to the works in ([Lin and Teräsvirta, 1994](#); [Eitrheim and Teräsvirta, 1996](#)).

Once G, S_t and p have been set, STAR model parameters can be estimated using a nonlinear optimization procedure. Autoregressive order p can be chosen by optimizing a model selection criterion.

5.4.2 Forecasting

After the STAR(p) model parameters $\{\phi_0^{(j)}, \dots, \phi_p^{(j)}, \sigma^2\}$ with $j = 1, 2$, and the shape parameters of the transition function G have been estimated from observations $\{z_t\}_{t=1}^T$, one-step ahead prediction is performed as follows:

$$\hat{Z}_{T+1} = f_{(S_{T+1})}(z_T, \dots, z_{T+1-p}) = (\hat{\phi}_0^{(1)} + \hat{G}(S_{T+1}) \hat{\phi}_0^{(2)}) + \sum_{i=1}^p z_{T+1-i} (\hat{\phi}_i^{(1)} + \hat{G}(S_{T+1}) \hat{\phi}_i^{(2)}). \quad (67)$$

As usual, past predicted values are used as new observations in multi-step ahead predictions.

5.5 Autoregressive Conditional Heteroscedasticity - ARCH(p)

In the course of a forecasting task, the ability to make accurate prediction may vary from one period to another. Therefore, the uncertainty associated with different forecast periods represented by the forecast variance g^2 may change over time. However, most time series models introduced in the literature assume a constant forecast variance g^2 (this is the case of all models presented so far in Sections 4 and 5). To release this constraint and obtain reliable forecast intervals $[f - g, f + g]$, [Engle \(1982\)](#) has introduced the ARCH model.

In the standard ARCH model, the conditional mean f is equal to 0 (hence a zero unconditional mean) and the forecast/conditional variance g^2 (equation 33, Section 4) is modeled as a quadratic function of

the past p values. A zero-mean process $\{Z_t\}$ follows a standard ARCH model if and only if

$$Z_t = \sigma_t \epsilon_t, \quad (68)$$

$$\sigma_t^2 | Z_{t-1}, \dots, Z_{t-p} = \phi_0 + \sum_{i=1}^p \phi_i Z_{t-i}^2, \quad (69)$$

where ϵ_t 's are i.i.d.(0,1) white noise processes (usually, the normal law is used), σ_t^2 is the conditional variance, $\{\phi_0, \phi_1, \dots, \phi_p\}$ are the model parameters and p is the ARCH process order.

Regarding ARCH process identification, Engle and Bollerslev (1986) proposed a statistical test that checks the evidence of ARCH(p) for a given time series data. Once the ARCH order has been fixed, the model parameters can be estimated through maximum likelihood maximization (Engle, 1982).

An ARCH process is said to be *volatile* since the *conditional variance* is time-varying while the *unconditional variance* $\text{Var}(Z_t)$ is assumed constant over time. Volatility is exhibited in many financial time series. When $\phi_0 > 0$, $\phi_1, \dots, \phi_p \geq 0$, a large value observed for Z_t will result in large *volatilities* (large conditional variances) for the next p time steps. Similarly, a small value observed for Z_t will lead to small volatilities for the next p time steps. Thus, an ARCH process tends to cluster large (respectively small) conditional variances. When it is not taken into account in time series models, the *volatility phenomenon* can lead to inaccurate predictions.

In Section 4.1, we have examined conditions to guarantee the stationarity for autoregressive processes. Similar conditions have been derived by Engle (1982) for the ARCH model: a standard ARCH(p) process with $\phi_0 > 0$, $\phi_1, \dots, \phi_p \geq 0$ is stationary if and only if all roots of the associated characteristic equation are outside the unit circle.

Other formulations of the conditional variance g^2 may be considered, such as exponential and absolute value forms. To simplify the parameter estimation procedure, Engle (1982) has suggested to choose g^2 symmetric, strictly positive and regular. The regularity conditions can be found in (Engle, 1982).

5.5.1 Generalized ARCH Model - GARCH(q, p)

The GARCH model is an extension of the ARCH model in which the conditional variances σ_t^2 's are autocorrelated (Bollerslev, 1986b). In the GARCH process, equation (69) becomes:

$$\sigma_t^2 | Z_{t-1}, \dots, Z_{t-p}, \sigma_{t-1}^2, \dots, \sigma_{t-q}^2 = \phi_0 + \sum_{i=1}^p \phi_i Z_{t-i}^2 + \sum_{j=1}^q \alpha_j \sigma_{t-j}^2, \quad (70)$$

where (q, p) characterizes the GARCH process orders and $\{\phi_0, \phi_1, \dots, \phi_p, \alpha_1, \dots, \alpha_q\}$ are parameters with $\phi_0 > 0$ and $\phi_1, \dots, \phi_p, \alpha_1, \dots, \alpha_q \geq 0$.

ARCH model extension to GARCH model is similar to the extension of AR to ARMA. Similarly, this extension allows a more parsimonious description of large-order ARCH processes. GARCH($q = 0, p$) and ARCH(p) processes coincide, and GARCH($p = 0, q = 0$) amounts to white noise process. GARCH($p = 0, q$) and ARCH($p = 0$) processes coincide.

Regarding GARCH process identification, that is the selection of (q, p) , Bollerslev (1986b) designed a procedure relying on the autocorrelation function and partial autocorrelation function for the squared process $\{Z_t^2\}$. To note, a similar procedure had been proposed for ARMA process identification (Box et al., 2015). Besides this informal graphical procedure, a statistical test checking the evidence of GARCH(q, p) for given time series data has been introduced in (Bollerslev, 1986b). Once (q, p) have been fixed, as with ARCH model, GARCH model parameters can be estimated through maximum likelihood maximization Bollerslev (1986b).

It has been proven that GARCH(q, p) process is stationary with $\mathbb{E}[Z_t] = 0$, $\text{Var}(Z_t) = \phi_0(1 - \sum_{i=1}^p \phi_i - \sum_{j=1}^q \alpha_j)^{-1}$ and $\text{Cov}(Z_t, Z_{t'}) = 0$ for $t \neq t'$, if and only if $\sum_{i=1}^p \phi_i + \sum_{j=1}^q \alpha_j < 1$ (Bollerslev, 1986b).

Finally, the GARCH model has been used in connection with other models. In practice, in models assuming a constant forecast variance, this assumption has been relaxed by incorporating residuals modeled through a GARCH process. Thus, better forecast intervals are obtained. For instance, ARMA (equation 48) and ARIMA (equation 52) models have been supplemented with a GARCH modeling of the residuals (Pham and Yang, 2010; Xin et al., 2018).

5.5.2 Forecasting

Let $\{\hat{\phi}_0, \hat{\phi}_1, \dots, \hat{\phi}_p, \hat{\alpha}_1, \dots, \hat{\alpha}_q\}$ the GARCH model parameters estimated from observations $\{z_t\}_{t=1}^T$. One-step ahead prediction is achieved as follows:

$$\hat{\sigma}_{T+1}^2 = g^2(z_T, \dots, z_{T+1-p}) = \hat{\phi}_0 + \sum_{i=1}^p \hat{\phi}_i z_{T+1-i}^2 + \sum_{j=1}^q \hat{\alpha}_j \hat{\sigma}_{T+1-j}^2, \quad (71)$$

$$\hat{Z}_{T+1} \sim \mathcal{D}(0, \hat{\sigma}_{T+1}^2),$$

where $\hat{\sigma}_T, \hat{\sigma}_{T-1}, \dots, \hat{\sigma}_{T+1-q}$ are computed from equation (70) and \mathcal{D} is the chosen distribution for white noise errors.

In multi-step ahead predictions, past predicted values are used as new observations.

5.5.3 Other Extensions of the Arch Model

The Markov-ARCH model (Cai, 1994) combines Hamilton's switching-regime model (MSAR, equation 60, Hamilton (1990)) with the ARCH model. The motivation behind this extension of ARCH is to address the issue of *volatility persistence*, or constancy of volatility during a relatively long period of time. The Markov-ARCH model handles this issue by allowing occasional shifts in the conditional variance g^2 governed by a Markov process. Namely, ARCH movements occur within "regimes", with occasional jumps occurring between two successive "regimes" characterized by different conditional variances. In the same line, further works have described MS-CGARCH, the Markov switching component GARCH model, in which volatility is modeled through the combination of two GARCH models (Alemohammad et al., 2016).

Besides, a smooth transition ARCH model was proposed, that combines a smooth transition autoregressive (STAR) model (equation 63, Section 5.4) with an ARCH model (Hagerud, 1997). In this model, the conditional variance g^2 is the one defined in equation (69), in which the ϕ_i terms depend on the logistic (equation 64) or exponential (equation 65) transition functions and on transition variable $S_t = X_{t-d}$. Finally, stochastic volatility models provide more realistic and flexible alternatives to ARCH-type models (Meyer et al., 2003). Therein, the conditional variance is stochastic, that is g is a nonlinear function of the past values of \mathbf{Z} plus random error terms.

6 Deep Learning

Amongst nonlinear models, artificial neural networks hold a place apart as deep learning has recently gained considerable attention.

To model time series, parametric models informed by domain expertise have been mainly used, such as autoregressive models and exponential smoothing frameworks. Not only did these established

statistical models gain their popularity from their high accuracy. They are also suitable for nonspecialists as they are efficient, robust and user-friendly.

In times series processing, deep neural networks (DNNs) hold a distinctive place. Recently, notable achievements have open up an avenue for deep learning. Deep learning is not a restricted learning approach, but it abides various procedures and topographies, to cope with a large spectrum of complex problems (Raghu and Schmidt, 2020). Deep learning relies on *deep* artificial neural networks (ANNs), that is ANNs with a high number of layers. Deep learning has become an active field of research in the next generation of time series forecasting models. DNNs are particularly suitable for finding the appropriate complex nonlinear mathematical function to turn an input into an output. Therefore, deep learning provides a means to learn temporal dynamics in a purely data-driven manner. In the remainder of this section, we briefly highlight how different classes of DNNs may be adapted to achieve the forecasting task in time series. The categories of models selected for illustration are the following:

- Multilayer Perceptrons,
- Recurrent Neural Networks,
- Long short-term memory networks,
- Convolutional neural networks,
- Transformers.

6.1 Multilayer Perceptrons

The most popular Artificial Neural Network (ANN) model, or perceptron, is composed of an input layer, hidden layers and output layer. Therein, except for an input node, an output y is computed as a weighted sum over the nodes connected to y in the preceding layer L : $y = A(\sum_{i \in L} x_i w_i + b)$, where x_i denotes an input from a node in L , b is a bias term, and A is a nonlinear activation function. A triggers the node activation. Amongst the most widely-used activation functions, illustrations are:

- sigmoid: $\sigma(z) = \frac{1}{1+e^{-z}}$
- hyperbolic tangent: $\tanh(z) = \frac{e^z - e^{-z}}{e^z + e^{-z}}$
- Rectified Linear Unit (ReLU): $R(z) = \max(0, z)$
- softmax: $\text{softmax}(z_i) = \frac{e^{z_i}}{\sum_j e^{z_j}}$, where z is a vector of reals.

6.1.1 Gradient-based Learning Algorithm

Beyond single-layer perceptrons, increasing the number of hidden layers in *multilayer* perceptrons (MLPs) allows to tackle more complex problems (Figure 7). This comes at a higher learning cost. Learning a perceptron is a supervised task that aims at instantiating the weights w of the connections between the layers, and the biases b , to minimize some cost function $C(w, b)$. The MLP learning algorithm proceeds by successive improvements. At a current point, a modification is made in the opposite direction to the gradient, so as to decrease the contribution to the cost ($w_{i,j} \leftarrow w_{i,j} - \alpha \frac{\partial C}{\partial w_{i,j}}$; $b_i \leftarrow b_i - \alpha \frac{\partial C}{\partial b_i}$), where α is the learning rate. This *gradient algorithm* is iterated until cost convergence. However, a neural network potentially consists in the composition of millions of functions. Therefore, the function modeled to turn the input into the output is not simple and a difficulty lies in the calculation of the different partial derivatives $\frac{\partial C}{\partial w_{i,j}}$ and $\frac{\partial C}{\partial b_i}$.

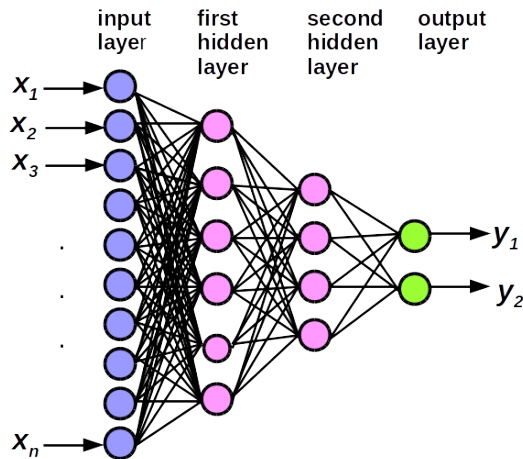


Figure 7 Example of Multilayer perceptron (MLP). The number of nodes in the input layer equals the number of features in each data row. Each layer is fully connected to its subsequent layer.

Gradient backpropagation is the cornerstone of MLP learning. Since we know the expected result in last layer and the calculations that took us from penultimate to last layer, it is possible to compute the error on the penultimate layer, and so on up to the first layer. Thus, potentially millions of partial derivatives may be computed efficiently through a unique forward and backward pass.

6.1.2 Enhancing Backpropagation Performance for Deep Learning

It soon quickly turned out that solving more and more complex problems requires an increasing number of layers in neural networks. However, the deeper a neural network is, the more computing power is needed to learn it, and the less the gradient backpropagation algorithm works satisfactorily. Technological and algorithmic advances have triggered the spectacular rise of deep learning in the last ten years: the increasing availability of massive data allows to train deeper models; neural network learning naturally lends itself to mass parallelization *via* GPUs; a set of new techniques facilitated the use of gradient backpropagation. Moreover, the provision of open-source frameworks is making a significant contribution to the upturn of deep learning, to facilitate backpropagation as well as the customisation of network architectures.

6.1.3 Forecasting

In time series forecasting, the data fed to an MLP (as well as to any other kind of neural network) must be prepared from a single sequence. The sequence must be splitted into multiple $\{x = \text{input} / y = \text{output}\}$ patterns (or samples) from which the model can be learned. For example, for a one-step prediction purpose, if three time steps are used for inputs, the time series $[10, 15, 20, 25, 30, 35, 40, 45, 50]$ will be divided into the following samples: $\{x = [10, 15, 20], y = 25\}$, $\{x = [15, 20, 25], y = 30\}$, $\{x = [20, 25, 30], y = 35\} \dots$. The MLP model will map a sequence of past observations as input to an output observation.

In time series forecasting as in other domains, the emergence of competing neural networks has relegated MLPs to the background.

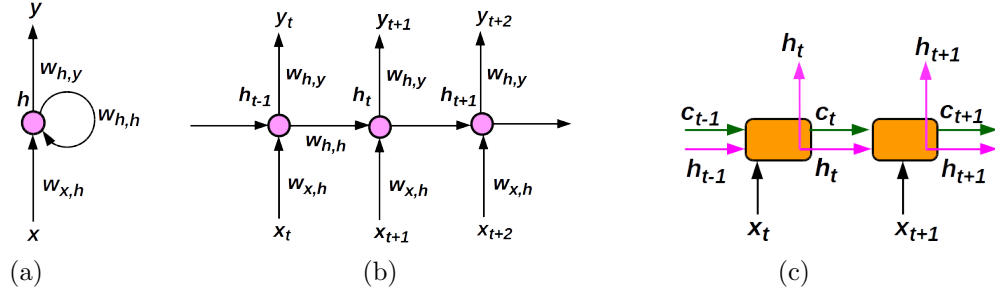


Figure 8 Examples of Recurrent Neural Network (RNN) and Long-Short Term Memory (LSTM) network. **(a)** RNN architecture. x , h and y respectively denote input, hidden state (or "memory") and output. At any time step, an element x_t of the time series is fed into the RNN module. h_t depends on previous hidden state h_{t-1} and on current value x_t . **(b)** Unfolding in time for the forward pass of the RNN in subfigure 8 (a). x_t : $h_t = f(w_{h,h}h_{t-1} + w_{x,h}x_t)$. The nonlinear function f is usually the \tanh or $ReLU$ function, and $y_t = \text{softmax}(w_{h,y}h_t)$. **(c)** Unfolding in time for an LSTM. x_t : input vector; h_t , c_t : hidden layer vectors. The LSTM module models a mathematical function that takes three inputs and yields two outputs: $(h_t, c_t) = f(h_{t-1}, c_{t-1}, x_t)$, where $h_t, h_{t-1}, c_t, c_{t-1} \in [-1, 1]$. The two outputs are fed back into the LSTM module at time step $t + 1$.

6.2 Recurrent Neural Networks

In the previous subsection, we have described how a univariate time series must be preprocessed to feed a MLP for one-step prediction purpose. However, two limitations appear when short-term predictions are made from a fixed sized window of inputs (three time steps in the illustration of Subsection 6.1): (i) the sliding window adds memory to the problem, for a contextual prediction, but defining the window size is challenging as there is no guarantee that sufficient knowledge is brought; (ii) a MLP takes as input a feature vector of fixed size, which defeats the purpose of processing series with no prespecified size.

6.2.1 Context-informed Prediction

Recurrent neural networks (RNNs) were designed to handle sequential information. Typically, RNNs are suitable to make predictions over many time steps, in time series. A RNN achieves the same task at each step (with varying inputs): the sequential sequence $(x_1, x_2, \dots, x_t, x_{t+1} \dots)$ is input to the RNN, element by element (one step at a time).

A RNN performs the same task for each element of a sequence, with the output being dependent on the previous computations. Conceptually, a RNN can be seen as a MLP architecture enriched with loops (Figure 8 (a)). In other words, a RNN has a memory to capture information about what has been calculated so far, and its decisions are impacted by what the RNN learnt from the past. Thus, in a RNN, not only are outputs influenced by weights associated with inputs as in standard feedforward NNs; a *hidden state vector* allows contextual decisions, based on prior input(s) and output(s).

6.2.2 Backpropagation Through Time

For a better understanding, Figure 8 (b) provides the RNN unfolded on the forward pass and along the input time series $\{x_t\}$. For instance, if the time series was of length T , the network would be unfolded into a T -layer neural network without cycles. The hidden states capture the dependencies that neighbor datapoints might have with each other in the series.

We have seen previously that MLPs use different parameters at each layer. In contrast, a RNN shares the same parameters across all steps ($w_{h,h}$, $w_{x,h}$, $w_{h,y}$, see Figure 8 (b)). This substantially diminishes the number of parameters to learn. However, in a deep learning context, RNN learning faces several major difficulties: (i) standard backpropagation cannot be applied as is, due to the loop connections; (ii) exploding or vanishing gradients are likely to generate instability, thus hampering the reliability of weight updates; (iii) theoretically, RNNs can exploit information from arbitrarily long time series, but in practice they are limited to model dependencies only within a few time steps.

The first issue is addressed using Backpropagation Through Time (BPTT): the network is unfolded into a standard MLP in which nodes involved in recurrent connections are replicated; backpropagation is then applied. Because the parameters are shared by all time steps in a RNN, the gradient at each output depends not only on the calculations of the current time step, but also on those of the previous time steps.

The second and third issues are tackled through using a novel class of architectures called Long Short-Term Memory networks, usually just called LSTMs.

6.2.3 Forecasting

Time series forecasting through deep RNNs is an active area (see for instance Chandra and Chand (2016) and Hiransha et al. (2018) in the financial domain). Recently, an extensive empirical study demonstrated that in many cases, RNNs outperform statistical methods which are currently the state-of-the art in the community (Hewamalage et al., 2021).

6.3 Long Short-Term Memory networks

LSTMs are the most widely-used subclass of RNNs, as they perform better than RNNs in capturing long dependencies. LSTMs are intrinsically RNNs in which changes were introduced in the computation of hidden states and outputs, using the inputs.

6.3.1 Keeping Track of Dependencies

We have seen that the RNN architecture is described as a chain of repeating modules. In standard RNNs, this repeating module will have a basic structure, such as a single *tanh* layer (see Figure 9 (a)). Typically, in the base module of a LSTM, a co-called long short-term memory cell and several gates interact in a more or less complex way. A gate may be triggered or not, depending on the sigmoid activation function. Thus are controlled the change of state and addition of information flowing through the module.

In a nutshell, these gates fall into three categories: (i) an input gate conditionally decides which values from the input will contribute to update the memory state, (ii) a forget gate conditionally determines what information will be discarded from the module, (iii) an output gate conditionally decides what will be output, based on module input and module memory state. Besides, the influence of these gates is controlled by weights, to be learnt during the training process. Each module therefore amounts to a mini state machine. Thus, the LSTM memory module improves over the common recurrent module used in RNNs by two points: (i) it allows to tune how new information is added to the previously stored information; (ii) it enables oblivion for some part of this previously stored information.

An illustration of the architecture of a single LSTM module is provided in Figure 9 (b). The unfolding in time of this single-module LSTM is shown in Figure 8 (c).

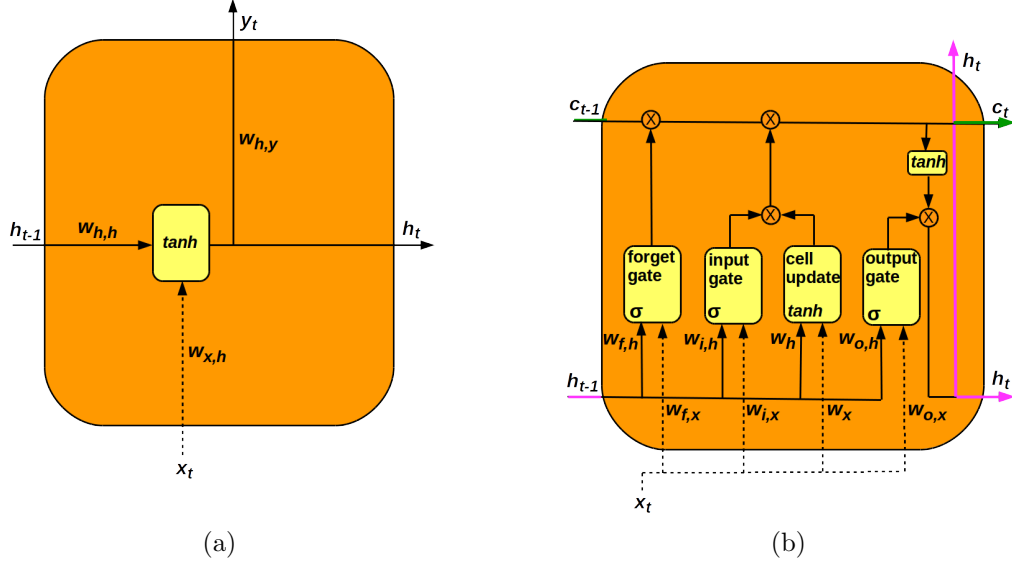


Figure 9 Illustrations for the repeating modules of a Recurrent Neural Network (RNN) and a Long-Short Term Memory (LSTM) network. **(a)** Standard RNN. $h_t = \tanh(w_{h,h} h_{t-1} + w_{x,h} x_t)$, $y_t = \text{softmax}(w_{h,y} h_t)$. **(b)** LSTM. Notations: x_t : input vector; h_t, c_t : hidden layer vectors; σ, \tanh : activation functions. To regulate the flow of information passing through modules, gates rely on the sigmoid activation function σ and on the pointwise multiplication operation (\otimes) as follows: $f^g(x_t, h_{t-1}) = \sigma(w_{f,x} x_t + w_{f,h} h_{t-1} + b_f) \in [0, 1]$ (forget gate) $i^g(x_t, h_{t-1}) = \sigma(w_{i,x} x_t + w_{i,h} h_{t-1} + b_i) \in [0, 1]$ (input gate) $o^g(x_t, h_{t-1}) = \sigma(w_{o,x} x_t + w_{o,h} h_{t-1} + b_o) \in [0, 1]$ (output gate) $c^u(x_t, h_{t-1}) = \tanh(w_x x_t + w_h h_{t-1} + b) \in [0, 1]$ (cell update), where $w_{f,x}, w_{i,x}, w_{o,x}, w_{f,h}, w_{i,h}, w_{o,h}, w_x, w_h$ and $b_f, b_i, b_o, b \in \mathbb{R}$ are respectively weight and bias parameters.

6.3.2 Refining the Architecture

Higher-order abstractions can be taken into account if we compose LSTM modules between them. First, the concatenation of n LSTM modules results in a layer of n LSTM modules. Further, stacking multiple such layers will increase the complexity of the function modeled by the network.

6.3.3 Learning Procedure

Since LSTMs are a specialization of RNNs, weight updates and optimization resort to the same techniques.

6.3.4 Forecasting

Due to their ability to address gradient explosion and vanishing gradient, LSTMs are actively investigated for time series forecasting purpose. LSTMs have been used for time series prediction in a number of domains, such as traffic speed (Ma et al., 2015), electricity price (Peng et al., 2018), electric load (Cheng et al., 2017), renewable energy power (Gensler et al., 2016) and financial markets (Selvin et al., 2017; Fischer and Krauss, 2018).

Some works dedicated to times series forecasting implement an optimization procedure to identify

the hyperparameters, prior to LSTM learning. For instance, LSTM learning is combined with a genetic algorithm to forecast stock markets, in (Chung and Shin, 2018). A solution using the differential evolution algorithm is described in (Peng et al., 2018), for the purpose of energy-related time series forecasting.

Interestingly, Hua, Zhao, Li, Chen, Liu, and Zhang (2018) introduced stochastic connectivity into conventional LSTM modules. A certain level of sparsity is thus obtained in the module architecture, which alleviates the computational burden in training.

6.4 Convolutional Neural Networks

The event that triggered the emergence of deep learning was an image recognition and classification contest (ImageNet, 2012). Very soon, a specific kind of deep neural networks, the convolutional neural networks (CNNs), were proposed and dedicated to image analysis. Having connections from all nodes of one layer to all nodes in the subsequent layer, as in MLPs, is extremely inefficient. CNNs arose from the observation that a careful pruning of the connections, based on domain knowledge, boosts performance. A CNN is a particular kind of artificial neural network aimed at preserving spatial relationships in the data, with very few connections between the layers. Moreover, CNNs exploit knowledge which is intrinsic to the data considered (for instance, spatial relationships in an image). The name Temporal Convolutional Networks (TCNs) was first referred to in (Bai et al., 2018), to emphasize the autoregressive property of CNNs used for a forecasting task, and the ability to process sequences of arbitrary length.

In the generic scheme, the input to a CNN is a matrix. This input is then converted into successive layers, throughout the CNN (see Figure 10). These layers (matrices in fact) capture relationships of increasing granularity, up to high-level details. For example, in image analysis, low-level features would be edges, corners, color or gradient orientation; a high-level feature could be a complete face. Consecutive layers of convolutions and activations, generally interspersed with pooling layers, construct the deep CNN.

6.4.1 Convolution

The two paradigms of CNNs are local connectivity and parameter sharing. In each convolutional layer, the convolution operation is performed by a specific filter (also known as the "kernel" or "receptive field"), which is applied on the preceding layer. Each unit in a convolutional layer is connected to only one local region of the preceding layer. In other words, a small set of neighbor units of the preceding layer is processed by the kernel, to calculate the unit in the convolutional layer. When the whole preceding layer has been convolved in this way, a novel feature map (the convolution layer) is obtained. A convolution operation involves weights. Importantly, all the units in the novel feature map are processed using the same weights. Thus, it is guaranteed that all units in the novel feature map will detect exactly the same pattern. Another no less important consequence of weight sharing is the decrease in the number of learnable parameters, which translates into a more efficient learning procedure.

In Temporal Convolutional Networks, the autoregressive characteristics implies that the value at time step t must only depend on past time-steps and not on future ones. To guarantee this behavior, the standard convolution operation is replaced with **causal convolution** (see Figures 11 (a) and (b)). Further, **dilated causal convolution** is a technique used to increase the receptive field of the TCN, thus allowing to learn long-term dependencies within the data (see Figure 11 (c)).

6.4.2 Dimension Reduction

Another building block of CNNs is the pooling layer, whose role is to subsample the feature map obtained. One aim is to reduce the spatial size of the data representation. Besides this impact on

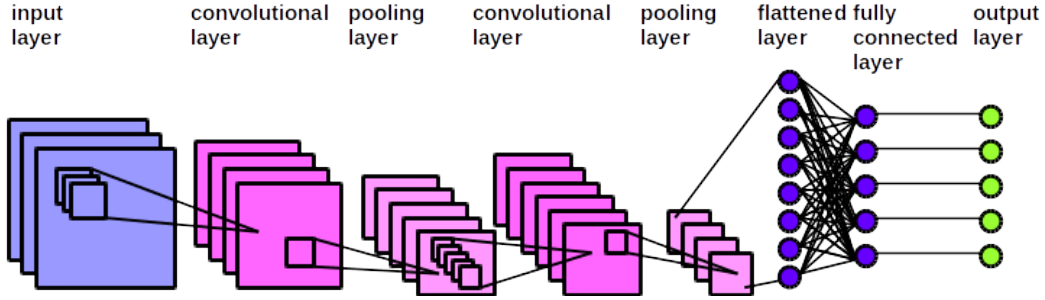


Figure 10 Example of Convolutional Neural Network (CNN) architecture. In CNNs, the number of convolution and pooling layers is larger greater than 2, as in this illustration. The value C_k of k^{th} unit in a convolutional layer is calculated as $C_k = f(x * W + b)$, where x is the vector of values for the units defining the local region (in the preceding layer), associated with k^{th} unit, W denotes the weights characterizing the filter driving the convolution, b is a bias, and f is an activation function (sigmoid, tanh or ReLU, for instance). When the whole preceding input layer has been convolved in this way, a novel feature map (the convolutional layer) is obtained. In complement to the convolutional layer, the pooling layer is responsible for reducing the spatial size of the convolved feature. Max pooling is generally employed. Through max pooling, the maximum value from the portion of the novel feature map covered by the filter is assigned to a dedicated unit in the pooling layer. At the end of the network, the feature maps (corresponding to as many channels) obtained through the latest convolution are flattened into a single (long) one-dimensional vector. The latter vector is fully connected to an additional layer \mathcal{L} . The softmax function is used to obtain the final output: $softmax(z_i) = \frac{e^{z_i}}{\sum_{j \in \mathcal{L}} e^{z_j}}$.

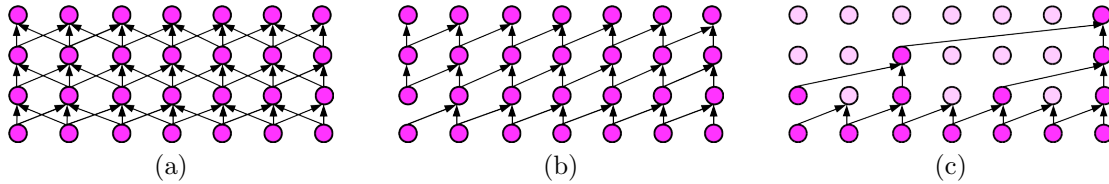


Figure 11 Convolution operation. (a) Standard convolution; kernel size = 3: as the convolutional kernel slides over the local region (or kernel) in the subsequent layer, the estimated value at time t depends on both past and future. (b) Three-layer CNN with causal convolution; kernel size = 2: the output at time t does not depend on past values. (c) Dilated causal convolution: kernel size = 2, dilatation rate = 2: the dilatation rate defines the spacing between the values in a kernel. Dilated causal convolution provides a wider field of view at constant computational cost. Thus it allows to handle long-term dependencies within the data.

learning complexity, a second aim is to make the feature captured by the convolutional layer invariant to local anomalies (such as distortions in image analysis, for instance). For example, max pooling returns the maximum value over neighbor units that belong to the novel feature map obtained.

6.4.3 Managing Data Seen from Different Perspectives

So far, we have given a simplified description of CNNs. The CNN model was initially developed for an image analysis purpose. In this case, the input data, an image, comprises multiple channels (for instance Red, Green, Blue). The consequence is that kernels, together with hidden layers, have the same depth as that of the input image (the number of channels). Convolutions are applied independently on

the channels. But one-dimensional data also often comes in the form of several parallel streams. For instance, electroencephalogram records are described by up to 128 channels.

Importantly, the number of channels may not be kept constant through later layers in the CNN. The channels (or feature maps) represent as many abstract versions of the initial data, with each channel focusing on some aspect of the information.

6.4.4 Adaptation to Time Series Data

Although initially designed to handle two-dimensional image data, CNNs can be used to model univariate time series. A one-dimensional CNN will just operate over a sequence instead of a matrix.

To note, whereas handling multivariate time series requires nontrivial multivariate extensions of traditional models, CNNs more naturally lend themselves to process multivariate time series. A multivariate time series will be fed to the CNN as various vectors corresponding to the initial channels. For instance, in the case of economic data, one channel will correspond to the unemployment rate, another channel to the gross domestic product, a third one to the number of companies created during the year. We have seen that convolutions are applied independently (in parallel) on the dimensions (or channels) of the data. Nonetheless, putative dependencies between the data dimensions will be taken into account by the fully connected layer at the end of the CNN.

6.4.5 Whole CNN Architecture

The first convolutional layer and pooling layer would capture low-level information from the input data. Multiple convolution, activation and pooling layers can be stacked on top of one another. Such architectures endow CNNs the ability to extract high-level features.

Additional operations complete the description of the CNN architecture (see Figure 10). The multi-channel vector obtained in the last pooling layer is flattened into a single-channel vector. This (long) vector is then fully connected to an additional layer. An activation layer generates the final output.

CNNs are trained using backpropagation as in standard artificial neural networks.

6.4.6 Forecasting

Notably, deep learning models have been widely investigated to address electric load forecasting (Gasparin et al., 2019). However, in this domain, CNNs had not been studied to a large extent until recently (Amarasinghe et al., 2017; Almalaq and Edwards, 2017; Kuo and Huang, 2018). The three latter works reported that CNNs have been proven comparable to LSTMs as regards electricity demand forecasting. Furthermore, CNNs outperformed LSTMs in works related to energy-related time series such as photovoltaic solar power prediction (Koprinska et al., 2018) and in experimentations focused on power demand at charging points for electric vehicles (Lara-Benítez et al., 2020). Importantly, all these works highlighted a better adequacy of CNNs for real-time applications, compared to other neural networks. The explanation lies in their faster training and testing execution times.

Hybrid models combining convolutional and LSTM layers have been proposed. In some of these works, the feature maps generated through a CNN are input into a LSTM which is in charge of prediction (see for instance the work of Cirstea et al. (2018), with its application to chemical concentration prediction). He (2017) relies on CNNs to extract features from multiple input sources, before an RNN captures the temporal dependencies in the data. Other works implement further model integration by combining the features extracted in parallel from a CNN and a LSTM. Tian et al. (2018) and Shen et al. (2019) illustrate this latter approach for the energy, meteorology and finance fields.

6.5 Transformers

Seq2Seq models allow to transform an input sequence into an output sequence. Sections 6.2 and 6.3 have spotlighted how RNNs, and a specialized version of RNNs, LSTMs, are suited to handle sequential data based on recurrent modules. Transformers are a class of deep learning Seq2Seq models that were recently introduced (Vaswani et al., 2017). Like RNNs, transformers were designed to handle sequential data and tackle problems in natural language processing (for instance translation). Transformers were repurposed to address forecasting in time series (see for instance Nino, 2019).

The encoder and decoder form the two parts of the transformer’s architecture (Figure 12). The encoder mainly consists of an input layer, an input encoding, a positional encoding mechanism, and a stack of identical encoder layers. In the seminal work of Vaswani et al. (2017), the decoder is composed of an input layer, an input encoding, a positional encoding mechanism, a stack of identical decoder layers and an output layer.

6.5.1 Transformers *versus* Recurrent Neural Networks

A first difference between RNNs and transformers is that in the former, the sequential data is input element by element (one step at a time). In Transformers, the entire sequence is input all at once while positional encoding preserves the sequential nature of the data. In natural language processing (NLP) tasks, transformers rely on word and phrase encodings to represent the input data with a gain of performance in the transformation. More generally, encoding an input sequence results in representing each input element as a vector of identifiers (for example co-occurring word identifiers in NLP). The encoding representation of the data is obtained by forcing the transformer to reconstruct the original sequence. The *encoder* is delegated this task. In time series applications, the *encoder* allows to summarize information and integrate temporal behavior from the time series under analysis.

In connection with this first difference, another difference with RNNs is that transformers do not require the input data to be processed sequentially. Namely, transformers do not need to process the beginning of the input sequence before its end. Therefore, transformers lend themselves to much further parallelization than RNNs, which decreases training times. Moreover, since the sequence is not fed sequentially to a transformer, training a transformer for a forecasting purpose requires specific mechanisms to ensure that predicting a data point will only depend on previous data points. This property is obtained through two mechanisms, look-ahead masking and one-position shifting between the decoder input and target output (to be further described).

A third difference occurs in the way RNNs and transformers capture the dependencies within the input sequential data for a forecasting purpose. RNN units can remember or forget parts of the previously stored information, depending on whether they find them important or not. Relying on a single RNN unit entails that this latter be able to memorize important events of the past and use these events to predict future values. In contrast, instead of a single multi-task unit, transformers rely on two specialized units. These units define the characteristic *encoder-decoder* architecture shown in Figure 12. In time series prediction, the encoder extracts the important features from the past events, whereas the decoder exploits this information to predict future values.

In LSTMs, an issue is that there is no way to assign more importance to some parts of the input sequence compared to others while processing the sequence. The attention mechanism, a corner stone in the transformer model, emerged as an improvement to capture dependencies, especially long-range dependencies, in a sequence. In the traditional encoder-decoder model, only is the final vector produced by the encoder used to initialize the decoder. However, summarizing a long input sequence into this single vector drastically decreases the transducer performance. The key idea behind attention consists in using all intermediate encodings generated by the encoder, to enrich the information passed to the decoder.

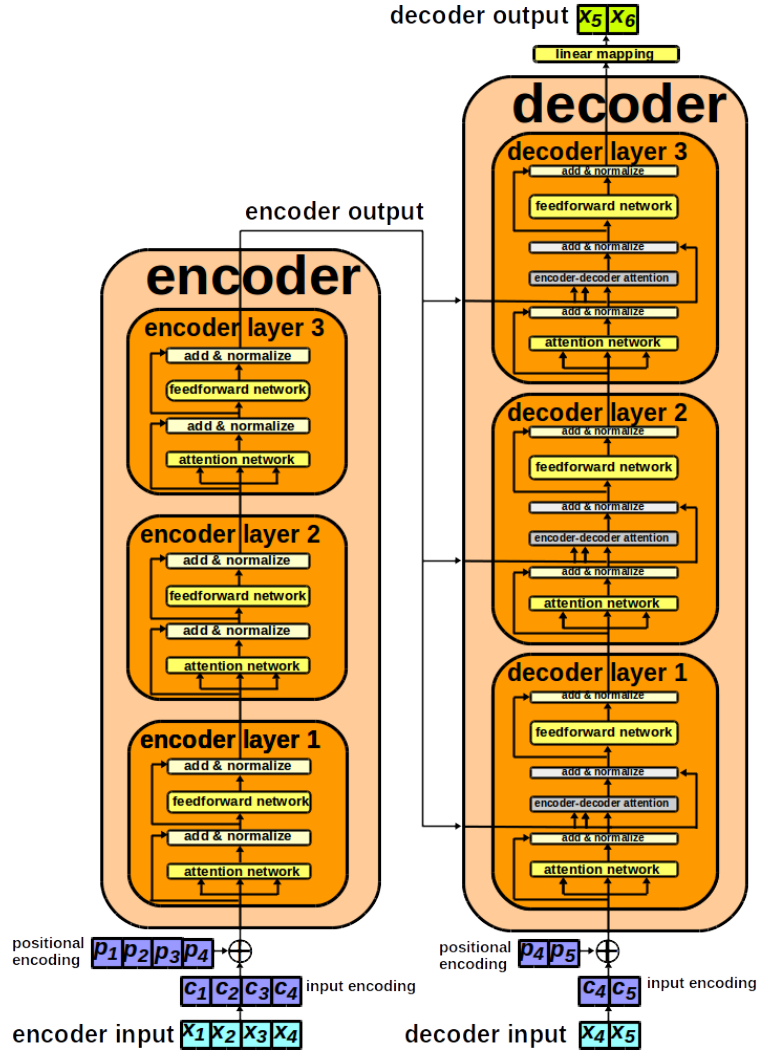


Figure 12 Example of transformer (or encoder-decoder) architecture. The inputs and outputs (target sentences in the training task) are first each encoded as a vector of d -dimensional vectors. • The encoder mainly consists of an input layer, an input encoding, a positional encoding mechanism, and a stack of identical encoder layers. The input layer maps the input time series data to a vector of d -dimensional vectors (input encoding). The positional encoding mechanism integrates sequential information to the model through element-wise addition with the original input encoding. In the end, the encoder yields a vector of d -dimensional vectors which is fed to the decoder. • In this illustration inspired from the seminal work of Vaswani et al. (2017), the decoder is composed of an input layer, an input encoding, a positional encoding, a stack of identical decoder layers and an output layer. The decoder input starts with the last data point of the encoder input (X_4 in this example). The decoder input is mapped to an encoded input layer. As in the first encoder layer, the input for the first decoder layer integrates positional information supplied by a positional encoding vector. Downstream the last decoder layer, an output layer maps the output of last decoder layer to the decoder output. • The encoder and decoder layer architectures are described in detail in Figure 13.

Recurrent networks were put forward as the best way to capture timely dependencies in sequences. Specifically, LSTMs are supposed to capture long-range dependencies but they may fail to meet this purpose in practice. The introduction of the transformer model brought to light the fact that attention mechanisms in themselves are powerful and dispense a sequential recurrent processing of the data (Vaswani et al., 2017). Instead, processing all input elements at the same time and calculating *attention weights* between them enables to relate different positions in a sequence. Thus long-range dependencies may be captured in the representation of the sequence.

Another difference is that RNNs only allow one-step-ahead prediction. Therefore, multi-step-ahead is handled in RNNs by iterating H times a one-step-ahead prediction: the newly predicted series value is fed back as an input for the future series value. A major flaw of this iterated scheme lies in error propagation. Instead, transformers allow direct forecast of $x_T + h$ with $h \in \{1, 2, \dots, H\}$.

Each encoder or decoder layer makes use of an attention mechanism to process each element of its input. Namely, the attention mechanism weights the relevance of every other element in the input sequence and extracts information accordingly, to generate the layer output. Similarly to kernels in CNNs, multiple attention heads allow to capture various levels of relevance relations. Each decoder layer also has an additional attention mechanism which applies self-attention over the encoder output.

6.5.2 Attention Mechanism

An attention mechanism computes weights representing the relevance of the elements in the input sequence (named keys hereafter) to a peculiar output (named query). Otherwise stated, weights indicate which elements in the input sequence are more important for predicting each output element.

Contextual information Given the input sequence of n elements x_1, x_2, \dots, x_n , each i^{th} element is mapped to an associated code c_i which is a d -dimensional vector. However, this encoding neither takes into account the surrounding context nor the position in the sequence of the elements.

To address the first issue, the key is to quantify how similar i^{th} element represented by c_i (**query**) is to each of the codes c_1, c_2, \dots, c_n (**keys**). The inner product operation, followed by exponentiating and normalizing, yields the relative relationship $r_{i \rightarrow j}$ that exists between i^{th} and j^{th} elements. Thus, $r_{i \rightarrow j}$ indicates how much attention should be paid to code c_j when constituting a new encoding \tilde{c}_i for element i . $\tilde{c}_i = \sum_{j=1}^n r_{i \rightarrow j} c_j$ is therefore informed by the context in which i^{th} element appears. This mechanism implements self-attention over a single sequence.

If element i is highly related to a particular element j , $r_{i \rightarrow j}$ will be large. Thus, the **value** c_j multiplied by relative weight $r_{i \rightarrow j}$ will contribute significantly to the revised code \tilde{c}_i . As a consequence, the same element i observed in different contexts c_1, c_2, \dots, c_n would be mapped to different codes \tilde{c}_i .

To generalize, the attention function is depicted as mapping a query and a set of key-value pairs to an output. The query, keys and values are all vectors. The output consists in a weighted sum of the values. In practice, the attention function is computed simultaneously on a set of queries which form the matrix Q . Similarly, keys and values are respectively stored into the matrices K and V . For queries and keys of dimension d , and values of dimension v , dot-product-based attention provides the vector outputs according to the following principle

$$weights(Q, K, V) = softmax\left(\frac{QK^T}{\sqrt{d}}\right) V, \tag{72}$$

where A^T denotes the transpose of matrix A and *softmax* allows to non-linearly scale the weight values between 0 and 1. For large d values, the dot-product is likely to produce very large magnitudes. Very small gradients would therefore be passed to the softmax function. To address this issue, scaling by \sqrt{d} factor is applied.

separate

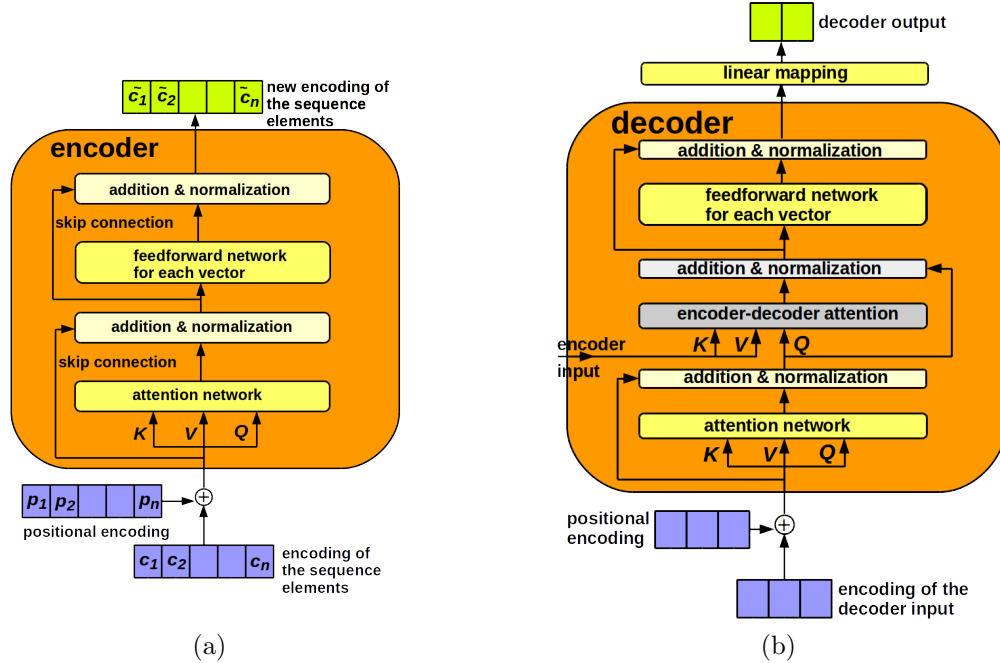


Figure 13 Attention mechanisms used in a transformer. (a) Attention mechanism in a single-layer encoder. (b) Attention mechanisms in a single-layer decoder. • Each encoder layer mainly consists of two sub-layers: a self-attention mechanism and a fully-connected feed-forward neural network. Each sub-layer is followed by a complementary sub-layer, where point-wise vector addition and normalization are performed, to implement the so-called skip connection. Except for first encoder layer, the self-attention mechanism is fed with the set of encodings generated by the previous encoder layer and weights their relevance to each other to generate a set of output attended encodings. • Besides a self-attention mechanism and a feed-forward neural network, a decoder layer includes a third sub-layer between the two former: the role of this encoder-decoder attention mechanism is to help the decoder focus on relevant parts of the input sentence.

Figure 13 describes in detail the architectures for the encoder and decoder layers. Besides a self-attention network present in both layers, a cross-attention mechanism is implemented through the so-called encoder-decoder attention network. Table 6 details Q , K and V for the three separate attention mechanisms of a transformer.

In the self-attention mechanism of an encoder layer, all the keys, values and queries come from the previous encoder layer. In the encoder-decoder attention mechanism of a decoder layer, the queries come from the previous decoder layer, whereas the keys and values come from the output of the encoder.

Positional information The attention mechanism described so far pays no attention to the order of the elements. To palliate this drawback, it has been found convenient to add a so-called **skip connection** to preserve the order of the elements: each original element encoding c_i is added to the output of the attention network, and the codes thus modified are normalized.

Further, this set-up is augmented with a positional encoding, to account for the positions of the elements. This positional encoding will be added to the original element embedding c_i . Since we have a

Encoder attention	Q:	vector associated with current element of input sequence
	K=V:	vectors corresponding to all elements of input sequence
Decoder attention	Q:	vector associated with current element of output sequence
	K=V:	vectors corresponding to all element of output sequence
Encoder-decoder attention	Q:	output of the decoder’s masked attention (output of the previous decoder layer)
	K=V:	all the vectors output by the encoder layers (ouput of the encoder)

Table 6 Details on queries, keys and values for the three separate attention mechanisms of a transformer. Q : queries, K :keys, V : values. Generically, attention is used to relate two different sequences to one another. In self-attention, different positions of the same input sequence are related to one another. Therefore, K and V are the same.

d-dimensional element encoding c_i for element i , we wish to produce a d-dimensional positional encoding p_i for this element. One standard way to construct p_i for an element i located at position pos is to use sinusoidal waves as follows:

$$\begin{aligned} p_i(pos, 2k) &= \sin(pos/c^{2k/d}), \\ p_i(pos, 2k + 1) &= \cos(pos/c^{2k/d}), \end{aligned} \tag{73}$$

with c some constant, $\omega_{2k} = 1/c^{2k/d}$ the sinusoidal wave frequency, and $2k$ and $2k + 1$ even and odd indexes in $1, \dots, d$. As we move from 1 to d , the sinusoidal wave oscillates faster. The original element encoding added to this positional encoding is input into the attention network as shown in Figures 13 (a) and (b). Finally, each of the n vectors output by the attention network is fed through a simple (feedforward) neural network. Again, skip connection, addition and normalization are applied to this part of the framework.

This scheme (attention, addition and normalization, [cross-attention, addition and normalization,] feedforward network, addition and normalization) can be repeated k times (a standard value for k is 6). This yields a final deep sequence encoder [decoder].

Multihead attention Finally, similarly to convolutional neural networks that rely on several kernels, several self-attention sub-layers can be used in parallel in Transformers. This so-called multi-head attention mechanism uses different linear projections of Q , K and V . Learning from different representations of Q , K and V is beneficial to the model. The encoding vectors obtained through these heads are concatenated, then a dimension reduction step is applied to yied the final encoding vector.

6.5.3 Forecasting

In the self-attention mechanism of a decoder layer, each position in the decoder only attends to positions in the decoder up to and including this position. Values corresponding to subsequent forbidden positions are masked out in the input of the softmax function.

Together with look-ahead masking, one-position shifting between the decoder input and target output (decoder output) ensures that the prediction for a given position only depends on the known outputs at positions stricly less than this position. Thus can be preserved the autoregressive property.

Given a time series containing N data points $x_{t-N+1}, \dots, x_{t-1}, x_t$, H -step ahead prediction is formulated as a supervised machine learning task: the input of the model is $x_{t-N+1}, \dots, x_{t-H}$, and the output is $x_{t-H+1}, x_{t-H+2}, \dots, x_t$. During model training, one-position shifting between the decoder input and the target output (decoder output) prevents learning the decoder to merely copy its input and contribute to ensure that the prediction for a given position only depends on the known outputs at positions stricly less than this position. This shifting mechanism is combined with look-ahead masking that restrains attention to datapoints in the past: in the self-attention mechanism of a decoder layer,

each position in the decoder only attends to positions in the decoder up to and including this position. Values corresponding to subsequent forbidden positions are masked out. In the training phase, the first neural network in an encoder layer reads the input sequence one time step at a time.

Transformer models have been applied in such various domains as influenza-like illness forecasting (Wu et al., 2020) and prediction of vehicle trajectories (Park et al., 2018). To guess the future trajectory of surrounding vehicles in real time, the latter work relies on the following architecture: LSTM-based encoders analyze the patterns underlying the past trajectory data, whereas LSTM-based decoders predict the future trajectories.

The point-wise dot-product self-attention in canonical transformers is agnostic of local surrounding context. This may entail confusion regarding whether an observed point is an anomaly, a change point or part of the patterns underlying the data. To increase prediction accuracy, Li et al. (2019) employ causal convolution to incorporate local contextual information such as local shapes in the attention mechanism. Further, the authors proposed a log-sparse self-attention mechanism, to increase forecasting accuracy for time series with fine granularity and long-term dependencies under memory limited budget.

Phandoidaen and Richter (2020) investigated transformers to forecast high-dimensional time series. In their paper, the authors impose a specific encoder-decoder structure as a reasonable approximation of the underlying autoregressive model f_0 . They assume that their model compresses the given information of the last r lags into a vector of much smaller size and afterwards expands this concentrated information to generate the observation of the next time-step ahead. A theoretical analysis of the forecasting ability of an estimator \hat{f} of f_0 was developed under various structural and sparsity assumptions. In particular, upper bounds were provided for the forecast errors. The performances of the various neural network estimators were analyzed on simulated data.

A specific kind of encoder-decoder architecture is the autoencoder (AE). An AE is a Multilayer Perceptron Network whose particular architecture is described as follows: an input layer and an output layer of same size are connected through one or more hidden layers; the hidden layers of the encoding side are mirrored to constitute the decoding side of the AE (see Figure 14). Reconstructing the input by minimizing the difference between the input and the output (predicted input) then allows to implement feature extraction in an unsupervised learning scheme.

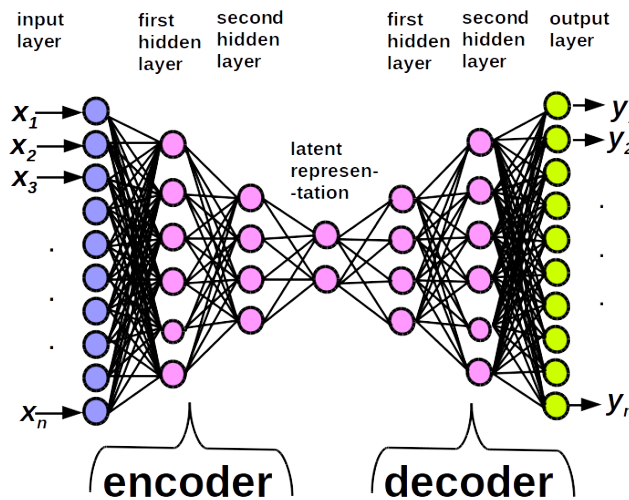


Figure 14 Example of autoencoder (AE) architecture.

Gensler et al. (2016) developed an approach combining an AE with an LSTM, to forecast power in renewable energy power plants. In the domain of financial time series forecasting, Bao et al. (2017) considered stacked AEs to extract features, together with an LSTM to generate the one-step-ahead output prediction. The stacked autoencoder architecture is constructed by stacking a sequence of single-hidden-layer AEs, layer by layer. In this scheme, the hidden layer of the previous AE serves as the input layer for the subsequent AE.

7 Available implementations

Table 7 gives a recapitulation of available *R* and *Python* implementations for methods/models presented throughout the present review of time series model analysis.

	Method/Model	Language	Package/Module (function/class)
Stationarity tests	Phillip-Perron test	<i>R</i> <i>Python</i>	tseries (<i>pp.test</i>) or urca (<i>ur.pp</i>) arch.unitroot (<i>PhillipsPerron</i>)
	(Augmented) Dickey-Fuller test	<i>R</i> <i>Python</i>	tseries (<i>adf.test</i>) or urca (<i>ur.df</i>) statsmodels.tsa.stattools (<i>adfuller</i>) or arch.unitroot (<i>ADF</i>)
	KPSS test	<i>R</i> <i>Python</i>	tseries (<i>kpss.test</i>) or urca (<i>ur.kpss</i>) statsmodels.tsa.stattools (<i>kpss</i>) or arch.unitroot (<i>KPSS</i>)
	Zivot-Andrew test	<i>R</i> <i>Python</i>	urca (<i>ur.za</i>) statsmodels.tsa.stattools (<i>zivot_andrews</i>) or arch.unitroot (<i>ZivotAndrews</i>)
Time series decomposition	Seasonal-trend decomposition using Loess	<i>R</i> <i>Python</i>	stats (<i>stl</i>) statsmodels.tsa.seasonal (<i>STL</i>)
	X11 and SEATS	<i>R</i> <i>Python</i>	seasonal (<i>seas</i>) statsmodels.tsa.x13 (<i>x13_arima_select_order</i>)
	Locally estimated scartterplot smoothing	<i>R</i> <i>Python</i>	stats (<i>loess</i>) statsmodels.nonparametric.smoothers.lowess (<i>lowess</i>)
Exponential smoothing methods		<i>R</i> <i>Python</i>	forecast (<i>ets</i>) statsmodels.tsa.holtwinters (<i>ExponentialSmoothing</i>)
Time series Transformation	Differentiation operator Δ_m^k	<i>R</i> <i>Python</i>	stats (<i>diff</i>) Pandas (<i>diff</i>)
	Box-Cox transformation	<i>R</i> <i>Python</i>	EnvStats (<i>boxcox</i>) or forecast (<i>BoxCox</i> , <i>BoxCox.lambda</i>) scipy.stats (<i>boxcox</i>)
Auto-correlation and Partial auto-correlation	Ljung-Box test	<i>R</i> <i>Python</i>	stats (<i>Box.test</i>) statsmodels.stats.diagnostic (<i>acorr_ljungbox</i>)
	Durbin-Watson test	<i>R</i> <i>Python</i>	stats (<i>dwttest</i>) statsmodels.stats.stattools (<i>durbin_watson</i>)
	(Partial) Autocorrelation function	<i>R</i> <i>Python</i>	stats (<i>(p)acf</i>) statsmodels.tsa.stattools (<i>(p)acf</i>)
Linear times models	AR model	<i>R</i> <i>Python</i>	tseries (<i>arma</i>) with $q = 0$ statsmodels.tsa.ar_model (<i>AutoReg</i>)
	MA model	<i>R</i> <i>Python</i>	tseries (<i>arma</i>) with $p = 0$ statsmodels.tsa.arma_model (<i>ARMA</i>) where $p = 0$
	ARMA model	<i>R</i> <i>Python</i>	tseries (<i>arma</i>) statsmodels.tsa.arma_model (<i>ARMA</i>)
ARIMA - SARIMA	ARIMA model	<i>R</i> <i>Python</i>	forecast (<i>Arima</i>) with $P = D = Q = 0$ statsmodels.tsa.arima_model (<i>ARIMA</i>) with $P = D = Q = 0$
	SARIMA model	<i>R</i> <i>Python</i>	forecast (<i>Arima</i>) statsmodels.tsa.arima_model (<i>ARIMA</i>)
Non-linear time series models	PAR	<i>R</i> <i>Python</i>	- -
	FAR	<i>R</i> <i>Python</i>	- -
	MSAR	<i>R</i> <i>Python</i>	MSwM (<i>msmFit</i>) statsmodels.tsa.regime_switching.markov_autoregression (<i>MarkovAutoregression</i>)
	STAR	<i>R</i> <i>Python</i>	tsDyn (<i>tar</i> , <i>setar</i> , <i>lstar</i>) -
	Angle's test for ARCH	<i>R</i> <i>Python</i>	- statsmodels.stats.diagnostic (<i>het_arch</i>)
	(G)ARCH	<i>R</i> <i>Python</i>	tseries (<i>garch</i>) arch (<i>arch_model</i>)

Table 7 Time series analysis methods and models presented throughout the present survey. Recapitulation of available *R* and *Python* implementations.

Acknowledgements

Fatoumata Dama is supported by a PhD scholarship granted by the French Ministry for Higher Education, Research and Innovation.

References

- Aghabozorgi S, Shirkorshidi AS, Wah TY (2015) Time-series clustering - a decade review. *Information Systems* 53:16–38
- Ailliot P, Prevosto M, Soukissian T, Diamanti C, Theodoulides A, Politis C (2003) Simulation of sea state parameters process to study the profitability of a maritime line. In: *The Thirteenth International Offshore and Polar Engineering Conference*, International Society of Offshore and Polar Engineers
- Ailliot P, Bessac J, Monbet V, Pene F (2015) Non-homogeneous hidden markov-switching models for wind time series. *Journal of Statistical Planning and Inference* 160:75–88
- Akaike H (1998) *Markovian representation of stochastic processes and its application to the analysis of autoregressive moving average processes*, Springer New York
- Alemohammad N, Rezakhah S, Alizadeh S (2016) Markov switching component garch model: stability and forecasting. *Communications in Statistics - Theory and Methods* 45(15):4332–4348
- Ali M, Alqahtani A, Jones MW, Xie X (2019) Clustering and classification for time series data in visual analytics: a survey. *IEEE Access* 7:181314–181338
- Almalag A, Edwards G (2017) A review of deep learning methods applied on load forecasting. In: *16th International Conference on Machine Learning and Applications (ICMLA)*, IEEE, pp 511–516
- Amarasinghe K, Marino DL, Manic M (2017) Deep neural networks for energy load forecasting. In: *IEEE 26th International Symposium on Industrial Electronics (ISIE)*, pp 1483–1488
- APTECH (2020) Introduction to the fundamentals of time series data and analysis. <https://www.aptech.com/blog/introduction-to-the-fundamentals-of-time-series-data-and-analysis/>
- Aryee G, Essuman R, Djagbletey R, Darkwa EO (2019) Comparing the forecasting performance of seasonal Arima and Holt-Winters methods of births at a tertiary healthcare facility in Ghana. *Journal of Biostatistics and Epidemiology*
- Avishek P, Prakash P (2017) *Practical Time Series Analysis: Master Time Series Data Processing, Visualization, and Modeling using Python*. Packt Publishing Ltd, Birmingham, UK
- Bai S, Kolter JZ, Koltun V (2018) An empirical evaluation of generic convolutional and recurrent networks for sequence modeling. arXiv:1803.01271
- Bao W, Yue J, Rao Y (2017) A deep learning framework for financial time series using stacked autoencoders and long-short term memory. *PLOS ONE* 12(7):e0180944
- Basu P, Rudoy D, Wolfe PJ (2009) A nonparametric test for stationarity based on local Fourier analysis. In: *IEEE International Conference on Acoustics, Speech and Signal Processing (ICASSP)*, Tapei, pp 3005–3008
- Bekleric S (2008) *Nonlinear prediction via Volterra series and applications to geophysical data*. Master's thesis, University of Alberta, Canada

- Bergmeir C, Hyndman RJ, Benítez JM (2016) Bagging exponential smoothing methods using STL decomposition and Box–Cox transformation. *International Journal of Forecasting* 32(2):303–312
- Bessac J, Ailliot P, Cattiaux J, Monbet V (2016) Comparison of hidden and observed regime-switching autoregressive models for (u, v)-components of wind fields in the Northeast Atlantic. *Advances in Statistical Climatology, Meteorology and Oceanography* 2(1):1–16
- Blázquez-García A, Conde A, Mori U, Lozano JA (2020) A review on outlier/anomaly detection in time series data. arXiv:2002.04236
- Bollerslev T (1986a) Generalized autoregressive conditional heteroskedasticity. *Journal of Econometrics* 31:307–327
- Bollerslev T (1986b) Generalized autoregressive conditional heteroskedasticity. *Journal of Econometrics* 31(3):307–327
- Bougerol P, Picard N (1992) Stationarity of GARCH processes and some nonnegative time series. *Journal of Econometrics* 52:115–127
- Box GE, Cox DR (1964) An analysis of transformations. *Journal of the Royal Statistical Society: Series B (Methodological)* 26(2):211–243
- Box GE, Jenkins GM, Reinsel GC, Ljung GM (2015) *Time series analysis: forecasting and control*, 5th edn. Wiley
- Braei M, Wagner S (2020) Anomaly detection in univariate time-series: a survey on the state-of-the-art. arXiv:2004.00433v1
- Brockwell PJ, Davis RA, Fienberg SE (1991) *Time series: theory and methods*. Springer
- Brooks C (2019) *Introductory Econometrics for Finance*, 4th edn. Cambridge University Press
- Brownlee J (2020a) Deep learning for time series forecasting. Predict the future with MLPs, CNNs and LSTMs in Python. <https://machinelearningmastery.com/deep-learning-for-time-series-forecasting/>
- Brownlee J (2020b) How to decompose time series data into trend and seasonality. <https://machinelearningmastery.com/decompose-time-series-data-trend-seasonality/>
- Cai J (1994) A markov model of switching-regime ARCH. *Journal of Business & Economic Statistics* 12(3):309–316
- Cardinali A, Nason GP (2013) Costationarity of locally stationary time series using costat. *Journal of Statistical Software* 55(1):1–22
- Chan NH, Yau CY, Zhang RM (2015) Lasso estimation of threshold autoregressive models. *Journal of Econometrics* 189(2):285–296
- Chandra R, Chand S (2016) Evaluation of co-evolutionary neural network architectures for time series prediction with mobile application in finance. *Applied Soft Computing* 49:462–473
- Chen R, Tsay RS (1993) Functional-coefficient autoregressive models. *Journal of the American Statistical Association* 88(421):298–308
- Cheng J, Xu C, Zhang Z, Li X (2017) Electric load forecasting in smart grids using Long-Short-Term-Memory based Recurrent Neural Network. In: 51st Annual Conference on Information Sciences and Systems (CISS), pp 1–6
- Cheung YW, Lai KS (1995) Lag order and critical values of the augmented Dickey–Fuller test. *Journal of Business & Economic Statistics* 13(3):277–280

- Chung H, Shin Ks (2018) Genetic algorithm-optimized long short-term memory network for stock market prediction. *Sustainability* 10:3765
- Cirstea R, Micu D, Muresan G, Guo C, Yang B (2018) Correlated time series forecasting using multi-task deep neural networks. In: 27th International Conference on Information and Knowledge Management, ACM, pp 1527–1530
- Cleveland RB, Cleveland WS, McRae JE, Terpenning I (1990) STL: a seasonal-trend decomposition. *Journal of Official Statistics* 6(1):3–73
- Cleveland WS, Grosse E, Shyu WM (2017) Local regression models. In: Hastie T (ed) *Statistical models in S*, Routledge, pp 309–376
- Dagum EB, Bianconcini S (2016) *Seasonal adjustment methods and real time trend-cycle estimation. Statistics for Social and Behavioral Sciences*, Springer
- van Delft A, Eichler M (2018) Locally stationary functional time series. *Electronic Journal of Statistics* 12:107–170
- Dette H, Preuß P, Vetter M (2011) A measure of stationarity in locally stationary processes with applications to testing. *Journal of the American Statistical Association* 106(495):1113–1124
- Dette H, Wu W, Zhou Z (2015) Change point analysis of second order characteristics in non-stationary time series. arXiv preprint arXiv:150308610
- Dickey DA, Fuller WA (1979) Distribution of the estimators for autoregressive time series with a unit root. *Journal of the American Statistical Association* 74(366):427–431
- Dolado JJ, Gonzalo J, Mayoral L (2002) A fractional dickey–fuller test for unit roots. *Econometrica* 70(5):1963–2006
- Durbin J (1959) Efficient estimation of parameters in moving-average models. *Biometrika* 46(3/4):306–316
- Durbin J (1960) The fitting of time-series models. *Review of the International Statistical Institute* 28(3):233–244
- Dürre A, Fried R, Liboschik T (2015) Robust estimation of (partial) autocorrelation. Tech. rep., TU Dortmund, report number: 12/14
- Dwivedi Y, Subba Rao S (2011) A test for second-order stationarity of a time series based on the discrete fourier transform. *Journal of Time Series Analysis* 32(1):68–91
- Eitrheim Ø, Teräsvirta T (1996) Testing the adequacy of smooth transition autoregressive models. *Journal of econometrics* 74(1):59–75
- Elliott G, Rothenberg TJ, Stock JH (1996) Efficient tests for an autoregressive unit root. *Econometrica* 64(4):813–836
- Engle RF (1982) Autoregressive conditional heteroscedasticity with estimates of the variance of United Kingdom inflation. *Econometrica* 50(4):987–1007
- Engle RF, Bollerslev T (1986) Modelling the persistence of conditional variance. *Econometric Reviews* 5(1):1–50
- Fan J, Gijbels I (1996) *Local polynomial modelling and its applications, Monographs on statistics and Applied Probability, vol 66*. Chapman and Hall, CRC Press
- Fawaz H, Forestier G, Weber J, Idoumghar L, Muller PA (2019) Deep learning for time series classification: a review. *Data Mining and Knowledge Discovery* 33(4):917–963

- Fernandes CAR, Mota JM, Favier G (2010) MIMO volterra modeling for nonlinear communication channels. *Learning and Nonlinear Models* 2(8):71–92
- Fischer T, Krauss C (2018) Deep learning with long short-term memory networks for financial market predictions. *European Journal of Operational Research* 270:654–669
- Franke J (1985) A Levinson-Durbin recursion for autoregressive-moving average processes. *Biometrika* 72(3):573–581
- Galbraith JW, Zinde-Walsh V (1994) A simple noniterative estimator for moving average models. *Biometrika* 81(1):143–155
- Gardner Jr E, Everette S (2006) Exponential smoothing: The state of the art - Part ii. *International Journal of Forecasting* 22(4):637–666
- Gardner Jr E, McKenzie E (1985) Forecasting trends in time series. *Management Science* 31:1237–1246
- Gardner Jr ES (1985) Exponential smoothing: The state of the art. *Journal of forecasting* 4(1):1–28
- Gasparin A, Lukovic S, Alippi C (2019) Deep learning for time series forecasting: the electric load case. [arXiv:1907.09207](https://arxiv.org/abs/1907.09207)
- Ge M, Kerrigan EC (2016) Short-term ocean wave forecasting using an autoregressive moving average model. In: 2016 UKACC 11th International Conference on Control (CONTROL), IEEE, pp 1–6
- Gelper S, Fried R, Croux C (2010) Robust forecasting with exponential and Holt–Winters smoothing. *Journal of Forecasting* 29(3):285–300
- Gensler A, Henze J, Sick B, Raabe N (2016) Deep learning for solar power forecasting - an approach using AutoEncoder and LSTM neural networks. In: International Conference on Systems, Man, and Cybernetics (SMC), IEEE, pp 2858–2865
- Gomes P, Castro R (2012) Wind speed and wind power forecasting using statistical models: autoregressive moving average (ARMA) and artificial neural networks (ANN). *International Journal of Sustainable Energy Development* 1(1/2)
- Gospodinov N (2005) Testing for threshold nonlinearity in short-term interest rates. *Journal of Financial Econometrics* 3(3):344–371
- Gruber JK, Bordons C, Bars R, Haber R (2010) Nonlinear predictive control of smooth nonlinear systems based on Volterra models. application to a pilot plant. *International Journal of Robust and Nonlinear Control* 20(16):1817–1835
- Guerrero VM (1993) Time-series analysis supported by power transformations. *Journal of Forecasting* 12(1):37–48
- Hagerud GE (1997) A smooth transition ARCH model for asset returns
- Hamilton JD (1989) A new approach to the economic analysis of nonstationary time series and the business cycle. *Econometrica* pp 357–384
- Hamilton JD (1990) Analysis of time series subject to changes in regime. *Journal of econometrics* 45(1-2):39–70
- Hamilton JD (1994) *Time series analysis, vol 2*. Princeton University Press, NJ
- Hannan EJ, Kavalieris L (1984) A method for autoregressive-moving average estimation. *Biometrika* 71(2):273–280

- Hannan EJ, Rissanen J (1982) Recursive estimation of mixed autoregressive-moving average order. *Biometrika* 69(1):81–94
- Hansen BE (2011) Threshold autoregression in economics. *Statistics and its Interface* 4(2):123–127
- Härdle W, Lütkepohl H, Chen R (1997) A review of nonparametric time series analysis. *International Statistical Review* 65(1):49–72
- He W (2017) Load forecasting via deep neural networks. *Procedia Computer Science* 122:308–314
- Hewamalage H, Bergmeir C, Bandara K (2021) Recurrent neural networks for time series forecasting: current status and future directions. *International Journal of Forecasting*, in press, doi:10.1016/j.ijforecast.2020.06.008
- Hiransha M, Gopalakrishnan E, Menon VK, Soman K (2018) NSE stock market prediction using deep-learning models. *Procedia Computer Science* 132:1351–1362
- Holt CC (1957) Forecasting seasonals and trends by exponentially weighted averages. Office of Naval Research Memorandum, No 52, Carnegie Institute of Technology, Pittsburgh USA
- Holt CC (2004) Forecasting seasonals and trends by exponentially weighted moving averages. *International Journal of Forecasting* 20(1):5–10
- Hossain MZ (2011) The use of Box-Cox transformation technique in economic and statistical analyses. *Journal of Emerging Trends in Economics and Management Sciences* 2(1):32–39
- Hua Y, Zhao Z, Li R, Chen X, Liu Z, Zhang H (2018) Deep learning with Long Short-Term Memory for time series prediction. <https://arxiv.org/pdf/1810.10161.pdf>
- Jones RH (1980) Maximum likelihood fitting of ARMA models to time series with missing observations. *Technometrics* 22(3):389–395
- Karakuş O, Kuruoğlu EE, Altinkaya MA (2015) Estimation of the nonlinearity degree for polynomial autoregressive processes with RJMCMC. In: 23rd European Signal Processing Conference (EUSIPCO), pp 953–957
- Karakuş O, Kuruoğlu EE, Altinkaya MA (2017) One-day ahead wind speed/power prediction based on polynomial autoregressive model. *IET Renewable Power Generation* 11(11):1430–1439
- Klimko LA, Nelson PI (1978) On conditional least squares estimation for stochastic processes. *The Annals of statistics* pp 629–642
- Koprinska I, Wu D, Wang Z (2018) Convolutional neural networks for energy time series forecasting. In: International Joint Conference on Neural Networks (IJCNN), IEEE, pp 1–8
- Kuo PH, Huang CJ (2018) A high precision artificial neural networks model for short-term energy load forecasting. *Energies* 11(1):213
- Kuruoglu EE (2002) Nonlinear least lp-norm filters for nonlinear autoregressive alpha-stable processes. *Digital Signal Processing* 12(1):119–142
- Kwiatkowski D, Phillips PC, Schmidt P, Shin Y (1992) Testing the null hypothesis of stationarity against the alternative of a unit root: How sure are we that economic time series have a unit root? *Journal of econometrics* 54(1-3):159–178
- Lahaye PJ, Poline JB, Flandin G, Dodel S, Garnero L (2003) Functional connectivity: studying nonlinear, delayed interactions between BOLD signals. *NeuroImage* 20(2):962–974

- Lara-Benítez P, Carranza-García M, Luna-Romera JM, Riquelme JC (2020) Temporal convolutional networks applied to energy-related time series forecasting. *Applied Sciences* 10(7):2322
- Lee D (2011) Short-term prediction of wind farm output using the recurrent quadratic Volterra model. In: 2011 IEEE Power and Energy Society General Meeting, IEEE, pp 1–8
- Lee S, Ha J, Na O, Na S (2003) The cusum test for parameter change in time series models. *Scandinavian Journal of Statistics* 30(4):781–796
- Li S, Jin X, Xuan Y, Zhou X, Chen W, Wang YX, Yan X (2019) Enhancing the locality and breaking the memory bottleneck of transformer on time series forecasting. In: 33rd Annual Conference on Neural Information Processing Systems (NeurIPS), pp 5244–5254
- Lim B, Zohren S (2020) Time series forecasting with deep learning: a survey. <https://arxiv.org/abs/2004.13408>
- Lin CFJ, Teräsvirta T (1994) Testing the constancy of regression parameters against continuous structural change. *Journal of econometrics* 62(2):211–228
- Ljung GM, Box GE (1978) On a measure of lack of fit in time series models. *Biometrika* 65(2):297–303
- Ma X, Tao Z, Wang Y, Yu H, Wang Y (2015) Long short-term memory neural network for traffic speed prediction using remote microwave sensor data. *Transportation Research Part C: Emerging Technologies* 54:187–197
- Maronna R, Martin R, Yohai V (2006) *Robust statistics*. J. Wiley, Chichester
- Martinez EZ, Aparecida Soares da Silva E, Lelis Dal Fabbro A (2011) A SARIMA forecasting model to predict the number of cases of dengue in Campinas, State of São Paulo, Brazil. *Revista da Sociedade Brasileira de Medicina Tropical* 44(4):436–440
- Meyer R, Fournier DA, Berg A (2003) Stochastic volatility: Bayesian computation using automatic differentiation and the extended Kalman filter. *The Econometrics Journal* 6(2):408–420
- Mohammadi M (2017) Prediction of α -stable GARCH and ARMA-GARCH-M models. *Journal of Forecasting* 36(7):859–866
- Montgomery DC, Jennings CL, Kulahci M (2016) *Introduction to Time Series Analysis and Forecasting*, 2nd edn. Wiley Series in Probability and Statistics, Wiley
- Murthy DP, Kronauer R (1973) Maximum likelihood estimation for moving average models. *Sankhyā: The Indian Journal of Statistics, Series A* 35(4):455–464
- Nason G (2013) A test for second-order stationarity and approximate confidence intervals for localized autocovariances for locally stationary time series. *Journal of the Royal Statistical Society: Series B (Statistical Methodology)* 75(5):879–904
- Nielsen A (2019) *Practical Time Series Analysis*. O’Reilly
- Nielsen B (2006) Correlograms for non-stationary autoregressions. *Journal of the Royal Statistical Society: Series B (Statistical Methodology)* 68(4):707–720
- Nino S (2019) *Transformers and time series forecasting*. PhD thesis, Princeton University, USA
- Nyoni T (2019) *Time series modeling and forecasting of the consumer price index in Belgium*. Mpra paper, University Library of Munich, Germany
- Osborne JW (2010) Improving your data transformations: Applying the Box-Cox transformation. *Practical Assessment, Research & Evaluation* 15(12):1–9

- Panorska A, Mittnik S, Rachev S (1995) Stable GARCH models for financial time series. *Applied Mathematics Letters* 8:33–37
- Paoella MS (2018) *Linear models and time-series analysis: regression, Anova, Arma and Garch*. Wiley Series in Probability and Statistics, John Wiley & Sons
- Paparoditis E (2010) Validating stationarity assumptions in time series analysis by rolling local periodograms. *Journal of the American Statistical Association* 105(490):839–851
- Park SH, Kim B, Kang CM, Chung CC, Choi JW (2018) Sequence-to-sequence prediction of vehicle trajectory via LSTM encoder-decoder architecture. In: *IEEE Intelligent Vehicles Symposium (IV)*, pp 1672–1678
- Pegels CC (1969) Exponential forecasting: some new variations. *Management Science* 15(5):311–315
- Peng L, Liu S, Liu R, Wang L (2018) Effective long short-term memory with differential evolution algorithm for electricity price prediction. *Energy* 162:1301–1314
- Perron P (1989) The great crash, the oil price shock, and the unit root hypothesis. *Econometrica* 57(6):1361–1401
- Perry MB (2010) The exponentially weighted moving average. In: Cochran JJ (ed) *Wiley Encyclopedia of Operations Research and Management Science*, John Wiley & Sons, Inc., pp 1–9
- Pham HT, Yang BS (2010) Estimation and forecasting of machine health condition using ARMA/GARCH model. *Mechanical Systems and Signal Processing* 24(2):546–558
- Phandoidaen N, Richter S (2020) Forecasting time series with encoder-decoder neural networks. [arXiv:2009.08848](https://arxiv.org/abs/2009.08848)
- Phillips PC (1987) Time series regression with a unit root. *Econometrica* 55(2):277–301
- Phillips PC, Perron P (1988) Testing for a unit root in time series regression. *Biometrika* 75(2):335–346
- Portilla JM (2018) Using Python and Auto ARIMA to forecast seasonal time series. <https://medium.com/@josemarcialportilla/using-python-and-auto-arima-to-forecast-seasonal-time-series-90877adff03c>
- Preuß P, Vetter M, Dette H (2013) A test for stationarity based on empirical processes. *Bernoulli* 19(5B):2715–2749
- Priestley M, Rao TS (1969) A test for non-stationarity of time-series. *Journal of the Royal Statistical Society: Series B (Methodological)* 31(1):140–149
- Puchstein R, Preuß P (2016) Testing for stationarity in multivariate locally stationary processes. *Journal of Time Series Analysis* 37(1):3–29
- Raghu M, Schmidt E (2020) Survey of deep learning for scientific discovery. [arXiv:2003.11755](https://arxiv.org/abs/2003.11755)
- Sakia R (1992) The Box-Cox transformation technique: a review. *Journal of the Royal Statistical Society: Series D (The Statistician)* 41(2):169–178
- Samal KKR, Babu KS, Das SK, Acharaya A (2019) Time series based air pollution forecasting using SARIMA and Prophet model. In: *International Conference on Information Technology and Computer Communications (ITCC)*, pp 80–85
- Sandgren N, Stoica P, Babu P (2012) On moving average parameter estimation. In: *20th European Signal Processing Conference (EUSIPCO)*, IEEE, pp 2348–2351

- Selvin S, Vinayakumar R, Gopalakrishnan E, Menon VK, Soman K (2017) Stock price prediction using LSTM, RNN and CNN-sliding window model. In: International Conference on Advances in Computing, Communications and Informatics (ICACCI), IEEE, pp 1643–1647
- Sezer OB, Gudelek MU, Murat A (2020) Financial time series forecasting with deep learning : a systematic literature review: 2005–2019. *Applied Soft Computing* 90:106181
- Shen Z, Zhang Y, Lu J, Xu J, Xiao G (2019) A novel time series forecasting model with deep learning. *Neurocomputing* 396(5):302–313
- So MK, Chen CW, Chen MT (2005) A bayesian threshold nonlinearity test for financial time series. *Journal of Forecasting* 24(1):61–75
- Solarwinds (2019) Holt-winters forecasting simplified. <https://orangematter.solarwinds.com/2019/12/15/holt-winters-forecasting-simplified/>
- Sreenivasan M, Sumathi K (1998) Innovation algorithm in ARMA process. *Korean Journal of Computational & Applied Mathematics* 5(2):331–340
- Susto GA, Cenedese A, Terzi M (2018) Time-series classification methods: review and applications to power systems data. In: *Big Data Application in Power Systems*, Elsevier, chap 9, pp 179–220, dOI: 10.1016/B978-0-12-811968-6.00009-7
- Taylor JW (2003a) Exponential smoothing with a damped multiplicative trend. *International Journal of Forecasting* 19(4):715–725
- Taylor JW (2003b) Short-term electricity demand forecasting using double seasonal exponential smoothing. *Journal of the Operational Research Society* 54(8):799–805
- Tian C, Ma J, Zhang C, Zhan P (2018) A deep neural network model for short-term load forecast based on long short-term memory network and convolutional neural network. *Energies* 11:3493
- Tong H (1990) *Non-linear time series: a dynamical system approach*. Oxford University Press
- Tsay RS (1989) Testing and modeling threshold autoregressive processes. *Journal of the American statistical association* 84(405):231–240
- Tsay RS, Chen R (2018) *Nonlinear time series analysis*. Wiley
- Ubilava D, Helmers CG (2013) Forecasting ENSO with a smooth transition autoregressive model. *Environmental modelling & software* 40:181–190
- Usman A, Sulaiman M, Abubakar I (2019) Trend of neonatal mortality in Nigeria from 1990 to 2017 using time series analysis. *Journal of Applied Sciences and Environmental Management* 23(5):865–869
- Valipour M (2015) Long-term runoff study using SARIMA and ARIMA models in the united states. *Meteorological Applications* 22(3):592–598
- Vaswani A, Shazeer N, Parmar N, Uszkoreit J, Jones L, Gomez AN, Kaiser L, Polosukhin I (2017) Attention is all you need. In: *31st Annual Conference on Neural Information Processing Systems (NeurIPS)*, pp 5998–6008
- Whittle P (1953) Estimation and information in stationary time series. *Arkiv för matematik* 2(5):423–434
- Winters PR (1960) Forecasting sales by exponentially weighted moving averages. *Management Science* 6(3):324–342
- Wold H (1954) *A study in the analysis of stationary time series*, vol Second revised edition. Almqvist and Wiksell Book Co., Uppsala

- Wu N, Green B, Ben X, O'Banion S (2020) Deep transformer models for time series forecasting:the influenza prevalence case. arXiv:2001.08317
- Xin J, Zhou J, Yang SX, Li X, Wang Y (2018) Bridge structure deformation prediction based on GNSS data using Kalman-ARIMA-GARCH model. Sensors 18(1):298
- Xu H, Ding F, Yang E (2019) Modeling a nonlinear process using the exponential autoregressive time series model. Nonlinear Dynamics 95(3):2079–2092
- Zhou Z (2013) Heteroscedasticity and autocorrelation robust structural change detection. Journal of the American Statistical Association 108(502):726–740
- Zivot E, Andrews DWK (2002) Further evidence on the great crash, the oil-price shock, and the unit-root hypothesis. Journal of business & economic statistics 20(1):25–44